

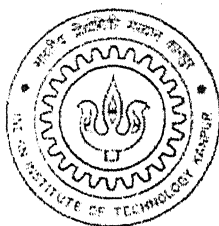
Seismic Response of RC Frame Buildings on Stilts

*A Thesis Submitted
In Partial Fulfillment of the Requirements
For the Degree of*

MASTER OF TECHNOLOGY

by

Perwez Ahmad



To the

DEPARTMENT OF CIVIL ENGINEERING
INDIAN INSTITUTE OF TECHNOLOGY
OCTOBER, 2004

Dedicated to

My Parents
&
Jainath Sir

TH
CE/2004/M
AR518

15 MAR 2005/CE

गुरुप्राप्तम काशीनाथ केलकर पुस्तकालय
भारतीय प्रौद्योगिकी संस्थान कानपुर
बप्रापि ड० ▲...150914...




A150914

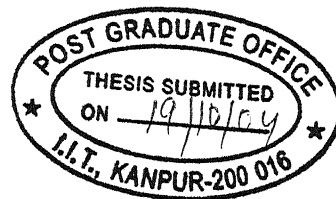
CERTIFICATE

It is certified that the work contained in this thesis entitled "Seismic Response of RC Frame Buildings on Stilts" by Perwez Ahmad (Roll No. Y210327) has been carried out under my supervision and that this work has not been submitted elsewhere for a degree.



October 2004


Dr. Sudhir K. Jain
Professor
Department of Civil Engineering
I.I.T. Kanpur





ACKNOWLEDGMENTS

All the praise and thanks is for Almighty as without His help and guidance nothing can be done and peace be upon all His messengers. I cannot be thankful to Almighty without being thankful to all who has helped me to reach here.

I express my earnest gratitude to my guruji, Dr. Sudhir K. Jain, for his invaluable guidance, technical as well as non-technical support during my stay in IIT Kanpur. His word of encouragement always forced me to excel and to work hard. Many academic and non-academic things that I have learn from him, I will try to instill in my personal and professional life. I wish to be dynamic and workaholic like him.

I feel deeply indebted to Professor C.V.R. Murty and Dr. D.C. Rai for their invaluable guidance and technical support. In spite of their busy schedule, they always showed a kind gesture to help me. The resources and the materials in Professor Murty's office have helped a lot in this work. I thank all the faculty members of the institute for whatever I have learnt from them. Special thanks to Ashwini sir and Vinay sir for their warm feelings and hospitality.

I do not have word to describe my sense of gratitude to Hemant Bhai. I used to call him "co-guru". He always guided me at each step like co-guru and showed affection like elder brother. Special thanks to Dipti Bhai, Rupen Da, Kaustubh Da, Goutam Da, Balu, Surajit, Akash, Aami, Bharati, Deepak, Kaushik, Debasis, and Sandip Da for their technical and non-technical helps in completing the program. My stay at IIT Kanpur has been most memorable and pleasant in the company of brother Quaff, Shahid, Faizaan, Basha, Tanwir, Dilshad, Asif, Shahzad, Ahmad, Shadab, and Sajid.

My friends helped and encouraged me a lot at every critical time, especially Nehal, Aadil, Tabish, Nehal Mirza, Manoj, Ejaz, Shadab, Imteyaz, Amit, Varun, and Babloo. Affections of my loving juniors Pundir, Wasim, Fahim, Aarzoo and Reshad are memorable. My relatives Shamsuz Zuha saheb, Iqbal Bhai, Khalid Bhai, Ekramul Hoda, Arshi saheb etc. guided and motivated me always. My teachers Abdur Rahman saheb, Jianath Babu, Maya Babu, Prem Babu, Ghazala Yasmeen saheba, Saifi saheb, Afzal saheb, Nasim saheb, Mumataz saheb, Sabih saheb, Nadim saheb, Hasan Irteza saheb taught and guided me affectionately.

Words are insufficient to describe my gratitude to my parents, brother, sisters, and brother in laws whose encouragement and affection have helped me to strive forward throughout the life.

I gratefully acknowledge the financial support received through a research grant from the Ministry of Human Resource Development.

Perwez

Table of Contents

Certificate	i
Abstract	ii
Acknowledgements	iii
Table of Contents	iv
List of Tables	vi
List of Figures	vii
1. Introduction and Literature Review	
1.0 General	1
1.1 Stilt Buildings	3
1.2 Performance of Stilt Buildings during the Past Earthquake	4
1.2.1 1997 Jabalpur (India) Earthquake	4
1.2.2 1998 Adana-Ceyhan (Turkey) Earthquake	6
1.2.3 1999 Kocaeli (Turkey) Earthquake	6
1.2.4 2001 Bhuj (India) Earthquake	7
1.2.5 2003 Bingol (Turkey) Earthquake	7
1.3 Codal Provision for Stilt Buildings	8
1.4 Previous Studies on Stilt Buildings	9
1.5 Scope and Research Objectives	13
1.6 Organization of Thesis	14
2. Analysis and Design	
2.0 General	15
2.1 Details of the Considered Building	15
2.2 Material Properties of Members	16
2.3 Modeling of Members	16
2.4 Analysis of the Frames	16
2.5 Design Cases	18
3. Pushover Analysis	
3.0 General	21
3.1 Material Properties of Infill	22
3.2 Modeling of Infills for Stiffness	23
3.3 Modeling of Infills for Strength and Deformation	25
3.4 Hinge Properties of Members	27
3.5 Locations of Plastic Hinges	29
3.6 Loads and Load Combinations	30
3.7 Pushover Analysis and Pushover Curve	31
4.0 Results and Discussions	
4.0 General	32
4.1 Design Case GRAV	33
4.1.1 Bare Frames	33
4.1.2 Stilt Frames	33
4.1.3 Infill Frames	34
4.1.4 Comparison	35

4.2	Design Case EQ2	36
4.2.1	Bare Frames	36
4.2.2	Stilt Frames	37
4.2.3	Infill Frames	38
4.2.4	Comparison	38
4.3	Design Case EQ3	39
4.3.1	Bare Frames	39
4.3.2	Stilt Frames	40
4.3.3	Infill Frames	41
4.3.4	Comparison	42
4.4	Design Case EQ5	43
4.4.1	Bare Frames	43
4.4.2	Stilt Frames	44
4.4.3	Infill Frames	44
4.4.4	Comparison	45
4.5	Design Cases EQC3 and EQCB3	46
4.5.1	Design Case EQC3	46
4.5.2	Design Case EQCB3	47
4.5.3	Comparison	48
4.6	All Bare Frames	50
4.7	All Stilt Frames	51
4.8	All Infill Frames	52
4.9	Overall Observations	53
5.	Summary and Conclusions	
5.0	General	55
5.1	Summary	55
5.2	Conclusions	56
5.3	Possible Future Work	57
	References	58
	Tables	61
	Figures	68

LIST OF TABLES

<i>Tables</i>	<i>Title</i>	<i>Page No.</i>
2.1	Base Shear Distribution in Frame-A	61
2.2	Base Shear Distribution in Frame-B	61
2.3	Section Properties of Columns of Frame-A	61
2.4	Section Properties of Beams of Frame-A	62
2.5	Section Properties of Columns of Frame-B	62
2.6	Section Properties of Beams of Frame-B	62
3.1	Flexural Hinge Properties of Columns of Frame-A	63
3.2	P-M Interaction Curve of Columns of Frame-A	63
3.3	Flexural Hinge Properties of Beams of Frame-A	63
3.4	Axial Hinge Properties of Struts of Frame-A	63
3.5	Flexural Hinge Properties of Columns of Frame-B	64
3.6	P-M Interaction Curve of Columns of Frame-B	64
3.7	Flexural Hinge Properties of Beams of Frame-B	64
3.8	Axial Hinge Properties of Struts of Frame-B	64
3.9	Shear Hinge Properties of Frame-A	65
3.10	Shear Hinge Properties of Frame-B	65
4.1	Lateral Strength (kN) of Frame-A and Frame-B	66
4.2	Maximum Roof Displacement (mm) of Frame-A and Frame-B	66
4.3	Lateral Stiffness (kN/mm) of Frame-A and Frame-B	66
4.4	Ductility of Frame-A and Frame-B	67
4.5	Column Overstrength Factor (COF) of Frame-A and Frame-B	67
4.6	Overstrength Factor of Frame-A and Frame-B	67
4.7	Ground Story Lateral Stiffness (kN/mm) of Frame-A and Frame-B	67

LIST OF FIGURES

<i>Figure</i>	<i>Title</i>	<i>Page No.</i>
1.1	Contrasting structural behavior of buildings without and with unreinforced masonry infill walls (Murty et al., 2002) (a) Bare frame: Predominant frame action (b) Infilled frame: Predominant truss action	68
1.2	Soft story is subject to severe deformation demands during earthquake shaking (Murty et al., 2002) (a) Open ground story (b) Bare frame	68
1.3	Damage to ground story columns in stilt buildings (Arlekar et al., 1997) (a) Damage to column in Hingiri apartment (b) Damage to columns of Youth Hostel Building	69
1.4	Soft story mechanism formed after the fall out of the infill in the bottom two stories (Mistakidis, et al., 2000)	69
1.5	Multistorey RC frame with masonry infill near Golcuk (Dolsek et al., 2001) (a) Concentration of damage in bottom 2-stories (b) Collapse in bottom 2-stories	70
1.6	Completely infilled RC frame sustained uniform damage (Murty et al., 2002)	70
1.7	Four-story building with infilled ground story had minor cracking- at frame-infill interface (Murty et al., 2002)	71
1.8	Severe damage to the ground story columns in the open ground story building (Murty et al., 2002)	71
1.9	Shear cracking of non-ductile columns of an open ground story building in Bhuj (Murty et al., 2002)	72
1.10	Damage of ground story columns of stilt building (Ellul et al., 2003) (a) Soft ground story building (b) Damage to column in Fig. (a)	72
1.11	Collapse of the ground floor where three shops were operating (Ellul et al., 2003)	73
2.1	Dead Load on frame-A	74
2.2	Imposed Load on frame-A	74
2.3	Dead Load on frame-B	75
2.4	Imposed Load on frame-B	75
2.5	Base Shear Distribution in Frame-B	76
2.6	Base Shear Distribution in Frame-B	76
2.7	Cross section of frame-A in GRAV case	77
2.8	Cross section of frame-A in EQ2 case	77
2.9	Cross section of frame-A in EQ3 case	77
2.10	Cross section of frame-A in EQ5 case	78
2.11	Cross section of frame-A in EQC3 case	78
2.12	Cross section of frame-A in EQCB3	78
2.13	Cross section of frame-B in GRAV case	79
2.14	Cross section of frame-B in EQ2 case	79
2.15	Cross section of frame-B in EQ3 case	79
2.16	Cross section of frame-B in EQ5 case	80
2.17	Cross section of frame-B in EQC3 case	80
2.18	Cross section of frame-B in EQCB3	80

3.1	Idealized pushover curve with salient features for infilled frame structure	81
3.2	Load-deformation relationship by Reinhorn et al. [Reinhorn et al., 1995]	81
3.3	Idealized axial load-axial deformation relationship for equivalent [Das, 2000] diagonal strut	82
3.4	Stress-strain curve for confined concrete [Razvi et al., 1999]	82
3.5	Stress-strain curve of HYSD steel bars [Dasgupta, 2000]	82
3.6	Moment-rotation relationship for frame members [FEMA 273]	83
3.7	Axial force-moment interaction curve for columns	83
3.8	Shear strength - shear deformation relationship for frame members [FEMA 273]	84
3.9	Type and location of hinges in infilled frame	84
4.1	Pushover curve of frame	85
4.2	Pushover curve of frame	85
4.3	Pushover curve of frame	86
4.4	Pushover curve of frame	86
4.5	Pushover curve of frame	87
4.6	Pushover curve of frame	87
4.7	Pushover curve of frame	88
4.8	Pushover curve of frame	88
4.9	Pushover curve of stilt and infill frames of frame	89
4.10	Pushover curve of stilt and infill frames of frame	89
4.11	Pushover curve of bare frame of frame	90
4.12	Pushover curve of bare frame of frame	90
4.13	Pushover curve of stilt frame of frame	91
4.14	Pushover curve of stilt frame of frame	91
4.15	Pushover curve of infill frame of frame	92
4.16	Pushover curve of infill frame of frame	92
4.17	Location of hinges at failure in frame	93
4.18	Location of hinges at failure in frame	93
4.19	Location of hinges at failure in frame	94
4.20	Location of hinges at failure in frame	94
4.21	Location of hinges at failure in frame	95
4.22	Location of hinges at failure in frame	95
4.23	Location of hinges at failure in frame	96
4.24	Location of hinges at failure in frame	96
4.25	Location of hinges at failure in stilt frame	97
4.26	Location of hinges at failure in stilt frame	97
4.27	Lateral strength of frame	98
4.28	Lateral strength of frame	98
4.29	Maximum roof displacement of frame	98
4.30	Maximum roof displacement of frame	99
4.31	Lateral stiffness of frame	99
4.32	Lateral stiffness of frame	99
4.33	Ductility of frame	100
4.34	Ductility of frame	100

Chapter 1

Introduction and Literature Review

1.0 General

Reinforced concrete (RC) moment resisting frames are popular compared to structural steel frames in developing countries including India, due to low cost of material and labors. The vertical spaces created by adjoining RC beams and columns are filled by masonry walls either to protect the inside of structure from rain, snow, wind etc. or to divide inside spaces according to functional requirements. Generally, in India unreinforced masonry of burnt clay brick with cement mortar is used. Thickness of infill walls is usually 230-250 mm. Use of half brick thick (~115 mm) walls to divide internal spaces of buildings in urban India is also common.

In general practice, infill panels are assumed as non-structural elements and their strengths and stiffnesses are neglected in the analysis and design of structures, while their mass is taken into account for load calculations. Infills alter the behavior of the building from predominant frame action [Fig. 1.1(a)] to predominant truss action [Fig. 1.1(b)], and carry the lateral seismic force as a compressive axial force along their diagonals [Murty et al., 2002].

In many past earthquakes, relatively weak and flexible RC frames, designed for only gravity loads could have been prevented from collapse if infills were distributed uniformly in plan and elevation. However, when infills are not uniformly distributed, it has many severe ill effects on seismic performance of frames. If infills are not uniformly distributed in plan, it causes stiffness and strength irregularity in plan, which may induce torsional moments in the building. Whereas uneven distribution of infills in elevation causes vertical irregularity. Soft-story effect occurs due to the absence of infill panels in a

particular story while short-column effect occurs in case of partially-filled infills causing stress concentration.

During past earthquakes across the world, numerous buildings with soft story have collapsed or suffered severe damage. Hence, it is crucial to incorporate the effect of infill to comprehend the seismic behavior of infilled frames; especially, when infill is not uniformly distributed.

Infill panel is not homogeneous as it is made of brick and mortar. Therefore, its behavior is dependent on brick and mortar both. Another difficulty in modeling of infills is uncertainties associated with properties of masonry and mortar. Due to this reason, there is a general lack of realistic and simple analytical models, which may be acceptable to designers. However, a large numbers of experimental and analytical researches have been carried out in the last fifty years, to understand the influence of infill on lateral strength and stiffness of framed structures.

Different analytical techniques/models have been proposed for idealizing the infill panels to study their global behavior (e.g., stiffness and strength) and local behavior (such as, failure patterns). These can be divided into two groups: micro-models and macro-models. The first group includes FEM models in which the structure is divided into numerous elements to account for the local effects in detail, whereas the second group includes simplified models (e.g., diagonal strut model) based on the physical behavior of infill panels. The FEM models can give fairly accurate results if the structure is idealized with care, but require large computational effort, and hence, are not suitable to practicing engineers. On the other hand, diagonal strut models give approximate results, and require less computational effort. Due to their simplicity, the macro-models are popular with the practicing engineers [Kumar, 2002].

1.1 Stilt Buildings

Owing to the high cost of land and small size of plots, parking is often accommodated in the ground story area of the multistory buildings in urban areas of India and many other countries. Ground story in such buildings does not have any partition walls between them, while infill walls are present in upper stories. Such buildings are often called “open ground story buildings” or “soft story buildings” or “buildings on stilts” [Murty, 2004]. Ground story may be kept open for making reception lobby or storage also. This type of building will be referred as “stilt building” for the sake of brevity in this document. Such buildings have mainly three types of vertical irregularities namely mass, strength, and stiffness irregularity. As compare to strength and stiffness irregularity, mass (or weight) irregularity has a smaller effect on seismic behavior [Al-Ali et al., 1998].

Stilt buildings are relatively flexible in ground story, i.e., the relative horizontal displacement in the ground story is much larger than that in each of the stories above it [Fig. 1.2(a)]. This flexible ground story is also termed as “soft story”. Such buildings are also weak in ground story, i.e., the total horizontal earthquake force that can be carried in the ground story is significantly smaller than the horizontal load carrying capacity of the upper stories. Thus, the open ground story may also be a weak story. Often, open ground story buildings are called soft story buildings, even though their ground story may be soft and weak. Generally, the soft or weak story usually exists at the ground story level, but it could be at any other story level too [Murty, 2004].

Infilled RC frames are commonly analyzed and designed as bare frames. However, the actual behavior of bare frames is entirely different from that of the bare frames. In stilt buildings, ground story is bare and upper stories are infilled with masonry.

Therefore, it is of interest to analyze and compare deformation profile, hinge formation sequence, strength, stiffness etc. of the same frame, modeling it as a bare frame, fully infilled frame, and as stilt frame. Such a comparison will be useful to understand how the performance of stilt frame is different from that of the bare and infilled frames.

The Indian seismic code classifies a soft story as one in which the lateral stiffness is less than 70 percent of that in the story above or less than 80 percent of the average lateral stiffness of the three stories above. A weak story is one in which the story lateral strength is less than 80 percent of that in the story above. The story lateral strength is the total strength of all seismic force resisting elements sharing the story shear in the considered direction [IS:1893, 2002].

1.2 Performance of Stilt Buildings during the Past Earthquakes

Stilt buildings have consistently shown poor performance during past earthquakes across the world (1971 San Fernando, 1994 Northridge, 1995 Kobe, 1998 Adana-Ceyhan, 1999 Kocaeli, 1999 Taiwan, 2001 Bhuj, and 2003 Algeria earthquakes); a significant number of them have collapsed. Major damage to many reinforced concrete and steel buildings in the 1995 Kobe earthquake, and to critical hospital facilities in the 1971 San Fernando earthquake, were attributed to the open ground story. Alarming amount of damage to the buildings with open basements for parking has been reported during the 1994 Northridge earthquake [Arlekar et al., 1997; Murty, 2004]. Performance of buildings with open ground story in some of the past earthquakes is discussed in the following.

1.2.1 1997 Jabalpur (India) Earthquake

The Jabalpur earthquake of 1997 for the first time illustrated the seismic vulnerability of Indian buildings with soft story. This earthquake, the first one in urban

vicinity in India, provided an opportunity to assess the performance of engineered buildings in the country during ground shaking. The damage incurred by Himgiri and Ajanta apartments in the city of Jabalpur are very good examples of the inherent seismic risk to buildings with soft ground story. Himgiri apartment was an RC frame building with open ground story on one side for parking, and brick infill walls on the other side. The infill portion of the building in the ground story was meant for shops. All the upper stories had brick infill walls. The ground story columns in the parking area were badly damaged including spalling of concrete cover, snapping of lateral ties, buckling of longitudinal reinforcement bars and crushing of core concrete [Fig. 1.3(a)]. The columns on the other side had much lesser level of damage. There was only nominal damage in the upper stories consisting of cracks in the filler walls. This is a clear case of columns damaged because of the soft ground story.

The Ajanta apartment buildings were a set of almost identical four-story RC frame building located side-by-side. In each of these buildings, there were two apartments in each story, except in the ground story. One building had two apartments in the upper stories, but only one apartment in the ground story. The open space on the other side was meant for parking, and hence had no infill walls. Whereas, only nominal damages were reported in the building with two apartments in the ground story, the ground story columns on the open side in the other building were badly damaged. The damage consisted of buckling of longitudinal bars, snapping of ties, spalling of cover, and crushing of core concrete. Another 3-story C-shaped RC frame building (Youth Hostel building) suffered extensive damage to the columns in the stilt story in the form of severe X-type cracking [Fig. 1.3(b)]. Here also, the upper two stories had brick infilled walls. This made the upper stories very stiff as compared to the stilt story. There was no damage

to the columns in the stories above. The soft ground story at the stilt level is clearly the primary reason for such a severe damage [Arlekar et al., 1997].

1.2.2 1998 Adana-Ceyhan (Turkey) Earthquake

During the 1998 Adana-Ceyhan (Turkey) earthquake, the most catastrophic failures were due to discontinuity of vertical elements of the lateral load resisting system. It is common in Turkey to construct multistory buildings with the ground story being left open for parking or storage. In some cases, such areas are enclosed by glass partitioning windows to be used as showrooms. Such relatively flexible stories are subjected to higher stresses under which they may fail with the upper stories usually moving as a unit. The almost vertical collapse of the buildings without considerable lateral movement indicated a very low shear and vertical load carrying capacity of the ground story. Another unique example of the soft story effect was observed in a 6-story building of similar type but having partially soft story; the portion of the building having infill in ground story experienced no damage while the portion with openings resulted in soft story formation and collapsed. In the near proximity, other similar types of buildings with reasonably symmetric geometry and without significant variation in stiffness and strength in plan and in elevation performed well, with only nominal damage, usually in the form of the cracking of brick infill walls [Adalier et al., 2001].

1.2.3 1999 Kocaeli (Turkey) Earthquake

In the 1999 Kocaeli (Turkey) earthquake, a large number of multistory RC framed buildings with masonry infills collapsed. Typically, a story mechanism was formed in the bottom story or in the bottom two stories. In some cases, the obvious reason was soft story effect due to absence of infill walls in bottom story. In many cases, however, a soft story mechanism was observed in structures with a uniform vertical distribution of infills

after the fall out of the infills in the bottom two stories [Fig. 1.4]. In Fig. 1.5, two similar buildings, located within the same complex of buildings, are shown after the earthquake. In one building [Fig. 1.5 (a)], which did not collapse, a concentration of damage in the bottom two stories can be clearly seen. The other building collapsed due to complete failure of the bottom two stories, as shown in Fig. 1.5(b) [Dolsek, 2001].

1.2.4 2001 Bhuj (India) Earthquake

Most of the residential apartment buildings in affected areas had weak RC frames; masonry infills played a crucial role in the survival of many buildings by providing lateral strength and stiffness. A completely infilled RC frame with uniform strength and stiffness sustained almost uniform damage along the height [Fig. 1.6]. A four-story uniformly infilled building in Gandhidham had suffered minor cracking at frame-infill interface [Fig. 1.7]. While its symmetric half, which had open ground story to facilitate parking, completely collapsed along with stair tower in the middle, the site in the foreground was leveled flat after clearing the debris [Murty et al., 2002].

A large number of stilt buildings in Ahmedabad, Bhuj, Gandhidham, and other towns suffered severe damage or catastrophic collapse. Almost all of the buildings that collapsed in Ahmedabad were having open ground story configuration. In many other buildings that did not collapse, the damage was confined to the open ground story columns with only nominal frame infill separation in upper stories [Fig. 1.8]. Many buildings were neither designed for seismic load nor detailed for ductile behavior. Hence, ground columns suffered brittle shear failure as shown in Fig. 1.9 [Murty et al., 2002].

1.2.5 2003 Bingol (Turkey) Earthquake

Most of the damage witnessed in this earthquake was due to the soft story effect, whereby the absence of masonry infills, in order to provide extra space for commercial

enterprises at ground floor, proved detrimental [Fig. 1.10]. Generally the larger the ground floor outlet and the smaller the area of the infills, the heavier was the damage observed. Furthermore, the buildings with ground story height significantly higher than the typical story height, suffered more damage. This was manifested generally in the brittle behavior of the columns, affected by diagonal shear cracks in them. The apartment building shown in Fig. 3.11 lies on gentle sloping ground, at the bottom of a steep hill. It suffered a weak story collapse in the ground floor, where three shops were operating. The underlying basement was undamaged whilst the overlying typical stories had infill damage [Ellul et al., 2003].

1.3 Codal Provision for Stilt Buildings

Generally, for the purpose of structural design, buildings are modeled as bare frame, i.e., strength and stiffness contributions of infill are neglected in analysis and design. As a result, soft story effect is not captured. Indian seismic code IS:1893 addressed this serious issue by including a clause on stilt buildings in the last revision in 2002. This clause suggests performing nonlinear dynamic analysis including strength and stiffness contribution of infill and members should be designed accordingly. Instead of nonlinear dynamic analysis, nonlinear static analysis is preferable, as it needs less computational effort while it works well if inelastic properties of all the members including infill are modeled accurately [Jain et al., 2004]. Alternatively, code recommends designing open ground story columns and beams for 2.5 times story shears and moments calculated as in bare frame (the code is silent about axial force). As another alternative, it permits designing columns and beams as usual provided shear walls are placed symmetrically in both directions and designed exclusively for 1.5 times lateral story shear calculated as in bare frame [IS: 1983, 2002].

1.4 Previous Studies on Stilt Buildings

For the sake of brevity henceforth in this document, buildings with no infill, with infills in all the stories of the frame, and those with infills only in the upper stories will be referred as “bare”, “infill”, and “stilt” frame, respectively. A large number of experimental and analytical researches have been carried out to understand the effect of infill on seismic behavior of RC buildings. However, research work exclusively on stilt buildings is limited.

Linear analysis of a four-story building with 4.4 m ground story height and 3.2 m height in upper stories having symmetrical plan was performed in ETABS [Arlekar et al., 1997]. The stiffness irregularity in stilt building model was evident from the fact that the ground story stiffness was only 5% of the first story stiffness. However, in bare and infill buildings, ground story stiffness was about 50% of the first story stiffness. The lateral deformation profile of bare and infill buildings were smooth, while that of stilt had abrupt slope change at first floor level, i.e., most of the total displacement was contributed by the ground story. The fundamental natural period of bare, stilt, and infill frames in transverse direction was 0.64 s, 0.43 s, and 0.18 s, respectively, while it was 0.42 s as per codal formula. Bending moments and shear forces reduced significantly due to presence of infill in upper stories of stilt frame and all stories of infill frame. The bending moment and shear force demands were severely higher for ground story columns in case of the stilt building.

A study was conducted to evaluate the effect of vertical structural irregularity on seismic performance of 5, 10, and 20 story plane frames [Valmundsson et al., 1997]. The frames were designed for moderate seismic zone according to UBC requirements. The frames were designed and detailed for ductility levels for 2, 6, and 10. The ductility

demand in the ground story increases noticeably as the strength and stiffness of that story is reduced. For a design ductility of 2 and a 30% decrease in strength and stiffness of the ground story, the increase in the ground story ductility demand was 80% for 5-story structures, 130% for 10-story structures, and more than 200% for 20-story structures. The increase in ductility demand is generally less for a design ductility of 6 and 10.

The overstrength and ductility were investigated for three-bay RC plane frames of 3, 6, and 10 stories using nonlinear pushover analysis [Balendra et al., 1999]. These frames were designed to resist gravity loads, wind loads, and a notional horizontal load in accordance with the British code BS 8110. The study showed that the overstrength decreases for bare frame as the number of stories increases. The ductility of bare frame was found to be slightly more than 2.0 in all frames (3, 6, and 10-story). Infill was modeled as bi-diagonal struts. Struts width was as per Mainstone formula and stress-strain curve for concrete masonry given by Priestley and Elder was adopted. The infill walls have increased the lateral strengths of 3, 6, and 10 story frames to 12.5, 14.5, and 15.4 percent of the seismic gravity loads from 11.3, 8.3, and 4.9 percent, respectively. The ductility factors for 3, 6, and 10-story stilt frame are 1.89, 1.47, and 1.01. This shows that ductility of stilt frames are lesser than that of bare frames.

A four-story RC frame structure was selected as a test example to represent a contemporary earthquake resistant building [Dolsek, 2001]. Story height was 3.5 m in the ground story and 3.0 m in the upper three stories. The bare frame structure was designed according to Eurocode 8, as a high ductility class structure. It was designed for 0.3g peak ground acceleration, which results in a base shear coefficient of 0.15. The lateral strength of bare frame is about 30-35% of its total weight. Pushover analysis shows a global beam-hinge mechanism formation over the bottom three stories. In the uniformly infilled

structure, both stiffness and strength were much higher. However, with increasing deformation, the infills failed, and base shear decreased. A hinge mechanism was formed in the ground story at a relatively large deformation, similar to the deformation of the bare frame. In the bare frame, damage was limited and more or less uniformly distributed. The presence of infill changed the response of the structure significantly. In the case of the stilt frame, a concentration of drift was observed in the ground story. In the uniformly distributed infill frame, both story drift and roof displacement was much reduced. The test led to the complete destruction of infill in the lower two stories, severe damage of infill in second story and almost no damage in top story.

A six-story three-bay framed structures with no infill, i.e., bare frame (BFR) and infill other than bottom story, i.e., stilt frame (PIF) were designed to satisfy the seismic requirements for ductility class “Medium” in accordance with EC8 (EC8-1994 which is changed now significantly), with design peak ground acceleration (PGA) of 0.30g [Lu, 2002]. EC8 adopts the concept of the behavior factor, q , to factor down the elastic spectrum for the determination of the seismic design lateral load. The value of the q factor is determined according to the ductility class chosen, taking into account the structure type and the irregularities involved. Specific detailing requirements are stipulated to satisfy the respective ductility demand. In the case of stilt frame, the contribution of infill walls is not considered in the final strength design but it is accounted for when evaluating the regularity index and determining the design seismic load. A general countermeasure in dealing with all vertical irregularities, as explicitly prescribed in EC8 is a reduction of the design q factor (thus an increase in the design base shear). The reduction coefficient is taken as a function of the regularity index, which is defined as the ratio of the minimum story-shear overstrength factor to the average. The

story-shear overstrength factor is calculated as the ratio of available story-shear strength (taking into account all vertical members including infills in the story) and design story shear force. A minimum regularity index of 0.55 is imposed. In fact, it was the minimum requirement that actually governed the proportioning of the open ground story columns in frame PIF and as a result, its ground story columns size was larger than that of frame BFR. The final design q factors were 3.5 for BFR and 2.4 for PIF. The proportioning of the structural members was carried out following capacity design procedures for a weak-beam, strong column design and to avoid premature shear failure. For the experiment, reduced scale (1:5.5) models were constructed and tested under the same scheme of simulated earthquakes on an earthquake simulator. Frame BFR exhibited a uniformly distributed cracking pattern. The severe damage at the fifth story is attributable to the abrupt reduction (over 20%) of the column cross section size and the subsequently intensified higher mode whipping effects. Its response remained stable, however, cracking widened substantially, indicating extensive yielding, while spalling of concrete occurred in the lower stories. In frame PIF, the enlarged ground story columns appeared to be effective in preventing what would usually be anticipated a soft story mechanism. Instead, the cracking spread into the beam column members as well as the masonry walls throughout the frame.

A five-story building with 3.0 m typical story height having symmetrical plan was designed for zone V as per Indian seismic codes [Kanitkar et al., 2004]. The stilt building was designed as per the code provision of 2.5 times and the bare and the stilt, both frames were detailed as per ductile detailing code IS:13920-1993. Then inelastic analysis of the bare and the stilt buildings were performed. The bare frame exhibited good hysteretic behavior with almost no decrease in lateral capacity even at high displacement levels.

While the stilt frame lateral capacity decreased in successive cycles. Its initial stiffness and lateral strength was much larger than that of the bare frame. The rapid drop in lateral strength could be attributed to the fact that the inelastic deformation was confined to open story columns. In the bare frame, the inelasticity propagated into the upper stories due to redistribution of the load within the structure. This did not happened in the stilt frame and consequently, lateral strength decreased in successive cycles. The lateral strength of the bare and the stilt frame were approximately equal to $1.0V_B$ (V_B is design base shear) and $2.4V_B$, respectively. Although a scale factor of 2.5 is specified for moments and shear in the open story members, the current provisions do not account for increase in column axial forces, which could compromise flexural capacity.

1.5 Scope and Research Objectives

In the present study, two simple frames are studied. Initially, the frames are designed as bare frame for only gravity loads (dead and imposed load) to simulate old buildings, not designed for earthquake load. Infill is incorporated by modeling it as diagonal compression strut. Pushover analysis is performed on bare, stilt, and infill frames using a structural analysis program 'SAP2000 NonLinear'. The initial stiffness, lateral strength, maximum roof displacement, hinge mechanism, etc. of bare, stilt, and infill frames are compared. The frames are also redesigned as bare frames without considering soft story effect for different earthquake load level for zones II, III, and V as per IS:1893-2002. Seismic performance of all three frames namely bare, stilt, and infill is compared separately for different design cases. Variation in strength, stiffness, and hinge mechanism for the frames designed for different zones is discussed. The ground story columns of both frames designed for zone III are redesigned for 2.5 times moment, story shear, and axial force in the view of soft story effect. In another case, the ground story

columns, and beams, both are redesigned for 2.5 times forces as per requirements of IS:1893-2002. In the light of above study, the provisions of Indian seismic code for stilt buildings are reviewed.

1.6 Organization of Thesis

The contents of thesis are divided into five chapters. Chapter 1 discussed the stilt buildings, their performance in the past earthquakes, codal provisions on stilt buildings, previous researches on stilt buildings, and states research objectives and its scope. Chapter 2 describes the considered buildings, material properties used, analysis-design procedures, and design cases. The modeling procedure in 'SAP2000 NonLinear' for nonlinear static pushover analysis of the moment resisting RC frames with unreinforced brick masonry infill is described in Chapter 3. Chapter 4 discusses the results of pushover analyses for different design cases. Chapter 5 includes summary and conclusions of the work.

Chapter 2

Analysis and Design

2.0 General

In many countries, including India, reinforced concrete (RC) framed buildings with masonry infill panels are analyzed and designed as bare frames, neglecting the strength and stiffness contributions of the infill. However, weight of infill is considered in load calculations. This chapter describes the considered frames, their modeling procedure for analysis and design, and design cases. A structural analysis software package “SAP2000 NonLinear” [CSI, 1999] has been used for analysis.

2.1 Details of the Considered Frames

Two typical residential buildings have been chosen in this study from which one two-dimensional frame has been considered and named as frame-A and frame-B, respectively. Gravity loads on frame-A and frame-B are shown in Fig. 2.1 to Fig. 2.4. Frame-A has 3 stories and height of each story and bay width are 3.0 m and 4.0 m, respectively. On the other hand, frame-B with bay width 3.5 m has 5 stories and its height in bottom story is 4.2 m, while in upper stories it is 3.0 m.

Thickness of infill wall is 230 mm in both frames. Dead load of infill is applied on beams as uniformly distributed load at which it is resting. However, in seismic weight calculations, half of the weight of infill is lumped at the floor above and half at the floor below. Self-weight of beams and columns are calculated from its cross-section area and unit weight of concrete. Vertical distribution of design base shear as per IS:1893 is shown in Fig. 2.5 and 2.6 and values are given in Table 2.1 and 2.2. While procedure to calculate the design base shear is discussed in section 2.4.

2.2 Material Properties of Members

Material properties of the members are required to model the stiffness and the strength of the members. The grade of concrete used is M20; and that of longitudinal and shear reinforcement used is Fe415. When frame-B is designed for only gravity load case, grade of shear reinforcement used is Fe250, while grade of concrete is M15. The Young's modulus of elasticity (E_c) of concrete in MPa is calculated by the empirical relation given in IS 456:2000 as

$$E_c = 5000 \sqrt{f_{ck}} \quad (2.1)$$

where f_{ck} is 28-days characteristic cube strength of concrete in MPa. The Young's modulus of elasticity of steel is taken as 2.0×10^5 MPa. The Poisson's ratio and unit weight of concrete are taken as 0.2 and 25 kN/m^3 , respectively.

2.3 Modeling of Members

The beams and columns are modeled as frame element. The constraints are assigned at floor levels so that lateral displacement of each node at same floor level is equal. The columns are assumed to be fixed at their base. The centre line dimension of the actual structure is used to create the analytical model. End offset is considered as semi rigid to incorporate finite size of joint as suggested by Mondal (2003). The effect of geometric nonlinearity (P- Δ effect) is considered for all loads, which may be considerable where columns are long.

2.4 Analysis of the Frames

The following load combinations are considered in the analysis according to IS:1893-2002.

$$\begin{aligned}
& 1.5(DL+IL) \\
& 1.2(DL+IL\pm EL) \\
& 1.5(DL\pm EL) \\
& 0.9DL\pm 1.5EL
\end{aligned} \tag{2.2}$$

In the above equations, DL is self-weight of beams, columns, slab, floor finishing, and infill; and IL is imposed load. As per IS:1893-2002, the design base shear V_B on the frame is given by,

$$V_B = WA_h \tag{2.3}$$

where W is the seismic weight of the frame, which is calculated as full DL plus 25% of IL if IL is less than 3 kN/m^3 , else 50% of IL . A_h is the design horizontal seismic coefficient, which is calculated as below.

$$A_h = \left(\frac{Z}{2} \right) \left(\frac{S_a}{g} \right) \left(\frac{I}{R} \right) \tag{2.4}$$

In above equation Z is seismic zone factor, which is 0.10, 0.16, and 0.36 for zone II, III, and V, respectively. I is importance factor taken as 1.0 for residential building; R is the response reduction factor taken as 5.0 for special RC MRFs when detailed as per IS:13920. S_a/g is obtained from design acceleration response spectrum for corresponding natural period of building. Soil type is taken as medium and the value of damping for building is assumed 5% of the critical. S_a/g on medium soil site is given as below.

$$\frac{S_a}{g} = \begin{cases} 1+15T & 0.00 \leq T \leq 0.10 \\ 2.5 & 0.10 \leq T \leq 0.55 \\ 1.36/T & 0.55 \leq T \leq 4.00 \end{cases} \tag{2.5}$$

The approximate fundamental natural period of vibration of MRF buildings with masonry infill is estimated as,

$$T = \frac{0.09h}{\sqrt{d}} \quad (2.6)$$

where T is the fundamental period in seconds, h is height of the building in meter and d is base dimension of the building along the applied earthquake load direction in meter. The design base shear (V_B) is distributed along the height of the building as per the following expression;

$$H_i = V_B \frac{W_i h_i^2}{\sum_{j=1}^n W_j h_j^2} \quad (2.7)$$

where H_i is lateral force at floor i , W_i is seismic weight of floor i , h_i is height of floor i , measured from base, and n is number of stories.

2.5 Design Cases

Both frames are designed as per IS:456-2000 limit state design procedures. Frames are detailed as per IS:13920-1993 in all cases in which earthquake loads are considered including in zone II. On the other hand, frames detailed as per IS:456-2000 in cases in where these are designed for only gravity load.

Frame-A serves larger area and its seismic weight is 2400 kN while frame-B has 1500 kN. The approximate fundamental natural periods of frame-A and frame-B calculated as per IS:1893-2002 are 0.41 s and 0.55 s respectively. The fundamental natural periods of vibration of both frames lie between 0.10-0.55 story; therefore, S_a/g is 2.5 for both the frames. Consequently, the design base shear coefficient for both the frames for a particular zone is same and its value for zone II, III, and V is 0.025, 0.04, and 0.09, respectively. Design base shears are distributed vertically as per Equation 2.7 and values are given in Table 2.1 and 2.2. The frames have been designed for following cases:

(i) **GRAV:** In this case, frames have been designed for only gravity load (DL and IL), and no earthquake load has been considered. This case is to simulate non-seismically designed older buildings in order to envisage seismic performance of such buildings. Therefore, it is analyzed for only one combination, i.e., $1.5(DL+IL)$ and detailed as per IS:456-2000.

(ii) **EQ2:** In this case, frames have been designed for DL , IL , and EL for zone II. The design base shear is 2.5% of seismic weight, which is 60 kN and 37.5 kN for frame-A and frame-B, respectively. Detailing is done as per IS:13920-1993.

(iii) **EQ3:** In this case, frames have been designed for DL , IL , and EL for zone III. The design base shear is 4% of seismic weight, which is 96 kN and 60 kN for frame-A and frame-B, respectively. Detailing is done as per IS:13920-1993.

(iv) **EQ5:** In this case, frames have been designed for DL , IL , and EL for zone V. The design base shear is 9% of seismic weight, which is 216 kN and 135 kN for frame-A and frame-B, respectively. Detailing is done as per IS:13920-1993.

(v) **EQC3:** These frames are designed for zone III. Further, the ground story columns of stilt frame have been designed for 2.5 times the bending moment, shear force, and axial force values coming from bare frame analysis. Detailing is done as per IS:13920-1993.

(vi) **EQCB3:** These frames are designed for zone III. Following the IS:1893-2002 provisions for stilt buildings, the ground story columns and first floor beams are designed for 2.5 times the bending moment, shear force, and axial force values coming from bare frame analysis. Detailing is done as per IS:13920-1993.

Reinforcement details are given in Table 2.3 to 2.6 and shown in the Fig. 2.6 to 2.18. Reinforcement details given in tables or shown in the figures are for near the

support regions, as plastic hinge will be introduced in these regions only. For simplifying the analysis and designs, the section size and reinforcement are kept same in all stories.

Chapter 3

Nonlinear Pushover Analysis

3.0 General

The buildings are not made earthquake-proof due to high cost and very less probability of occurrence of strong shaking during the service life of the building. Rather the buildings are made earthquake-resistant to ensure the safety of occupants and contents. Thus, buildings are allowed to be damaged during earthquakes. The earthquake-resistant design philosophy is that the structural members should not be damaged under minor shaking; however, repairable and even irreparable damage is allowed in moderate and strong shaking, respectively. In other words, earthquake-resistant buildings are designed for a lower level of seismic force and members are allowed to deform inelastically under severe ground shaking. Therefore, a nonlinear analysis is essential to understand seismic performance of the building.

Nonlinear dynamic analysis is more appropriate than static nonlinear analysis, as structures are subjected to dynamic loading during ground shaking. Dynamic analysis is quite sensitive to the characteristics of the input motions, thus the selection of suitable representative acceleration time-history is mandatory. As a result, dynamic nonlinear analysis needs very high computational efforts. However, static nonlinear analysis that is also known as “pushover analysis” is a simple option to trace the sequence of yielding and failure of the members and estimate the lateral strength of the building. Nonlinear static analysis is suitable for practical design applications as well as adequate to envisage the seismic behavior of a building. Hence, a nonlinear static pushover analysis has become popular in recent years to determine parameters such as initial stiffness, yield strength, yield displacement, maximum base shear, and maximum displacement.

In pushover analysis, the nonlinear load-deformation characteristics of individual members are modeled and predefined lateral load pattern is applied along the building height. The lateral forces are then monotonically increased in constant proportion with displacement control at the top of the building until a certain level of deformation is reached. Response of structure beyond maximum strength can be determined only by displacement-controlled analysis. Hence, in the present study, displacement-controlled pushover method is used for analysis of infilled RC frames. A structural analysis software package "SAP2000 NonLinear" [CSI, 1999] has been used for this purpose. A typical pushover curve of infilled RC frame is shown in Fig. 3.1.

3.1 Material Properties of Infill

Much variation is found in material properties of brick masonry due to associated uncertainties in clay type from which it is made, level of heating undergone during burning, grade of mortar, etc. Material properties of brick masonry manufactured in India were surveyed in available literature and taken as describe below.

Compressive strength of brick masonry is taken as 5 MPa and Poisson's ratio 0.2. The unit weight of masonry is assumed as 20 kN/m³. Maximum compressive strain in the infill panel ϵ_m is taken as 0.0053 as reported by Choubey [Choubey, 1990]. The coefficient of friction between frame and infill panel μ_f is taken as 0.45 [Saneinejad et al., 1995]. The Indian masonry code [IS:1905, 1987] recommends that the permissible shear of masonry walls resisting in-plane horizontal forces will be calculated on the area of the bed joint as per following expression

$$f_s = 0.1 + \frac{f_d}{6} \leq 0.5 \text{ MPa} \quad (3.1)$$

where f_s is the permissible shear stress of the masonry (MPa) and f_d is the compressive stress due to dead loads (MPa). Although this recommendation is for masonry structures,

but it is used in this study also as there is no exclusive provision for masonry used as filler in RC frames. In this study, f_d is calculated as half of the self-weight of infill panel divided by area of bed joint, while the other loads are assumed to be taken by frame. Shear failure may occur at any height in the panel. Although it is assumed to fail at mid height and half of self-weight of infill panel is considered. The ultimate shear stress of masonry is taken as 2.5 times the permissible shear stress. The same value is suggested by Hatziniklas (2000).

Several empirical relationships are available in the literature to estimate modulus of elasticity of masonry. Grimm (1984) conducted a series of experiments for different types of masonry units and different mixes for mortar. His results show a large scatter. As per Dayaratnam (1987), elastic modulus of brick masonry in MPa may be taken as

$$E_m = 4000\sqrt{f'_m} \quad (3.2)$$

where f'_m is the compressive strength of brick masonry in MPa. Paulay et al. (1992) have recommended another expression

$$E_m = 750 f'_m \quad (3.3)$$

Drysdale et al. (1993) have recommended that modulus of elasticity of brick masonry should be calculated as

$$E_m = k f'_m \quad (3.4)$$

where k lies between 500-600. FEMA-273 and proposed draft code IS:1905 (Rai, 2004) recommends value of k as 550, which is used for the modeling of stiffness of the infilled frames in this study.

3.2 Modeling of Infills for Stiffness

Stiffness of an infilled frame is very high until the boundary separation of infill occurs at the tension diagonal corners. The initial stiffness of the infilled frames may be

10 to 80 times that of the bare frame due to presence of infill [Bertero et al., 1983; Moghaddam et al., 1987]. The separation between the infill panel and the confining frame depends upon their relative stiffness. As boundary separation occurs, only the portion of infill panel in contact with the confining frame takes part in the transfer of applied load. At this stage, the stiffness of the infill frame degrades and it is about 5 to 10 times that of the bare frame [Moghaddam et al., 1987]. This stiffness remains constant up to the appearance of diagonal cracking in the infill panel. After full diagonal cracking of the infill panel, it loses its stiffness and the stiffness of the infill frame depends only on that of the confining frame [as reported by Kumar, 2002].

Several macro models have been proposed to define stiffness of the infilled frames. However, single diagonal strut model is popular as compared to multi-diagonal model due to its simplicity. Infill panel is modeled as single diagonal strut connected between two compressive diagonal corners. The diagonal strut is assumed to be connected to the frame through pin connections at both ends. The modeling of infill panel as single diagonal strut is based on the assumption that the masonry is very weak in tension and the bond strength at the panel-frame interface is very low. The length of a diagonal strut is slightly longer than the actual diagonal length of the panel because of centre line modeling of frame. However, this difference is insignificant in most of the cases. The area of cross-section of the diagonal strut is a function of the width of the strut, as thickness of the strut is taken equal to that of the infill panel. The accuracy in estimation of stiffness of infilled frame very much depends upon the assumed width of strut. In this study, empirical relation proposed by Holmes (1961) is used for calculating the width of the strut. Its suitability is supported by Mondal (2003). Mondal (2003) compared the stiffness calculated by modeling infill as single diagonal strut using different width formulae with FEM analysis results. He found that Holmes width formula

is most accurate in case of infill panel with opening. Holmes empirical relation for calculating the width of the strut (w) is given below:

$$w = \frac{d}{3} \quad (3.5)$$

where d is the diagonal length of the infill panel (not the length of strut).

3.3 Modeling of Infills for Strength and Deformation

An infill panel strengthens the frame structure in both lateral and vertical directions. For studying the overall seismic response of a building, only the in-plane lateral strength of the infill panels is of interest. The lateral strength of the infilled frame depends upon the strength of the infill panel and the confining frame. The modes of failures depend upon the materials used in the infill panel and the frame. For a strong-frame weak-infill structure, generally used in the construction of seismic resistant buildings, the failure takes place in masonry panel first and the possible modes of failures in masonry panel can be classified as (a) bond shear failure, (b) diagonal tension failure, and (c) compression failure. In case of weak-frame strong-infill, shear failure in the columns, or flexural failure in beams or columns takes place first followed by corner crushing of infill panels [Liauw et al., 1983].

The properties required to define the strut model depend on the type of analysis (linear elastic versus non-linear) and on the type of loading (monotonic, cyclic or dynamic). For linear elastic analysis, only the area and length of diagonal strut and the modulus of elasticity are required whereas the force-displacement relationship of the material is also required for non-linear static analysis, and for non-linear dynamic analysis, hysteretic behavior of material needs to be specified.

The strength of an infill panel depends on the mortar strength, compressive strength of bricks, and bond between these two materials. It also depends on the aspect

ratio of the panel and the contact length between the infill panel and the confining frame. In modeling, the strength properties of the infill panel are defined in terms of diagonal compressive stress-strain relationship or in terms of diagonal strength-deformation relationship. The strength-deformation curve requires the strength and deformation capacity of the infill panel at various stages such as at boundary separation stage, at initial cracking stage, and at fully cracked stage. The strength-deformation relation of infill panel given by Reinhorn et al. (1995) is used in this study.

The strength-deformation criterion proposed by Reinhorn et al. (1995) is based on experimental and analytical studies; they developed a hysteretic model (Fig. 3.2) to describe the lateral strength-deformation relationship of masonry infill panel. The maximum lateral load required for complete crushing of infill panel and maximum deformation of infill panel are given as

$$H_m = A_d f'_m \cos \theta \leq \begin{cases} \frac{\tau_s t l'}{(1 - 0.45 \tan \theta')} \\ 0.83 \gamma_l t l' \end{cases} \quad (3.6)$$

$$u_m = \frac{\varepsilon_m L_d}{\cos \theta} \quad (3.7)$$

where l' and h' are length and height of masonry panel, respectively; θ is $\tan^{-1}(h'/l')$; A_d and L_d are the cross-sectional area of diagonal strut and effective length of diagonal band respectively, which depends upon the length of contact between the infill panel and the surrounding frame; τ_s is $2.5f_s$ and f_s is basic shear strength of masonry that is calculated by Equation 3.1; ε_m is the maximum strain in the infill panel; γ_l is load factor for shear strength of masonry, which is taken equal to 1.5 in the present study; and θ' is sloping angle of masonry diagonal strut at shear failure. The procedure for calculation of A_d , L_d ,

and θ' are given by Saneinejad et al. (1995). They also defined the initial stiffness of infill panel (K_i) and related to the lateral yield force (H_y) and lateral yield displacement (u_y) for the infill panel as

$$K_i = 2 H_m / u_m \quad (3.8)$$

$$H_y = (H_m - \kappa K_i u_m) / (1 - \kappa) \quad (3.9)$$

$$u_y = H_y / K_i \quad (3.10)$$

where κ is the stiffness degradation ratio, which is taken equal to 0.1. Based on these expressions, the idealized axial force-deformation curve for infill panel [Das, 2000] is shown in Fig. 3.3. The yield force (P_y), maximum force (P_m), yield displacement (δ_y) and maximum displacement (δ_m) for axial force-deformation relationship of the diagonal strut are defined by

$$\left. \begin{aligned} P_y &= H_y / \cos \theta \\ P_m &= H_m / \cos \theta \\ \delta_y &= u_y \cos \theta \\ \delta_m &= u_m \cos \theta \end{aligned} \right\} \quad (3.11)$$

Strut hinge properties are calculated using computer program developed by Dasgupta [Dasgupta, 2000], which is based on Reinhorn et al. (1995) and Saneinejad et al. (1995).

3.4 Hinge Properties of Members

One of the essential requirements for nonlinear analysis is to define the hinge properties for each member. These properties are flexural, shear, and axial capacity of the members in the nonlinear region. A member may have more than one hinges at one location; and one member may have hinges at more than one locations. The hinge properties are defined in terms of moment-rotation ($M-\theta$) curve, axial force-moment interaction ($P-M$) curve, and shear force-shear deformation $V-\delta$ curve. $M-\theta$ curve for

beams and columns are obtained using computer program PM_INT [Dasgupta, 2000]. The program uses the stress-strain model for confined concrete as per Razvi et al. (1999) (Fig. 3.4). For the stress-strain curve for HYSD bars, the program assumes the ultimate stress as 1.25 times yield stress and ultimate strain as 14.5% (Fig. 3.5). The idealized curve for moment-rotation relationship for frame members is shown in Fig. 3.6 and that for axial force-moment interaction relationship for columns is shown in Fig. 3.7. Flexural and axial hinge properties of frame-A and frame-B are listed in Table 3.1 to Table 3.6. In idealized moment rotation curve (Fig. 3.6), residual strength after reaching ultimate moment is taken as 20% of yield moment and θ_{max} is taken as $1.5\theta_u$.

The shear strength capacity of beams and columns is taken as per the recommendations of ATC-40 and FEMA-273. The ultimate shear capacity of frame members is given by

$$V_u = V_s + V_c \quad (3.12)$$

where V_s and V_c are the shear strength capacity of reinforcing bars and concrete respectively, which are calculated for normal-weight aggregate concrete in the regions of low ductility as

$$V_s = A_{sh} f_{yh} \frac{d}{0.6s} \quad (3.13)$$

$$V_c = 3.5 b_w d \left(1 + \frac{P_u}{2000 A_g} \right) \sqrt{0.8 f_{ck}} \quad (3.14)$$

where P_u is the axial compressive force in the member which can be neglected in case of beams; A_{sh} and f_{yh} are the area of cross-section and yield strength of the shear reinforcement, respectively; A_g is the gross sectional area of the member; b_w and d are the width of web and effective depth of the member, respectively; and s is the spacing of

shear stirrups. The ultimate shear deformation of frame members to define V - δ relation for frame members is given by

$$\delta_u = \frac{V_u}{G_c (A_g / L)} \quad (3.15)$$

where L is the length of the member and G_c is the shear modulus of rigidity, defined as

$$G_c = \frac{E_c}{2(1 + \nu_c)} \quad (3.16)$$

where E_c and ν_c are the Young's modulus of elasticity and Poisson's ratio for concrete, respectively. The V - δ relation for frame member can be idealized using Table 6.7 of FEMA-273 (Fig. 3.8). δ_m is taken as four times of δ_u .

Shear hinge is not formed in the models of this study when beams and columns are detailed as per ductile detailing code IS:13920. It is verified by performing pushover analysis after assigning shear hinges in frame-A, designed for zone II and detailed as per IS:13920. Therefore, to save computational efforts, shear hinges are assigned in frame-A and frame-B in design case GRAV only, wherein frames are designed for gravity loads only and detailed as per IS:456. Shear hinge properties of frame-A and frame-B of GRAV design case are listed in Table 3.9 and Table 3.10.

3.5 Location of Plastic Hinges

Lateral loading generally leads to hinge formation near the end of a frame member. However, inelastic deformations may occur at other locations, especially when large gravity loads are present. Several experiments indicate that hinges in the frame members form near the joints and not exactly at the joint. It is assumed that these plastic hinges in the frame members form at a distance equal to half the average plastic hinge

length l_p , from the member ends. The plastic hinge length is calculated using Baker's formula [Park and Pauley, 1975]:

$$l_p = 0.8k_1k_3\left(\frac{z}{d}\right)c \quad (3.17)$$

Where z is the distance of critical section to the point of contraflexure, c is the neutral axis depth at the ultimate moment; d is effective depth of the section; k_1 is taken as 0.7 for mild steel and 0.9 for HYSD steel; and k_3 is given by

$$k_3 = \begin{cases} 0.6 & f_{ck} \geq 44 \text{ MPa} \\ 0.6 + 0.01(44 - f_{ck}) & 44 \text{ MPa} < f_{ck} < 14.6 \text{ MPa} \\ 0.9 & f_{ck} \leq 14.6 \text{ MPa} \end{cases} \quad (3.18)$$

where f_{ck} is 28-days characteristic cube strength of concrete. l_p for beams and columns are obtained using computer program PM_INT [Dasgupta, 2000], which also gives $M-\theta$ curve. The locations and type of the plastic hinges in the various members of an infilled frame are shown (Fig. 3.9). Plastic hinge in beam is assigned at a distance of l_{beam} from centre line dimension and it is calculated as

$$l_{beam} = 0.5(l_p + D_{column}) \quad (3.19)$$

In columns, plastic hinge is assigned at a distance of l_{column} from centre line dimension and it is calculated as

$$l_{column} = 0.5(l_p + D_{beam}) \quad (3.20)$$

where l_p is plastic hinge length calculated as per Equation 3.18 for beams and columns, D_{column} and D_{beam} are depth of column and beam, respectively.

3.6 Loads and Load Combinations

Nonlinear static pushover analysis is done under displacement-controlled arrangement, in which target displacement is assigned generally in term of roof

displacement. Lateral loads on the models are applied at each floor levels in the ratio of that applied at the roof level. In displacement-controlled pushover analysis, the ratio in which the loads are applied at floor levels alters the response of structures. In this study, inverted triangular lateral load pattern is applied. These lateral loads are applied at beam-column joints at each floor level with the combinations of gravity loads. During the earthquake, dead load is acting on the frame and imposed load may or may not be present fully. Therefore, lateral loads are applied in combination with full dead load plus 25% imposed load in this study.

3.7 Pushover Analysis and Pushover Curve

After assigning all properties of the models, the displacement-controlled pushover analyses of the models are carried out. The models are pushed in monotonically increasing order until target displacement is reached or structure loses equilibrium; whichever occurs first. For this purpose, target displacement at roof level and number of steps in which this displacement must be applied, are defined. In this study, target displacement is taken as 4% of building height. The global response of structure at each displacement level is obtained in terms of the base shear versus roof displacement. The parameters useful for design purpose such as axial force, shear force, moments, deflection, etc., for any member can be obtained by this analysis. Pushover curve is a base shear force versus roof displacement curve. The peak of this curve represents maximum lateral load carrying capacity of the structure; the initial stiffness of the structure is obtained from the tangent at pushover curve at zero load level. The collapse is assumed when structure loses its 75% strength and corresponding roof displacement is called "maximum roof displacement".

Chapter 4

Results and Discussions

4.0 General

The two RC frames are designed for different seismic zones and pushover analysis is performed for bare, stilt, and infill frames as per the procedures described in the previous chapter. The base shear versus roof displacement, termed as pushover curve, is obtained for all these cases. Also the pushover curve is obtained for stilt frames, wherein ground story is designed for higher forces to assess the efficacy of provisions of IS:1893-2002. The effect of infill walls, modeled as single diagonal strut, on the seismic response of the frames is studied through different response quantities particularly lateral strength, lateral stiffness (hereafter referred as strength and stiffness, respectively), and maximum roof displacement. Sequence of formation of hinge mechanism is observed in frames designed for different zones. Strength of frames is expressed as a percentage of corresponding seismic weights (%W) while roof displacement is expressed in terms of percentage of the respective frame height (%H). When any hinge is in strain hardening region, it will be described as yielding (shown in figures as solid circles) and just after ultimate moment/force, it will be assumed to have failed (shown in figures as rings).

The behavior of 3-story frame-A and 5-story frame-B are generally different in all the design cases. The ground story height of frame-B is 4.2 m whereas height of all upper stories is 3.0 m. Therefore, ground story of frame-B is flexible compare to the upper stories, as column size is same in all stories. On the other hand, height of each story is 3.0 m in frame-A. Overstrength factor is calculated as ratio of maximum strength to design base shear (when designed for earthquake load also), and values are tabulated in Table 4.5. Column-overstrength factor (COF) is defined here as ratio of flexural strength of column and minimum (out of sagging and hogging) flexural strength of beam.

Column-overstrength factor of both frames are give in Table 4.5, where M_{yc} and M_{yb} are yield moments of column and beam, respectively.

4.1 Design Case GRAV

In this design case, frames are designed for only gravity loads, i.e., dead loads plus imposed loads, and detailed as per IS:456 (ordinary detailing). Pushover curves of frame-A and frame-B are shown in Fig. 4.1 and Fig. 4.2, respectively, while locations of hinges at failure are shown in the Fig. 4.17 and Fig. 4.18.

4.1.1 Bare Frames

The strength of frame-A and frame-B are 6.9%W and 9.1%W, respectively while their stiffnesses are 5.2 and 3.5 kN/mm in the same order. Maximum roof displacements reached before collapse, are 1.73%H and 1.16%H, respectively. Their ductility is about 5. In frame-A, all the beams yield first before the yielding starts in ground story columns at a roof displacement of 0.54%H. However, frame collapsed due to failure of ground story columns as being less ductile compare to beams (Table 3.1 and Table 3.3). Upper two story columns are intact [Fig. 4.17(a)]. In frame-B, after the hinge formation in the beams of first and second floors, yielding occurs at the base of ground story columns at 0.33%H roof displacement. Yielding spreads in upper floor beams also except at the roof. Hinges form in first story columns also. The frame collapsed due to failure of first floor beams [Fig. 4.18(a)].

4.1.2 Stilt Frames

The strength of frame-A and frame-B are 15.2%W and 14.9%W, respectively whereas their stiffnesses are 21.5 and 9.6 kN/mm, respectively. Maximum roof displacements reached before collapse, are 0.95%H and 0.64%H, respectively. Their ductility are 5.1 and 4.4, respectively. In frame-A, yielding initiates in first story strut then soon ground story column and first floor beam yield at a very low roof displacement

of 0.18%H. The first story strut fails at 0.56%H roof displacement and then yielding propagates in third story. The ground story columns fail at a roof displacement of 0.94%H, and frame collapses thereafter due to failure of ground story columns [Fig. 4.17(b)]. About half of the total drift occurs in ground story at collapse. Top story beam and columns are intact. In frame-B, yielding initiates at the base of ground story columns at a roof displacement of 0.12%H. All columns other than ground story and all beams except first floor are intact and the frame collapsed due to failure of ground story columns [Fig. 4.18(b)]. Ground story drift is 82% of roof displacement at collapse i.e. a major part of total deformation is concentrated in the ground story and therefore, inelastic deformation is mainly confined to this story.

4.1.3 Infill Frames

The strength of frame-A and frame-B are 21.3%W and 49.0%W, respectively; maximum roof displacements reached before collapse are 1.05%H and 0.67%H correspondingly. Their stiffnesses are 41.6 and 27.2 kN/mm, respectively and ductility are 7.7 and 4.0, respectively. In frame-A, yielding starts from ground story strut and gradually spreads in upper story struts, then first floor beam yields. The ground story columns yield at their base at a roof displacement of 0.35%H whereas second floor beam at 0.48%H. At a roof displacement of 0.62%H, struts of the bottom two stories failed and subsequently yielding occurs in second story columns. The frame collapses at a roof displacement of 1.05%H due to failure of ground story columns while top story beam and columns are undamaged [Fig. 4.17(c)]. In frame-B, a few of the bottom two stories struts yield first, and then ground story exterior column yields at 0.14%H roof displacement. At 0.36%H roof displacement, yielding propagates in ground story interior column, beams of bottom two floors and to the second and third story struts. The first story struts failed before the ground struts at 0.52%H and consequently, yielding was initiated in first story

interior column and soon all three columns of first story yield. The frame collapses at 0.67%H roof displacement due to first story columns failure [Fig. 4.18(c)]. At collapse, about half of the total drift is confined to first story while in ground story it is only 16%.

4.1.4 Comparison

Strength increment due to infills in stilt frame-A and frame-B are 8.3%W and 5.8%W, respectively, i.e., strength of stilt frame-A and frame-B are 2.2 and 1.6 times the strength of the corresponding bare frames. On the other hand, strength contribution of infills in infill frame-A and frame-B are 14.5%W and 39.9%W, i.e., 3.1 and 5.4 times that of the respective bare frames. Contribution of infills towards the total strength of stilt and infill frame-A are 55% and 68%, respectively, whereas contribution of infills in stilt and infill frame-B are 39% and 81%. This shows that RC frame is weak as compared to the infill panel. Strength enhancement in stilt frame-B due to infill is not as significant as in frame-A [Fig. 4.2 and Fig. 4.1]. Because in frame-B, struts do not play any major role, most of the struts are intact even at collapse of frame; and frame collapsed due to failure of ground story columns. Upper stories moved as a single unit without any considerable deformation. Therefore, its behavior is like single story bare frame.

Deformation capacity of infill and stilt frames drastically decreases due to presence of infill, which is apparent from Fig. 4.1 and 4.2. Deformation capacities of stilt and infill frames are 55% and 60% of that of respective bare frames. Stiffnesses of stilt frame-A and frame-B are 4.1 and 2.8 times the corresponding bare frame stiffnesses. However, stiffnesses of infill frames are 8 times the corresponding bare frames. Ductility is increased due to presence of infill in frame-A, though this increment in stilt frame is negligible. Conversely, ductility is decreased 8 to 17% in frame-B due to infills.

The bare frames are quite flexible and ductile compare to stilt and infill frames, despite the fact that the detailing is nonductile or ordinary [Fig. 4.1- 4.2]. The strength

and stiffness of stilt and infill are significantly enhanced because of infill while deformation capacity is drastically reduced. The frames that collapse owing to failure of ground story columns are bare, stilt, infill frame-A, and stilt frame-B. Although bare frame-B collapses due to failure of first floor beams and infill frame-B due to first story columns failure.

4.2 Design Case EQ2

In this design case, frames are designed for dead loads, imposed loads, and earthquake load for zone II; detailed as per IS:13920 (ductile detailing). Pushover curves of frame-A and frame-B are shown in Fig. 4.3 and Fig. 4.4, respectively, while locations of hinges at failure are shown in the Fig. 4.19 and Fig. 4.20.

4.2.1 Bare Frames

The strength of frame-A and frame-B are 10.7%W and 14.0%W, respectively, while their stiffnesses are 8.1 and 4.8 kN/mm correspondingly. Maximum roof displacements reached before collapse, are 3.38%H and 1.96%H, respectively. Their ductility are 9.7 and 8.8, respectively. In frame-A, yielding starts from first floor beam and spreads in upper floors beams. Yielding initiates in column at a roof displacement of 0.45%H in ground story. Beams begin to lose strength at a roof displacement of 2.66%H and fail at 3.38%H. A desirable strong-column weak-beam hinge mechanism is formed, owing to high column-overstrength factor 2.7 (Table 4.5) and higher ductility in columns compare to beams i.e. 1.6 times (Table 3.1 and Table 3.3). At collapse, all the three beams fail, yet upper two stories columns are intact; only ground story columns yield [Fig. 4.19(a)].

In frame-B, yielding starts from first floor beam; and spread in upper floors beams and ground story columns. Hinge formation begins in column at a roof displacement of 0.25%H. At collapse, yielding is quite evenly distributed in bottom three stories while

upper two stories are almost undamaged. First floor beams starts to lose strength at 1.90%H and consequently, frame fails at 1.96%H roof displacement. Frame collapses due to first floor beams failure [Fig. 4.20(a)]. Ground story columns yield, but do not fail at even collapse. Frame fails in beam hinging mechanism due to high column-overstrength factor 1.3 (Table 4.5) and higher ductility in columns compare to beams i.e. 2 times (Table 3.5 and Table 3.7).

4.2.2 Stilt Frames

Strength of frame-A and frame-B are 19.0%W, and 18.4%W, respectively and deformation capacity are 2.09%H and 1.47%H correspondingly. Their stiffnesses are 28.5 and 12.3 kN/mm, respectively and ductility are 11.7 and 10.6 correspondingly. In frame-A, first yield is observed in first story strut; and ground story columns and first floor beam yield at roof displacement of 0.20%H. At a roof displacement of 0.52%H, first story strut fails, and hinges form in second floor beam and top story strut. First floor beam starts losing strength at 1.76% H drift, soon ground story columns fail; and as a result, frame collapses. Bottom two stories become soft and weak after failure of first floor strut, and consequently drift of these two stories increases considerably. Drift of ground story and first story are 44% and 43% of the total drift at failure. However, top story drift is only 13% of the total drift as top story columns and top floor beam are intact [Fig. 4.19(b)].

In frame-B, yielding initiates first at the base of ground story column at 0.10%H roof displacement and hinge forms at both ends of all three columns of ground story while all other members are intact at a roof displacement of 0.19%H. However, yielding spreads in few struts of upper stories and first floor beam before collapse. Frame fail due to failure of ground story columns. Ground story drift is 88% of the total drift at collapse, as hinges are mainly confined in this story [Fig. 4.20(b)].

4.2.3 Infill Frames

Frame-A and frame-B show 24.3% and 51.9%W strength, respectively and maximum roof displacements undergo before collapse are 2.10%H and 1.12%H in the same order. Their stiffnesses are 45.0 and 30.9 kN/mm, respectively and ductility are 14.6 and 7.3 correspondingly. In frame-A, yielding propagates in order from bottom story strut to top story strut. All the three struts yield at a roof displacement of 0.16%H. In the next step, hinge form in the beams of bottom two floors and ground story column at a roof displacement of 0.33%H. Bottom two struts fail at 0.62%H and first floor beam starts losing strength at 1.78%H roof displacement. When roof displacement reaches 2.08%H, bottom story columns starts degrading and finally at 2.10%H frame collapsed. Top story beam and columns are intact [Fig. 4.19(c)].

In frame-B, yielding begins in first story strut then spreads in ground and second story struts. Yielding initiates in column at a roof displacement of 0.12%H in ground story exterior column. In the next step, first floor beam and interior column of ground story yield at 0.29%H drift. At a drift of 0.47%H, yielding propagates in first and second stories columns, beams, and upper stories struts. First story drift increases rapidly after failure of first story struts. Finally, frame collapses due to failure of first story columns at 1.16%H roof displacement [Fig. 4.20(c)]. First story drift is about two-third (62%) of roof displacement at failure.

4.2.4 Comparison

Strength increment due to infills in stilt frame-A and frame-B are 8.4%W and 4.4%W, respectively i.e. strength of stilt frame-A and frame-B are 1.8 and 1.3 times the corresponding bare frame strengths. On the other hand, strength contribution of infills in infill frame-A and frame-B are 13.7%W and 37.9%W i.e. 2.3 and 3.7 times respective bare frames. Contribution of infills in the total strength of stilt and infill frame-A are 44%

and 56%, respectively, whereas infills contribution in stilt and infill frame-B are 24% and 73%. Deformation capacity of infill and stilt frames considerably decreases due to presence of infill, which is apparent from Fig. 4.3 and 4.4. Deformation capacity of stilt and infill frame-A is 62% of bare frame. While deformation capacities of stilt and infill frame-B are 74% and 56% of bare frame. Stiffnesses of stilt frame-A and frame-B are 3.5 and 2.6 times the corresponding bare frame stiffnesses. However, stiffnesses of infill frame-A and frame-B are 5.5 and 6.4 times the corresponding bare frames. Overstrength factors of bare, stilt, and infill frame-A are 4.3, 7.6, and 9.7, respectively, while for frame-B is 5.6, 7.4, and 20.8 in the same order. Ductility is increases about 20% due to infill in both stilt frames. Ductility is increased about 50% in infill frame-A, whereas 18% decrease in infill frame-B owing to infills.

4.3 Design Case EQ3

In this design case, frames are designed for dead loads, imposed loads, and earthquake loads for zone III; and detailed as per IS:13920 (ductile detailing). Pushover curves of frame-A and frame-B are shown in Fig. 4.5 and Fig. 4.6, respectively, whereas locations of hinges at failure are shown in the Fig. 4.21 and Fig. 4.22.

4.3.1 Bare Frames

The strength of frame-A and frame-B are 15.3%W and 16.9%W, respectively, while their stiffnesses are 11.1 and 6.7 kN/mm, respectively. Their deformation capacities are 2.88%H and 1.33%H, respectively and ductility are 9.0 and 5.7 in the same order. In frame-A, first yielding is observed in first floor beam, which propagates to second floor beam. Yielding starts in column at the base of ground columns at a roof displacement of 0.45%H. Subsequently, yielding propagates to top story beam. In the next step, first floor beam fails at 2.55%H roof displacement and second floor beam at 2.66%H. Finally, frame fails when top floor beam fails at 2.88%H roof displacement.

Upper two stories columns are having no hinge formation and even ground story columns do not fail, but yield [Fig. 4.21(a)]. A perfect strong-column weak-beam hinge mechanism is formed, due to high column-overstrength factor 2.1 (Table 4.5) and higher ductility in columns compare to beams i.e. 1.7 times (Table 3.1 and Table 3.3).

In frame-B, yielding starts from first floor beam and subsequently, yielding occurs in second floor beams and ground story columns at a 0.22%H roof displacement. Hinges form in third floor beam and first story column at 0.36%H roof displacement. In the next step, yielding occurs in second story column at 0.52%H roof displacement. At a roof displacement of 1.10%H, first floor beam starts losing strength and frame collapses at 1.33%H, when first floor both beams fail completely. Upper two stories are completely undamaged [Fig. 4.22(a)]. Frame fails in beam hinging mechanism, due to higher ductility in columns compare to beams i.e. 2.6 times (Table 3.5 and Table 3.7) and higher column strength compare to beam.

4.3.2 Stilt Frames

Strength of frame-A and frame-B are 22.7%W and 18.7%W, respectively. Their deformation capacities are 1.99%H and 1.45%H roof displacement, respectively. Stiffness of frame-A is 30.6 kN/mm and that of frame-B is only 14.5 kN/mm. Ductility of frame-A and frame-B are 15.7 and 12.1 correspondingly. In frame-A, yielding spreads from first floor strut to first floor beam and top story strut. Yielding initiates in columns from ground story at 0.26%H roof displacement. At a roof displacement of 0.51%H, first floor strut fails and consequently, bottom two stories drift increases suddenly due to becoming weak and soft story. Yielding spreads in first story columns at 0.87%H. First floor beam begins losing strength at 1.76%H and ground story column at 1.99%H and as a result, frame fails. Bottom two stories become soft and weak after failure of first floor strut, and consequently drift of these two stories increases significantly. Drift of ground

story and first story are 44% and 43% of the total drift at failure. However, top story drift is only 13% of the total drift as top story columns and top floor beam are intact [Fig. 4.21(b)].

In frame-B, yielding begins from the base of ground story columns at 0.09%H roof displacement and spreads to upper ends of ground story columns at 0.15%H. Upper stories struts and first floor beam yield; and ground story column starts losing strength at 1.36%H roof displacement and finally, frame collapse at 1.45%H due to failure of ground story columns. Ground story drift is 89% of the total drift at collapse, as hinges are mainly confined in this story [Fig. 4.21(b)].

4.3.3 Infill Frames

Strengths of frame-A and frame-B are 27.9%W and 53.2%W, respectively. Maximum roof displacement, they sustain are 1.99%H and 1.11%H, respectively. Their stiffnesses are 47.6 and 32.5 kN/mm in the same order, whereas their ductility are 19.8 and 7.3, respectively. In frame-A, hinge formation starts from ground story strut and propagates to upper stories struts and first floor beam. In the next step, first floor beam yields. Yielding initiates in columns from ground story at a 0.34%H roof displacement. First floor strut fails at 0.47%H roof displacement. However, ground story strut fail at a higher displacement of 0.59%H. Yielding occurs in first story columns at 0.87%H. At a roof displacement of 1.76%H, first floor beam begins losing strength; and ground story columns also starts losing strength and as a result frame fail at 1.99%H. Top story beam and columns are intact [Fig. 4.21(c)].

In frame-B, yielding starts from first floor strut and subsequently spreads in lower and upper stories struts. Yielding starts in columns from ground story at a 0.12%H roof displacement. In the next step, yielding spreads in upper stories struts and beams. Hinge forms in first story column at a roof displacement of 0.36%H. First story strut fails at

0.54%H roof displacement and subsequently, many other struts also fail. Yielding propagates to even top story beams, yet upper two stories columns are undamaged. Frame collapse due to failure of ground story column [Fig. 4.22(c)].

4.3.4 Comparison

Strength increment due to infills in stilt frame-A and frame-B are 7.4%W and 1.8%W, respectively i.e. strength of stilt frame-A and frame-B are 1.5 and 1.1 times the corresponding bare frame strengths. On the other hand, strength contribution of infills in infill frame-A and frame-B are 12.5%W and 36.3%W i.e. 1.8 and 3.1 times respective bare frames. Contribution of infills in the total strength of stilt and infill frame-A are 10% and 45%, respectively. While infills contribution in stilt and infill frame-B are 39% and 68%. Deformation capacity of stilt and infill frame-A is 69% of bare frame. However, deformation capacity of stilt frame-B is slightly more than that of bare frame, whereas deformation capacity of infill frame-B is less than that of bare frame. Stiffnesses of stilt frame-A and frame-B are 2.8 and 2.2 times the corresponding bare frame stiffnesses. However, stiffnesses of infill frame-A and frame-B are 4.3 and 4.8 times the corresponding bare frames. Overstrength factor of bare, stilt, and infill frame-A is 3.8, 5.7, and 7.0, respectively, while for frame-B is 4.2, 4.7, and 13.3 in the same order.

In frame-B, pushover curves of stilt and infill frames coincide after failure of struts. In both frames, there is considerable base shear drop due to failure of struts. Infill frame-B shows quite similar behavior. However, bare and stilt frame-B shows ductile and flexible behavior. Stilt frame-B behaves like bare frame, because mainly ground story takes part in load bearing while upper portion is intact almost. Due to same reason, its strength is also quite close to bare frame. Both bare frames fail in beam hinging mechanism. However, both stilt frames collapse due to formation of story mechanism in bottom story in spite of high column-overstrength factor and more ductility in columns

compare to beams. In infill frames collapse due to columns failure mainly, but beam failure also contributes.

4.4 Design Case EQ5

In this design case, frames are designed for dead loads, imposed loads, and earthquake load for zone V; and detailed as per IS:13920 (ductile detailing). Pushover curve of frame-A and frame-B are shown in Fig. 4.7 and Fig. 4.8, respectively, whereas locations of hinges at failure are shown in the Fig. 4.23 and Fig. 4.24.

4.4.1 Bare Frames

The strength of frame-A and frame-B are 36.1%W and 35.2%W, respectively while their stiffnesses are 19.1 and 13.2 kN/mm, respectively. Maximum roof displacements reached before collapse, are 2.79%H and 1.36%H, respectively. Their ductility is same that is 5.5. In frame-A, yielding starts from ground story column at a roof displacement of 0.40%H and yielding occurs in first floor beam at 0.47%H. Yielding propagates to second floor beam at 0.57%H. In the next step, hinge forms in top story beam and first story column at 1.18%H. Frame is further pushed and as a result, ground story column starts losing strength and top story column yields at 2.76%H. Finally, frame collapses at 2.79%H due to failure of ground story columns. Hinges are distributed in all stories.

In frame-B, hinging initiates from ground story column at 0.17%H roof displacement and gradually spreads in other ground story columns and first floor beams. At a roof displacement of 0.62%H, yielding occurs in first story column and first floor beam. In the next step, ground story column starts losing strength and yielding occurs in third floor beam at 1.21%H; and finally, frame falls down due to complete failure of ground story columns at 1.36%H. Hinge is mainly confined to bottom two stories; only one beam of third floor yields.

4.4.2 Stilt Frames

Strength of frame-A and frame-B are 37.5%W, and 35.5%W, respectively and deformation capacity are 2.07%H and 1.05%H correspondingly. Their stiffnesses are 41.7 and 23.9 kN/mm, respectively and ductility are 8.6 and 7.6 correspondingly. In frame-A, yielding begins from first story strut and propagates to top story strut. Hinge formation initiates in columns from ground story at a roof displacement of 0.32%H. In the next step, first floor beam yields at 0.43%H roof displacement and soon first story strut fails. Yielding occurs in second floor beam at a roof displacement of 0.67%H. Ground story columns starts losing strength at 2.02%H roof displacement and frame falls down at 2.07%H. Bottom two stories become soft and weak after failure of first floor strut, and consequently drift of these two stories increases significantly. Drift of ground story and first story are 44% and 42% of the total drift at failure. However, top story drift is only 14% of the total drift as top story columns and top floor beam are intact [Fig. 4.23(b)].

In frame-B, yielding starts from ground story columns at only 0.10%H roof displacement; and then it propagates to other ground story columns and first story struts. Strut of second story yields at 0.60%H roof displacement. Ground story column starts losing strength at 1.01%H and finally, frame fails at 1.05%H roof displacement. The beams and columns of upper four stories are intact. However, upper stories struts yield. Ground story drift is 84% of the total drift at collapse, as hinges are mainly confined in this story [Fig. 4.24(b)].

4.4.3 Infill frames

Strengths of frame-A and frame-B are 42.7%W and 68.7%W, respectively. Maximum roof displacement, they sustain are 2.07%H and 1.25%H, respectively. Their stiffnesses are 54.8 and 40.2 kN/mm in the same order, whereas their ductility are 10.0

and 7.9, respectively. In frame-A, yielding begins from first story strut. In the next step, yielding propagates to other struts and ground story columns at 0.37%H roof displacement. At a roof displacement of 0.46%H, first floor beam yields. Struts of first and ground story fail at a roof displacement of 0.48%H and 0.54%H, respectively. Yielding spreads to second floor beam and second story columns at 0.66%H and 0.88%H roof displacements, respectively. At a roof displacement of 2.03%H, column of ground story starts losing strength and frame fall down at 2.07%H roof displacement. However, top story beam and columns suffer no damage.

In frame-B, yielding starts from first story strut and soon, bottom three stories all struts yield. Yielding initiates in columns from ground story at a roof displacement of 0.21%H. Beams of first floor yield at 0.29%H roof displacement. Yielding propagates to upper stories; hinge forms in first story column at 0.32%H roof displacement. Yielding occurs in struts of upper stories, while few struts of bottom two stories fail.

4.4.4 Comparison

Strength increment due to infills in stilt frame-A and frame-B are 1.5%W and 0.3%W, respectively. On the other hand, strength contribution of infills in infill frame-A and frame-B are 6.6%W and 33.5%W i.e. 1.2 and 2.0 times the respective bare frames. Contribution of infills in the total strength of stilt and infill frame-A are 4% and 16%, respectively, whereas infills contribution in stilt and infill frame-B are 1% and 49%. This shows that contribution of infills in the strength of stilt frame is negligible as frame is quite strong compare to infills. Deformation capacity of infill and stilt frames considerably decreases due to presence of infill, which is apparent from Fig. 4.7 and 4.8. Deformation capacity of stilt frame-A, infill frame-A, and stilt frame-B is about 75% of respective bare frame, while that of infill frame-B is 92% of bare frame-B. Stiffnesses of stilt frame-A and frame-B are 2.2 and 1.8 times the corresponding bare frame stiffnesses.

However, stiffnesses of infill frame-A and frame-B are 2.9 and 3.0 times the corresponding bare frames. Overstrength factors of bare, stilt, and infill frame-A are 4.0, 4.2, and 4.7, respectively, while for frame-B is 3.9, 3.9, and 7.6 in the same order. Ductility is increases about 60-80% due to presence of infill in frame-A., whereas increase in frame-B is 40%.

4.5 Design Cases EQC3 and EQCB3

These two cases are related to stilt frames, in which some preventive measures are taken to avoid formation of story mechanism in the ground story of such buildings; and effectiveness of these measures is evaluated.

4.5.1 Design Case EQC3

In fact, this is a special case of stilt frame of EQ3 design case. Ground story columns of stilt frame of EQ3, is redesigned for 2.5 times bare frame forces. Each member of this design case is same as in EQ3 case except ground story columns. No infill and bare frame is studied in this case, only stilt frames. Strength of frame-A and frame-B are 34.1%W (818.4 kN) and 40.9%W (613.5 kN), respectively, and deformation capacity are 2.45%H and 1.03%H in the same order. Their stiffnesses are 49.9 and 22.8 kN/mm, respectively; ductility are 13.4 and 6.2 in the order.

In frame-A, yielding begins from strut of first story and propagates to strut of top story. At a roof displacement of 0.34%H, first floor and second floor beams yield. In the next step, strut of first floor fail at a 0.43%H. At 0.54%H roof displacement, yielding in columns starts from ground story and top floor beam also yields at same displacement level. Further, strut of top story fails at 0.63%H roof displacement. Gradually, yielding propagates to first story column at 0.75%H and second floor beam starts losing strength at 1.82%H roof displacement. Finally, frame falls down at 2.45%H roof displacement. At collapse, upper two beams fail completely. Top story columns are intact [Fig. 4.25(b)].

Ground story drift is only 3.6% of the total drift, which clearly indicates that stiffness of ground story is very high compare to that of upper stories, even at collapse. In the elastic range, stiffness of bottom story of frame-A is 170 kN/mm, while that of frame-A is about 50 kN/mm. On the other hand, stiffness of bottom story of frame-B is 50 kN/mm, and that of frame-B is about 23 kN/mm.

In frame-B, yielding starts from first floor beam and then propagates to struts of first story. Hinge forms in ground story column at a 0.18%H roof displacement. Gradually, yielding spreads to columns of first story at 0.29%H roof displacement. Strut of first story fails at a roof displacement of 0.41%H. At 0.94%H roof displacement, first floor beam starts losing strength. Consequently, frame fails but yielding is limited to bottom two stories and in the struts of second story [Fig. 4.26(b)]. Frame collapses due to failure of first floor beams and struts. Drift in bottom two stories is 88% of the total drift at collapse, as hinges are mainly confined in these two stories.

4.5.2 Design Case EQCB3

This is also a special case of stilt frame of EQ3 design case, in which ground story columns as well as first floor beams of stilt frame of EQ3, is redesigned for 2.5 times forces. Other than ground story columns and first floor beams, each element is same as in EQ3 case. No infill and bare frame is studied in this case, only stilt frames. Strength of frame-A and frame-B are 37.4%W and 51.9%W and deformation capacity are 2.24%H and 0.96%H. Their stiffnesses are 55.6 and 22.9 kN/mm; ductility are 12.5 and 4.6.

In frame-A, hinge formation initiates from strut of first story and propagates to strut of top story. First and second floor beams yield at 0.30%H roof displacement. In the next step, strut of first story fails and top floor beam yields at 0.44%H roof displacement. First story columns yield at 0.54%H roof displacement. Top story strut fails at 0.56%H roof displacement. Further, second floor beam starts losing strength at 1.70%H roof

displacement and top floor beam at 1.82%H. Finally, frame fails at 2.24%H roof displacement. However, ground story and top story columns are intact [Fig. 4.25(c)]. Frame collapses due to failure of upper floor beams. Ground story drift is only 2.4% of the total drift, which clearly indicates that stiffness of ground story is very high compare to that of upper stories, even at collapse. In the elastic range, stiffness of bottom story of frame-A is 212 kN/mm, while that of frame-A is 56 kN/mm. On the other hand, stiffness of bottom story of frame-B is 50 kN/mm, and that of frame-B is 23 kN/mm.

In frame-B, yielding begins from strut of first story and propagates to strut of second story soon. Hinge formation starts in column from ground story at 0.20%H roof displacement. In the next step, yielding spreads in first story columns and second story beams at 0.29%H roof displacement. Strut of first story fails at 0.42%H roof displacement. At 0.77%H roof displacement, both struts of first story fail and as a result first story drift increases excessively. Finally, second story columns, struts, and second floor beams fail and consequently, frame collapses. First story and second story damage heavily and hence most of drift is confined to these two stories. Upper two stories are intact. Drifts of ground and first story are 31% and 54% of the total drift at collapse. In other words, drift in bottom two stories is 85% of the total drift, as hinges are mainly confined in these two stories.

4.5.3 Comparison

Seismic performance of stilt frames of design case EQ3, EQC3, and EQCB3 is compared in terms of strength, stiffness, and deformation capacity. These three stilt frames are also compared with infill frame of EQ3 design case. Pushover curves of these four frames are shown in Fig. 4.9 and Fig. 4.10. Locations of hinges in stilt frames EQ3, EQC3, and EQCB3 at failure are shown in the Fig. 4.25 and Fig. 4.26.

Strength of infill frame-A in EQ3 case is 27.9%W and it reduces in case of stilt to 22.7%W. Strength of stilt frame-A in EQC3 and EQCB3 are 34.1%W and 37.4%W. This shows that the strength deficiency due to absence of infills in ground story is over compensated by designing even only ground story columns for 2.5 times forces. On the other hand, strength of infill frame-B in EQ3 case is 53.2%W, which drastically reduces in stilt frame to 18.7%W. Strength of stilt frame-B in EQC3 and EQCB3 increase to 40.9%W and 51.9%W. This implies that the strength deficiency in stilt frame-B compare to infill frame-B is nearly compensated, if bottom story columns and beams both are designed for 2.5 times forces.

Stiffness of frame-A is reduces to 30.6 kN/mm from 47.6 kN/mm due to absence of infills in ground story in design case EQ3. Stiffness of stilt frame-A in design case EQC3 and EQCB3 are 49.9 and 55.6 kN/mm, which are more than that of infill frame-A in EQ3. However, stiffness of stilt frame-B in EQC3 and EQCB3 are about 23 kN/mm, which is less than that of infill frame-B (32.5 kN/mm).

Stilt frame-A of design case EQC3 and EQCB3 collapses due to failure of upper two floor beams, although ground story columns yield in EQC3 [Fig. 4.25]. In EQCB3, hinges are confined to upper two stories and as a result, deformation capacity is less than EQC3. Desirable mechanism of collapse is that all the beams should fail first then hinge should form at the base of ground story columns. So, designing first floor beam for higher forces reduces deformation capacity and confines the hinges in upper stories. In stilt frame-B, yielding occurs in ground story columns in both design case EQC3 and EQCB3. Designing first floor beams for higher forces, cause reduction in deformation capacity and columns of first story fails as ground story becomes quite stiff. Although, hinges propagates in upper stories by designing first floor beams for higher forces. Designing ground story columns for 2.5 times prevents the formation of column hinging

mechanism in the ground story; causes propagation of yielding in upper stories and enhances deformation capacity. However, designing columns and beams both for 2.5 times forces is not seems to be appropriate due to above mentioned reasons.

4.6 All Bare Frames

Pushover curves of bare frames of design case GRAV, EQ2, EQ3, and EQ5 are shown in Fig. 4.11 and 4.12. Strength of bare frames-A of design cases GRAV, EQ2, EQ3, and EQ5 is 6.9%W, 10.7%W, 15.3%W, and 36.1%W, respectively; while that of frame-B are 9.1%W, 14.0%W, 16.9%W, 35.2%W in that order. Overstrength factor of frame-A are 4.3, 3.8, and 4.0 in design case EQ2, EQ3, and EQ5, respectively; whereas these values for frame-B are 5.6, 4.2, and 3.9 in that order. Strength increment in EQ2, EQ3 and EQ5 case compared to GRAV, in frame-A are 55%, 122%, and 423%, respectively; while in frame-B are 54%, 86%, and 287% in the same order.

Maximum roof displacement of frame-A of design cases GRAV, EQ2, EQ3, and EQ5 is 1.73%H, 3.38%H, 2.88%H, and 2.79%H, respectively, whereas for frame-B are 1.16, 2.00, 1.33, and 1.36. It is apparent from Fig. 4.11 and 4.12 that maximum roof displacement is quite low in GRAV case in both frames; and it decreases from EQ2 to EQ5. Low deformation capacity in GRAV case is obviously due to ordinary detailing and smaller sections in spite of very high column-overstrength factor. Column-overstrength (COF) factor decreases in higher seismic zones; consequently, frame having low COF fails in weak-column strong-beam mechanism and have low deformation capacity. Both frames in EQ2 and EQ3 collapse due to failure of beams, while both frames in EQ5 fail due to columns failure [Fig. 4.19-4.24]. Ductility of both frames in design case EQ2 is almost double than that of in GRAV case, whereas ductility of frame-A in EQ3 is 1.8 times the ductility in GRAV case. However, increment in ductility in EQ5 is about 15% only compare to GRAV case. Stiffness increment in EQ2, EQ3, and EQ5 case compared

to GRAV, in frame-A are 55%, 111%, and 264%, respectively; while in frame-B are 38%, 93%, and 279% in the same order.

4.7 All Stilt Frames

Pushover curves of stilt frames of design case GRAV, EQ2, EQ3, and EQ5 are shown in Fig. 4.13 and 4.14. Pushover curves of frame-A for all the design cases shows drop in base shear due to failure of struts. On the other hand, pushover curves of frame-B for all design cases are similar to that of bare frames, i.e., flexible, ductile and without any drop in base shear due to strut failure. The alteration in seismic behavior due to infill is not significant in frame-B in all design. The ground story height of frame-B is 1.4 times the height of stories above it. Consequently, ground story of stilt frame is quite flexible and weak compare to upper stories owing to the fact that column and beams are same in all stories. Most of the struts of upper stories are intact or slightly damaged and frame collapses due to ground story columns failure.

Strength increment due to infills is negligible due to the same reason. Strength of stilt frame-A of design cases GRAV, EQ2, EQ3, and EQ5 is 15.2%W, 19.0%W, 22.7%W, and 37.5%W, respectively; while that of frame-B are 14.9%W, 18.4%W, 18.7%W, and 35.5%W in the same order. Strength increment in EQ2, EQ3, and EQ5 case compared to GRAV, in frame-A are 26%, 50%, and 148%, respectively; while in frame-B are 23%, 26%, and 138% in the same order. Overstrength factor decreases for higher seismic zones, which is evident from Table 4.5. Overstrength factor of frame-A of design cases EQ2, EQ3, and EQ5 are 7.6, 5.7, and 4.2; whereas 7.4, 4.7, and 3.9 for frame-B in the same order. The contribution of infills in strength of frame-A in GRAV, EQ2, EQ3, and EQ5 are 55%, 44%, 33%, and 4%; while in frame-B 39%, 24%, 10%, and 1% in the same order. In other words, about half of the strength contribution is of infills in GRAV

case, whereas infills contribution is almost negligible in EQ5. Stiffness increments in seismic design cases compare to GRAV is 55-264% in frame-A and 38-279% in frame-B.

In frame-A, deformation capacity in design case GRAV is less than 50% of deformation capacity in seismic design cases. Deformation capacity is almost equal for all the seismic design cases (Fig. 4.13). In frame-B also, deformation capacity is quite low in GRAV case compare to seismic design cases. Deformation capacity of frame in EQ5 is less than that in EQ2 and EQ3. Both frames in all design cases, collapse due to failure of ground story columns (Fig. 4.17 to 4.26). Ductility is least in GRAV case in both frames. It increases in seismic cases due to ductile detailing. However, least increment is in EQ5 case due to column hinging mechanism (Fig. 4.33-4.34). Ductility of both frames in design case EQ2 and EQ3 is more than twice than that of in GRAV case. However, increment in ductility in EQ5 is 50-70% compare to GRAV case.

4.8 All Infill Frames

Pushover curves of infill frames of design case GRAV, EQ2, EQ3, and EQ5 are shown in Fig. 4.15 and 4.16. Strength of infill frame-A of design cases GRAV, EQ2, EQ3, and EQ5 is 21.3%W, 24.3%W, 27.9%W, and 42.7%W, respectively; while that of frame-B are 49.0%W, 51.9%W, 53.2%W, and 68.7%W in the same order. Strength increment in EQ2, EQ3, and EQ5 case compared to GRAV, in frame-A are 14%, 31%, and 100%, respectively; while in frame-B are 6%, 9%, and 40% in the same order. Overstrength factor decreases for higher seismic zones, which is evident from Table 4.5. Overstrength factor of frame-A of design cases EQ2, EQ3, and EQ5 are 9.7, 7.0, and 4.7; whereas 20.8, 13.3, and 7.6 for frame-B in the same order. The contribution of infills in strength of frame-A in GRAV, EQ2, EQ3, and EQ5 are 68%, 56%, 45%, and 16%; while in frame-B 81%, 73%, 68%, and 49% in the same order. This means contribution of infills is more than two-third in GRAV case.

In frame-B, the strength of ground story struts is more than 1.6 times the strength of upper stories struts, due to more height. Design cases in which strength contribution of infills is considerable, ground story is more stiff and strong than first story. As a result, frame collapses due to first story failure instead of ground story in GRAV and EQ2 case. Deformation capacity of frame-A in GRAV case is about 1%H, whereas in seismic design cases it is about 2%H. In frame-B, deformation capacity is 0.67%H in GRAV and almost double is in the seismic design cases. Ductility is least in GRAV case in both frames. It increases in seismic cases due to ductile detailing (Fig. 4.33-4.34).

4.9 Overall Observations

Following salient points have been observed after studying all the frames:

1. Strength increment due to infills in stilt frames-A is about 8%W in all design cases except in EQ5 case, in which it is only 1.5%W.
 2. Strength increment due to infills in infill frames-A is about 14%W in all design cases except in EQ5 case, in which it is only 6.6%W. However, strength increment is about 37%W in infill frames-B.
 3. Strength increment in stilt and infill frames as compared to bare frame are up to 120% and 440%, respectively.
 4. Strength of stilt frames is 1.0-2.2 times the corresponding bare frames. Whereas strength of infill frames is 1.2-5.4 times the respective bare frames.
 5. Contribution of infills in the total strength of frames decreases in frames designed for higher seismic zone.
 6. Strength reduction due to absence of infills in the ground story in stilt frames is 12-70%.
-

7. Strength of stilt frames-B is nearly equal to corresponding bare frames strength. However, strength increment in stilt frames-A as compared to bare frame is significant.
 8. Overstrength factor of both the bare frames in all seismic design cases is found to be about four. Whereas it is 3.9-7.6 for stilt frames and 4.7-20.8 for infill frames.
 9. Deformation capacity increases up to 100% owing to the ductile detailing.
 10. Deformation capacity decreases considerably in most of the frames due to infill and reduction is up to 45%.
 11. Yielding initiates in the ground story columns of stilt frames at a very low deformation level as compared to bare and infill frames.
 12. Both the stilt frames in all design cases collapse due to failure of ground story columns.
 13. In stilt frames, the ground story displacement at collapse is more than 40% of the roof displacement in frame-A. However, it is more than 80% in frame-B.
 14. Reduction in the ground story stiffness is 50-90% due to absence of infills, while overall stiffness deficit is 25-65%.
 15. Stiffness of stilt frames is 1.8-4.1 times the corresponding bare frames. Whereas stiffness of infill frames is 2.9-7.9 times the corresponding bare frames.
 16. Ductility is increased in most of the frames due to infills. However, decrease was noted in few frames.
 17. Seismic performance of stilt frames significantly improved in terms of strength and stiffness if bottom story components are designed for higher forces.
-

Chapter 5

Summary and Conclusions

5.0 General

RC frame buildings infilled with unreinforced brick masonry are very common in practice. Many such buildings have open ground story for parking. Such buildings have consistently shown poor performance during past earthquakes. Open ground story feature is not captured in design as strength and stiffness contribution of infill is not taken into account. Indian seismic code suggests designing open ground story components for 2.5 times moments and shears if infill is not considered in analysis and design.

5.1 Summary

In the present study, two frames three-story one-bay and five-story two-bay are designed for only gravity loads, and gravity loads plus seismic loads corresponding to seismic zones II, III, and V. Frames designed for seismic loads are detailed as per ductile detailing code, else detailing is ordinary. Ground story columns of stilt frames designed for zone III is redesigned for 2.5 times bending moments and shear forces. In the next case, first floor beams are also redesigned for 2.5 times bending moments and shear forces. The masonry infill panels are modeled as equivalent diagonal struts. Width of strut is taken as one-third of diagonal length of infill panel according to Holmes (1961) formula. Hinge properties of strut are defined as per Reinhorn et al. (1995). Moment-rotation hinge is assigned in both ends of beams and moment-rotation coupled with P-M interaction hinge is assigned in both ends of columns. Nonlinear pushover analysis is performed using structural analysis software package "SAP2000 NonLinear" [CSI, 1999]. Pushover analysis is performed for bare, stilt, and infill frames of each design case. Base-shear versus roof displacement is plotted for each frame. The performance of

stilt frames are compared with bare and infill frames in terms of strength, stiffness, deformation capacity, ductility, and hinge mechanism. The efficacy of designing bottom story components for higher forces to avoid soft/weak story formation is also evaluated.

5.2 Conclusions

The following are the salient conclusions drawn from the present study:

1. Both the stilt frames in all design cases collapse due to failure of ground story columns. It implies that ground story columns are more susceptible to failure than first floor beams in stilt frames.
 2. Strength and stiffness deficit in ground story caused by absence of infills is more prominent if ground story height is more.
 3. Deficit in ground story stiffness is 50-90% due to absence of infills, while overall stiffness deficit is 25-65% and strength deficit is 10-70%.
 4. Strength and stiffness deficit in ground story caused by absence of infills is less prominent in the frames designed for higher seismic zone.
 5. Increase in overstrength factor due to infills is more significant in infill frames compared to stilt frames. Overstrength factor decreases in the frames designed for higher seismic zones.
 6. Deformation capacity in most of the seismic design cases due to ductile detailing is considerably increased.
 7. Deformation capacity decreased up to 45% due to presence of infills.
 8. Ground story columns and first floor beams both are designed for 2.5 times forces then strength and stiffness increases but deformation capacity decreases compare to when only ground story columns are designed for 2.5 times forces.
 9. Ground story columns do not fail in stilt frames if designed for 2.5 times forces. Frames collapse due to failure of beams or upper stories columns.
-

10. In frame-A, strength and stiffness deficit is compensated if only ground story columns are designed for 2.5 times forces; while in frame-B, strength and stiffness deficit is nearly compensated if columns beams both are designed for 2.5 times forces. Strength and stiffness deficit caused by absence of infills vary zone to zone for even same frame. This 2.5 times factor may be quite conservative in zone V, while it may be low for zone II. Therefore, this factor needs more refinement and it should be based on extent of irregularity in strength and stiffness.

5.3 Possible Future Work

Observations from previous and present research on RC frame buildings on stilt show the need for more work to understand the seismic behavior of such buildings and find out some rational, simple, and economical method of design to avoid formation of weak/soft story. Following work may be carried out in future:

1. Analyzing and designing RC infill frame after incorporating infill.
 2. This work was done on two-dimensional frames. Future work may be extended to three- dimensional buildings.
 3. How seismic performances of buildings on stilts vary with the height of ground story can be studied.
 5. Opening in the infill panel of upper stories may be considered in future work to simulate the response of buildings with more precision.
 6. Ground story members of buildings on stilts may be designed for different force level (less than and more than 2.5 times) and seismic response and economy may be compared.
-

References

- Adalier, K., and Aydingun, O., (2001), "Structural Engineering Aspects of the June 27, 1998 Adan-Ceyhan (Turkey) Earthquake", *Engineering Structures*, Vol. 23, pp 343-355.
- Al-Ali, A.A.K. and Krawinkler, H., (1997), "Effects of vertical irregularities on seismic behavior of building structures", *Rep. No. 130*, John A. Blume Earthquake Engineering Centre, Stanford Univ., Stanford, Calif., 98.
- Al-Chaar, G., Issa, (2002), "Evaluating Strength and Stiffness of Unreinforced Masonry Structures", *US Army Corps of Engineers, Engineer Research and Development Center*, Vicksburg.
- Al-Chaar, G., Issa, M., and Sweeney, S., (2002), "Behavior of Masonry-Infilled Nonductile Reinforced Concrete Frames", *Journal of Structural Engineering, ASCE*, Vol. 128, No. 8, pp 1055-1063.
- AIJ, 1995, "Preliminary Reconnaissance Report of the 1995 Hyogoken-Nanbu Earthquake, Architectural Institute of Japan, Tokyo, Japan.
- Arlekar, J. N., Jain, S.K., and Murty, C. V. R., (1997), "Seismic Response of RC Frame Buildings with Soft First Storeys", *Proceedings of the CBRI Golden Jubilee Conference Natural Hazards in Urban Habitat*, New Delhi, India.
- ATC 40, (1996), "*Seismic Evaluation and Retrofit of Concrete Buildings*", Applied Technology Council, California.
- Balendra, T., Tan, K.H., and Kong, S.K., (1999), "Vulnerability of Reinforced Concrete Frames in Low Seismic Regions When Designed according to BS 8110", *Earthquake Engineering and Structural Dynamics*, Vol. 28, pp 1361-1381.
- Bertero, V. V., and Brokken, S. T., (1983), "Infills in Seismic Resistant Building", *Journal of structural Engineering, ASCE*, Vol. 109, No. 6, pp 1337-1361.
- Chintanapakdee, C., and Chopra, A.K., (2004), "Seismic Response of Vertically Irregular Frames: Response History and Modal Pushover Analyses", *Journal of Structural Engineering, ASCE*, Vol. 130, No. 8, pp 1177-1185.
- Das, D., (2000), "Beneficial Effects of Brick Masonry Infills in Seismic Design of RC Frame Buildings", *M.Tech. Thesis*, Department of Civil Engineering, Indian Institute of Technology, Kanpur.
- Dasgupta, P., (2000), "Effect of Confinement on Strength and Ductility of Large RC Hollow Sections", *M.Tech. Thesis*, Department of Civil Engineering, Indian Institute of Technology, Kanpur.
- Dolsek, M., and Fajfar, P., (2001), "Soft Storey Effects in Uniformly Infilled Reinforced Concrete Frames", *Journal of Earthquake Engineering*, Vol. 5, No. 1, pp 1-12.
-

Dayaratnam, P., (1987), "*Brick and Reinforced Brick Structures*", Oxford and IBH Publishing Corporation Private Limited, India.

Drysdale, R. G., Hamid, A. A., and Baker, A. L., (1993), "*Masonry Structures-Behavior and Design*", Prentice Hall Incorporation, New Jersey.

Ellul, F., Dayala, and D., (2002), "Field Report," The 2003 Bingol, Turkey Earthquake Field Report, Bath, Turkey: University of Bath, July 2003

FEMA 273, (1997), "*NEHRP Guidelines for the Seismic Rehabilitation of Buildings*", Federal Emergency Management Agency, Washington.

FEMA 306, (1999), "*Evaluation of Earthquake Damaged Concrete and Masonry Wall Buildings*", Federal Emergency Management Agency, Washington.

Grimm, C. T., (1975), "Strength and Related Properties of Brick Masonry", *Journal of the Structural Division, ASCE*, Vol. 101, No. 1, pp 217-232.

Hall, J.F., (Editor), 1994, "Northridge Earthquake January 17, 1994 - Preliminary Reconnaissance Report," Report No.94-01, *Earthquake Engineering Research Institute*, Oakland, USA.

IS:456-2000, (2000), "*Indian Standard Code of Practice for Plain and Reinforced Concrete*", Bureau of Indian Standards, New Delhi.

IS:1893-2002 (Part-I), (2002), "*Indian Standard Criteria for Earthquake Resistant Design of Structures*", Bureau of Indian Standards, New Delhi.

IS:13920-1993, (1993), "*Indian Standard Code of Practice for Ductile Detailing of Reinforced Structures Subjected to Seismic Forces*", Bureau of Indian Standards, New Delhi.

IS:1905-1987, (1987), "*Indian Standard Code of Practice for Structural Use of Unreinforced Masonry*", Bureau of Indian Standards, New Delhi.

Jain, S.K., and Murty, C.V.R., (2004), "Proposed Draft Provisions and Commentary on Indian Seismic Code IS 1893 (Part 1)", Department of Civil Engineering, Indian Institute of Technology, Kanpur.

Kanitkar, R., and Kanitkar, V., (2004), "Seismic Performance of Conventional Multistory Buildings with Open Ground Floors for Vehicular Parking", *The Indian Concrete Journal*, Vol. 78, No. 2, pp 99-104.

Kumar, S., (2002), "A Study on Modeling of Unreinforced Masonry Infilled RC Frames for Seismic Response", *M.Tech. Thesis*, Department of Civil Engineering, Indian Institute of Technology, Kanpur.

Lee, H.S., and Woo, S.W., (2002), "Effect of Masonry Infill on Seismic Performance of a 3-Storey R/C Frame with Non-Seismic Detailing", *Earthquake Engineering and Structural Dynamics*, Vol. 31, pp 353-378.

Lu, Y., (2002), "Comparative Study of Seismic Behavior of Multistory Reinforced Concrete Framed Structures", *Journal of Structural Engineering, ASCE*, Vol. 128, No. 2, pp 169-178.

- Moghaddam, H. A., and Dowling, P. J., (1987), "The State of Art in Infilled Frames", ESEE Imperial College of Science and Technology, Research Report, No. 87-2.
- Mondal, G., (2003), "Lateral Stiffness of Unreinforced Brick Infilled RC Frame with Central Opening", *M.Tech. Thesis*, Department of Civil Engineering, Indian Institute of Technology, Kanpur.
- Murty, C.V.R., (2004), "IITK-BMTPC Earthquake Tip 21" Department of Civil Engineering, Indian Institute of Technology, Kanpur.
- Murty, C.V.R., Goel, R.K., and Goyal, A., (2002), "Reinforced Concrete Structures," In *2001 Bhuj, India Earthquake Reconnaissance Report*, ed.
- Jain, S.K., Lettis, V.C., Murty, C.V.R., and Bardet, J.P., (2002) "Earthquake Spectra, supplement A to volume 18", Oakland, CA: Earthquake Engineering Research Institute, July 2002, pp. 149 - 185.
- Murty., C.V.R., (2004), "Earthquake Tip-21 IITK-BMTPC",
- Ono, T., Zhao, Y.G., and Ito, T., (2000), "Probabilistic Evaluation of Column Overdesign Factors for Frames", *Journal of Structural Engineering, ASCE*, Vol. 126, No. 5, pp 605-610.
- Pinto, A., Verzeletti, G., Molina, J. and Varum, H., (1999), "Pseudo-dynamic tests on non-seismic resisting RC frames (bare and selective retrofit frames)", *ICONS Topic (Assessment, Strengthening and Repair)*, JRC-ISIS Report, September.
- Paulay, T., and Priestley, M. J. N., (1992), "Seismic Design of Reinforced Concrete and Masonry Buildings", John Wiley and Sons Incorporation, New York.
- Rai, D.C., (2004), "Proposed Draft for Structural Use of Masonry IS 1905", Department of Civil Engineering, Indian Institute of Technology, Kanpur.
- Razvi, S., and Saatcioglu, M., (1999), "Confinement Model for High-Strength Concrete", *Journal of structural Engineering, ASCE*, Vol. 125, No. 3, pp 281-289.
- Reinhorn, A. M., Madam, A., Valles, R. E., Reichmann, Y., and Mander, J. B., (1995) "Modeling of Masonry Infill Panels for Structural Analysis", *National Center for Earthquake Engineering Research*, Technical Report, NCEER-95-0018.
- Saneinejad, A., and Hobbs, B., (1995), "Inelastic Design of Infilled Frames", *Journal of Structural Engineering, ASCE*, Vol. 121, No. 4, pp 634-650.
- Valmundsson, E.V., and Nau, J.M., (1997), "Seismic Response of Building Frames with Vertical Structural Irregularities", *Journal of Structural Engineering, ASCE*, Vol. 123, No. 1, pp 30-40.
- Vasandani, N., (1997), "Comparison of the Experimental Cyclic Response of RC Frames with and without Brick Masonry Infills", *M. Tech. Thesis*, Department of Civil Engineering, Indian Institute of Technology Kanpur, Kanpur.

Table 2.1: Base Shear Distribution in Frame-A

Floor	Earthquake Force (kN)		
	Zone II	Zone III	Zone V
Third (H_3)	39.0	62.0	140.0
Second (H_2)	17.5	28.0	63.0
First (H_1)	4.5	7.0	16.0
V_B	61.0	97.0	219.0

Table 2.2: Base Shear Distribution in Frame-B

Floor	Earthquake Force (kN)		
	Zone II	Zone III	Zone V
Fifth (H_5)	12.5	20.0	46.1
Fourth (H_4)	12.5	20.0	44.5
Third (H_3)	7.5	12.0	26.6
Second (H_2)	3.8	6.0	13.2
First (H_1)	1.2	2.0	4.5
V_B	37.5	60.0	135.0

Table 2.3: Reinforcement Details of Columns of Frame-A

Design Case	Width (mm)	Depth (mm)	Longitudinal Reinforcement		Shear Reinforcement
			(%)	Detailing	
GRAV	300	500	1.70	10Y18	Y8@280
EQ2	300	600	1.41	10Y18	Y8@75
EQ3	300	630	1.66	10Y20	Y8@75
EQ5	350	700	2.00	10Y25	Y10@85
EQC3*	500	800	2.01	10Y32	Y10@100
EQCB3**	500	800	2.01	10Y32	Y10@100

*This is the size of ground story columns. Columns in all other stories are same as in EQ3

** All columns are same as in case EQC3

Table 2.4: Reinforcement Details of Beams of Frame-A

Design Case	Width (mm)	Depth (mm)	Tension Reinforcement		Compression Reinforcement		Shear Reinforcement
			(%)	Detail	(%)	Detailing	
GRAV	200	400	0.75	3Y16	0.50	2Y16	2Y8@275
EQ2	200	450	0.85	3Y18	0.57	2Y18	2Y8@100
EQ3	250	500	0.91	3Y22	0.61	2Y22	2Y8@110
EQ5	250	600	1.31	4Y25	1.31	4Y25	2Y10@110
EQC3*	250	500	0.91	3Y22	0.61	2Y22	2Y8@110
EQCB3**	300	650	0.78	4Y22	0.58	3Y22	2Y8@130

* All beams are same as in case EQ3

** This is the size of ground story beam. All other stories beams are same as in case EQ3

Table 2.5: Reinforcement Details of Columns of Frame-B

Design Case	Width (mm)	Depth (mm)	Longitudinal Reinforcement		Shear Reinforcement
			(%)	Detailing	
GRAV	230	460	1.07	10Y12	4Y6@180*
EQ2	250	470	0.96	10Y12	4Y8@75
EQ3	250	500	0.91	10Y12	4Y8@75
EQ5	300	600	1.12	10Y16	4Y10@75
EQC3**	300	650	1.95	10Y22	4Y8@75
EQCB3***	300	650	1.95	10Y22	4Y8@75

* Grade of shear reinforcement is Fe250

** This is the size of ground story columns. All other stories columns are same as in EQ3

*** All columns are same as in case EQC3

Table 2.6: Reinforcement Details of Beams of Frame-B

Design Case	Width (mm)	Depth (mm)	Tension Reinforcement		Compression Reinforcement		Shear Reinforcement
			(%)	Detailing	(%)	Detailing	
GRAV	230	400	0.49	4Y12	0.25	2Y12	2Y6@130*
EQ2	200	450	0.67	3Y16	0.45	2Y16	2Y8@100
EQ3	250	500	0.64	4Y16	0.32	2Y16	2Y8@110
EQ5	300	600	0.57	4Y18	0.57	4Y18	2Y8@120
EQC3**	250	500	0.64	4Y16	0.32	2Y16	2Y8@110
EQCB3***	250	500	1.52	5Y22	0.91	3Y22	2Y10@110

* Grade of shear Reinforcement is Fe250

** All beams are same as in case EQ3

*** This is the size of ground story beam. All other stories beams are same as in EQ3

Table 3.5: Flexural Hinge Properties of Columns of Frame-B

Design Case	P_y (kN)	M_y (kN-m)	θ_y (10^{-3} radian)		M_u/M_y	θ_u/θ_y
			Upper Story	Ground Story		
GRAV	1587	96	0.757	1.060	1.000	20.3
EQ2	2379	102	0.693	0.970	1.003	70.0
EQ3	2522	111	0.626	0.876	1.002	70.4
EQ5	3800	231	0.631	0.883	1.021	47.9
EQC3	4765	428	-	1.281	1.059	29.4

Table 3.6: P-M Interaction Curve of Columns of Frame-B

Design Case	P_c (kN)	P_t/P_c	P_b/P_c	M_o (kN-m)	M_b/M_o
GRAV	1587	0.3696	0.30	96	1.2352
EQ2	2379	0.2447	0.35	102	1.5088
EQ3	2522	0.2326	0.37	111	1.5514
EQ5	3800	0.2744	0.34	231	1.4065
EQC3	4765	0.4139	0.26	428	1.1684

Table 3.7: Flexural Hinge Properties of Beams of Frame-B

Design Case	M_y (kN-m)	θ_y (10^{-3} radian)	M_u/M_y	θ_u/θ_y
GRAV (HOG)	75	1.054	1.000	17.2
GRAV (SAG)	41	0.572	1.000	34.0
EQ2(HOG)	113	1.278	1.008	34.6
EQ2 (SAG)	79	0.896	1.000	47.0
EQ3(HOG)	167	1.103	1.000	26.6
EQ3(SAG)	91	0.598	1.000	50.9
EQ5(HOG)	275	0.874	1.006	23.4
EQ5 (SAG)	275	0.874	1.006	23.4
EQCB3 (HOG)	349	2.301	1.079	20.0
EQCB3 (SAG)	248	1.631	1.015	23.0

Table 3.8: Axial Hinge Properties of Struts of Frame-B

Design Case	Upper Story		Ground Story		P_m/P_y	δ_m/δ_y
	P_y (kN)	δ_y (mm)	P_y (kN)	δ_y (mm)		
GRAV	316	8.872	517	10.700	1.125	2.25
EQ2	307	8.723	501	10.458	1.125	2.25
EQ3	305	8.585	490	10.298	1.125	2.25
EQ5	276	8.045	447	9.611	1.125	2.25
EQC3	-	-	474	9.721	1.125	2.25
EQCB3	-	-	444	9.374	1.125	2.25

Table 3.9: Shear Hinge Properties of Frame-A

Members	V_u (kN)	δ_u (mm)
Ground Story Columns	268	0.69
First Story Columns	223	0.574
Second Story Columns	178	0.458
Beams	140	0.903

Table 3.10: Shear Hinge Properties of Frame-B

Members	Exterior		Interior	
	V_u (kN)	δ_u (mm)	V_u (kN)	δ_u (mm)
Ground Story Columns	95	0.56	113	0.67
First Story Columns	89	0.375	103	0.434
Second Story Columns	83	0.351	93	0.391
Third Story Column	77	0.326	83	0.35
Fourth Story Column	71	0.301	73	0.309
Beams	40	0.228	40	0.228

Table 4.1: Lateral Strength (kN) of Frame-A and Frame-B

Design Case	Frame-A			Frame-B		
	Bare	Stilt	Infill	Bare	Stilt	Infill
GRAV	6.9	15.2	21.3	9.1	14.9	49.0
EQ2	10.7	19.0	24.3	14.0	18.4	51.9
EQ3	15.3	22.7	27.9	16.9	18.7	53.2
EQ5	36.1	37.5	42.7	35.2	35.5	68.7
EQC3	-	34.1	-	-	40.9	-
EQCB3	-	37.4	-	-	51.9	-

Table 4.2: Maximum Roof Displacement (%H) of Frame-A and Frame-B

Design Case	Frame-A			Frame-B		
	Bare	Stilt	Infill	Bare	Stilt	Infill
GRAV	1.73	0.95	1.05	1.16	0.64	0.67
EQ2	3.38	2.09	2.10	1.96	1.47	1.12
EQ3	2.88	1.99	1.99	1.33	1.45	1.11
EQ5	2.79	2.07	2.07	1.36	1.05	1.25
EQC3	-	2.45	-	-	1.03	-
EQCB3	-	2.24	-	-	0.96	-

Table 4.3: Initial Lateral Stiffness (kN/mm) of Frame-A and Frame-B

Design Case	Frame-A			Frame-B		
	Bare	Stilt	Infill	Bare	Stilt	Infill
GRAV	5.2	21.5	41.6	3.5	9.6	27.2
EQ2	8.1	28.5	45.0	4.8	12.3	30.9
EQ3	11.1	30.6	47.6	6.7	14.5	32.5
EQ5	19.1	41.7	54.8	13.2	23.9	40.2
EQC3	-	49.9	-	-	22.8	-
EQCB3	-	55.6	-	-	22.9	-

Table 4.4: Ductility of Frame-A and Frame-B

Design Case	Frame-A			Frame-B		
	Bare	Stilt	Infill	Bare	Stilt	Infill
GRAV	4.9	5.1	7.7	4.8	4.4	4.0
EQ2	9.7	11.7	14.6	8.8	10.6	7.3
EQ3	9.0	15.7	19.8	5.7	12.1	7.3
EQ5	5.5	8.6	10.0	5.5	7.6	7.9
EQC3	-	13.4	-	-	6.2	-
EQCB3	-	12.5	-	-	4.6	-

Table 4.5: Column Overstrength Factor (COF) of Frame-A and Frame-B

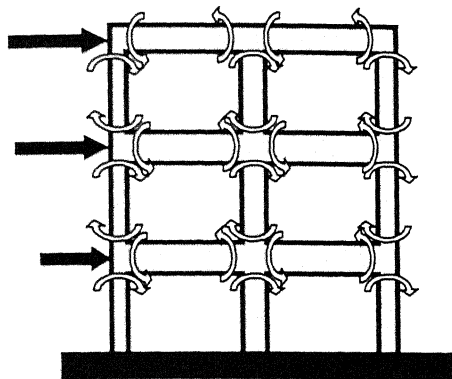
Design Case	Frame-A			Frame-B		
	M _{yc}	M _{yb}	COF	M _{yc}	M _{yb}	COF
GRAV	211	70	3.0	96	41	2.3
EQ2	279	104	2.7	102	79	1.3
EQ3	354	167	2.1	111	91	1.2
EQ5	594	511	1.2	231	275	0.8

Table 4.5: Overstrength Factor of Frame-A and Frame-B

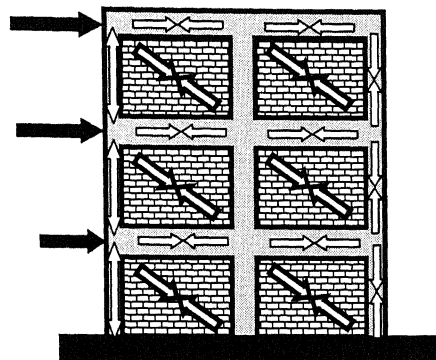
Design Case	Frame-A			Frame-B		
	Bare	Stilt	Infill	Bare	Stilt	Infill
GRAV	-	-	-	-	-	-
EQ2	4.3	7.6	9.7	5.6	7.4	20.8
EQ3	3.8	5.7	7.0	4.2	4.7	13.3
EQ5	4.0	4.2	4.7	3.9	3.9	7.6

Table 4.6: Ground Story Lateral Stiffness (kN/mm) of Frame-A and Frame-B

Design Case	Frame-A			Frame-B		
	Bare	Stilt	Infill	Bare	Stilt	Infill
GRAV	32	39	149	13	14	139
EQ2	53	65	172	18	19	147
EQ3	66	77	182	23	24	152
EQ5	106	119	222	46	48	178

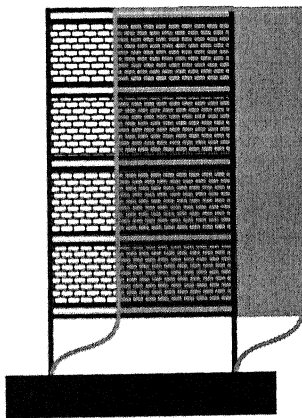


(a) Bare frame:
Predominant frame action

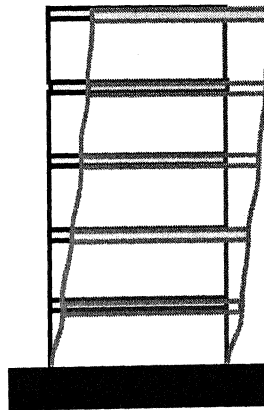


(b) Infilled frame:
Predominant shear action

Fig. 1.1: Contrasting structural behavior of buildings without and with unreinforced masonry infill walls (Murty et al., 2002)

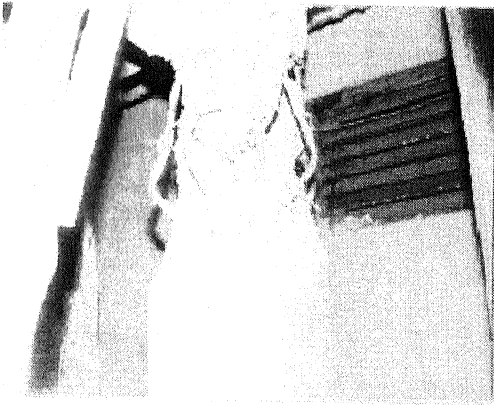


(a) Open ground story

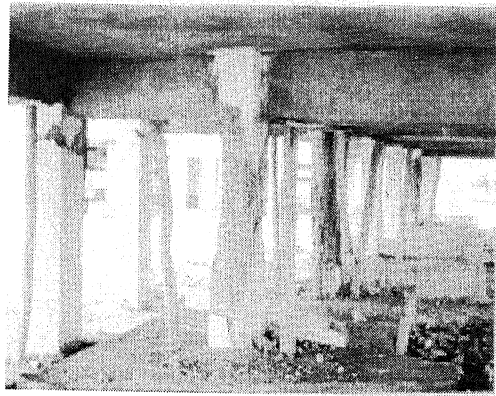


(b) Bare frame

Fig. 1.2: Soft story is subject to severe deformation demands during earthquake shaking (Murty et al., 2002)



(a) Damage to column in Himgiri apartment



(b) Damage to columns of Youth Hostel building

Fig. 1.3: Damage to ground story columns in stilt buildings (Arlekar et al., 1997)



Fig. 1.4: Soft story mechanism formed after the fall out of the infill in the bottom two stories (Mistakidis, et al., 2000)



(a) Concentration of damage in bottom 2-stories



(b) Collapse in bottom 2-stories

Fig. 1.5: Multistory RC frame with masonry infill near Golcuk
(Dolsek et al., 2001)

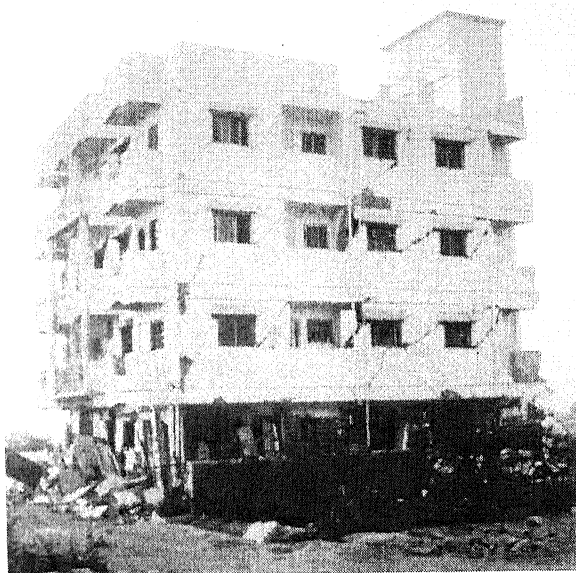


Fig. 1.6: Completely infilled RC frame sustained uniform damage
(Murty et al., 2002)



Fig. 1.7: Four-story building with infilled ground story had minor cracking at frame-infill interface (Murty et al., 2002)

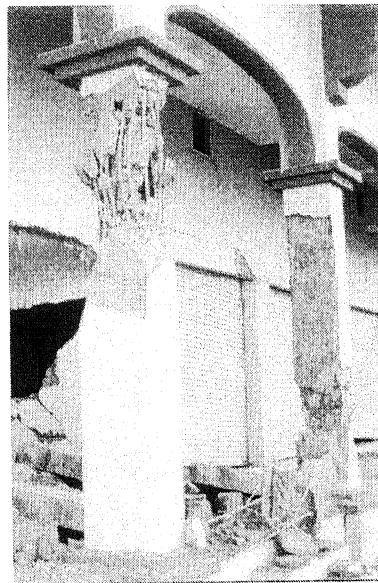
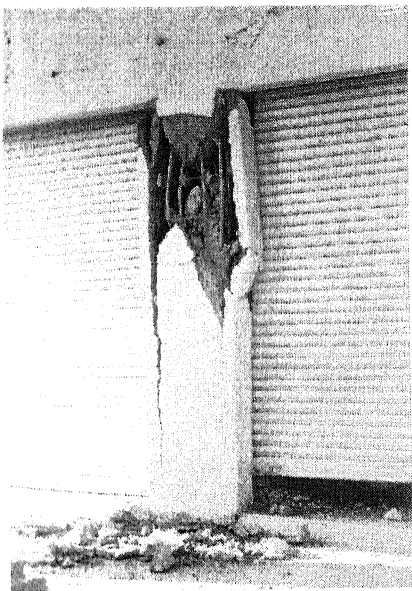


Fig. 1.8: Severe damage to the ground story columns in the open ground story building (Murty et al., 2002)

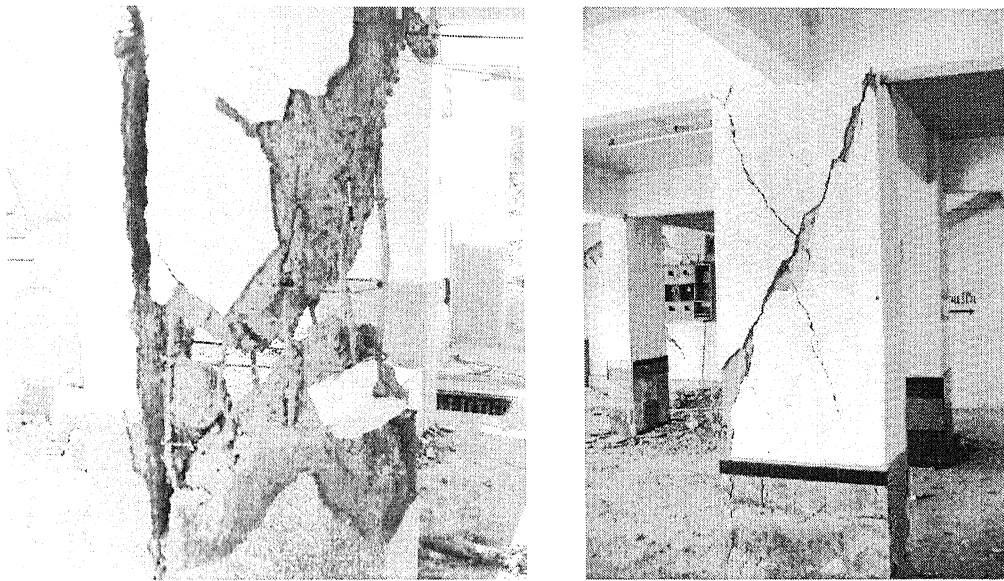


Fig. 1.9: Shear cracking of non-ductile columns of an open ground story building in Bhuj (Murty et al., 2002)



(a) Soft ground story building



(b) Damage to column in Fig. (a)

Fig. 1.10: Damage of ground story columns of stilt building (Ellul et al., 2003)



Fig. 1.11: Collapse of the ground floor where three shops were operating
(Ellul et al., 2003)

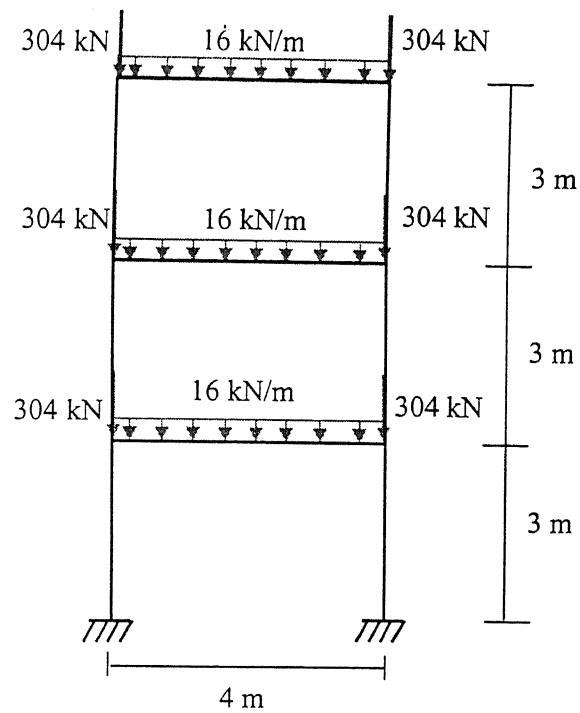


Fig. 2.1: Dead Load on frame-A

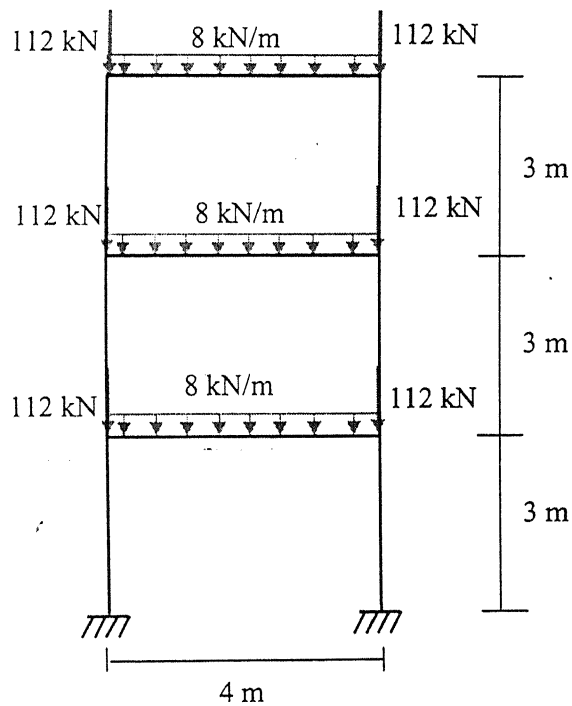


Fig. 2.2: Imposed Load on frame-A

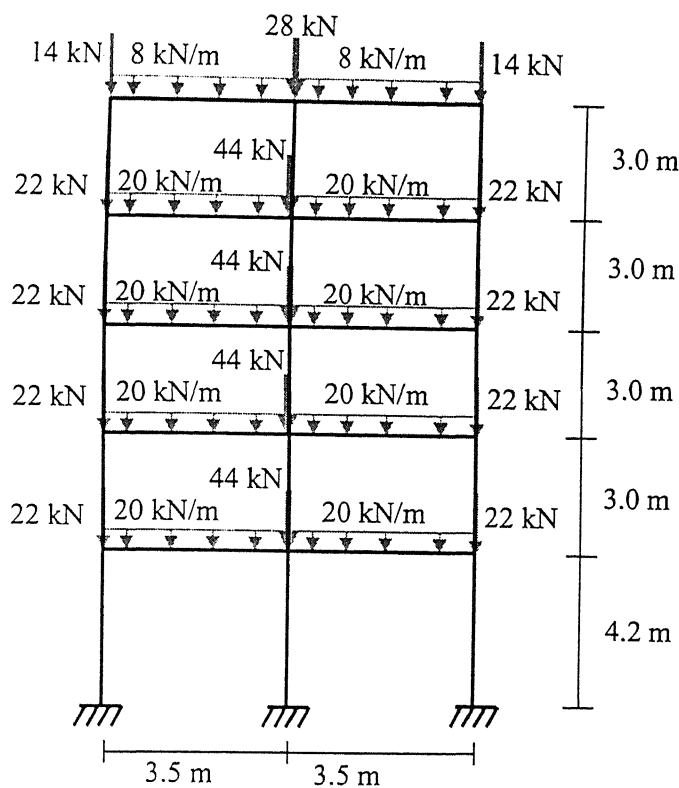


Fig. 2.3: Dead Load on frame-B

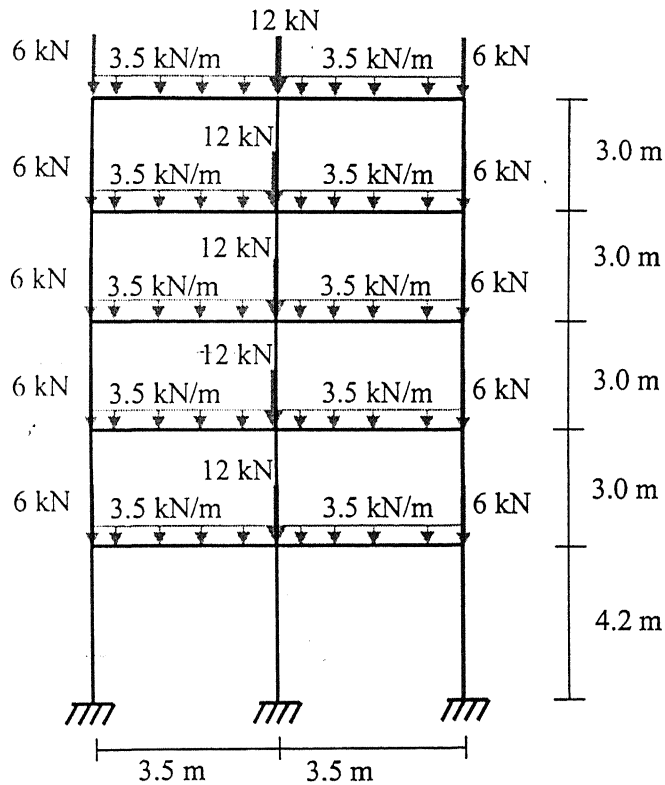


Fig. 2.4: Imposed Load on frame-B

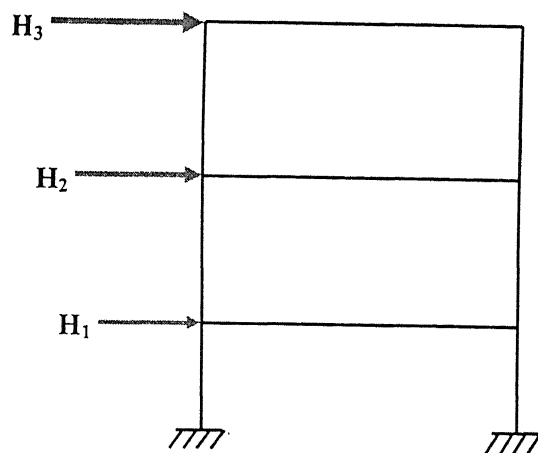


Fig. 2.5: Base Shear Distribution in Frame-B

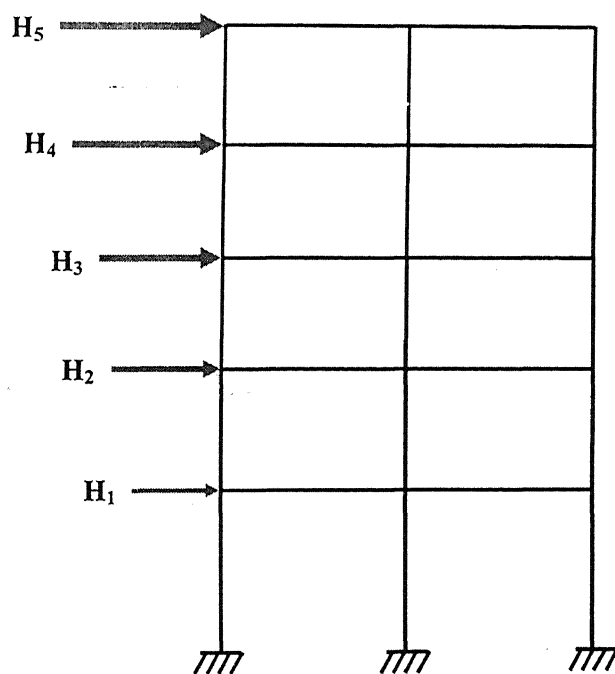


Fig. 2.6: Base Shear Distribution in Frame-B

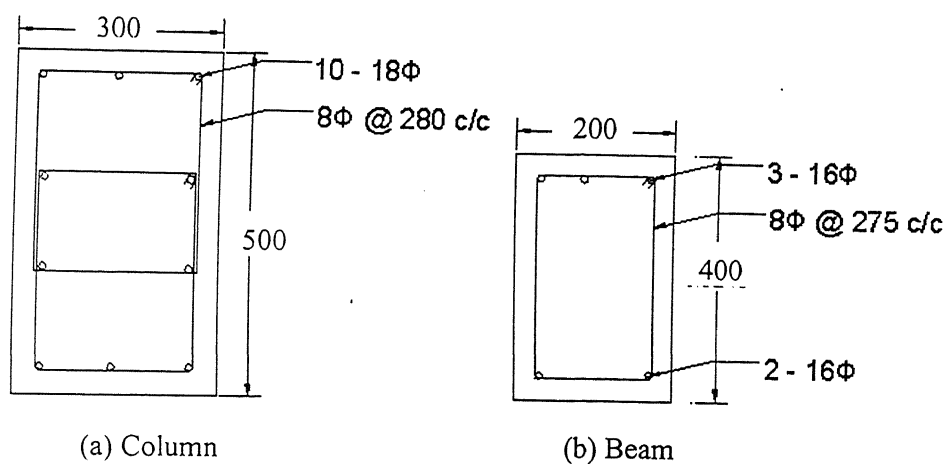


Fig. 2.7: Cross section of frame-A in GRAV case

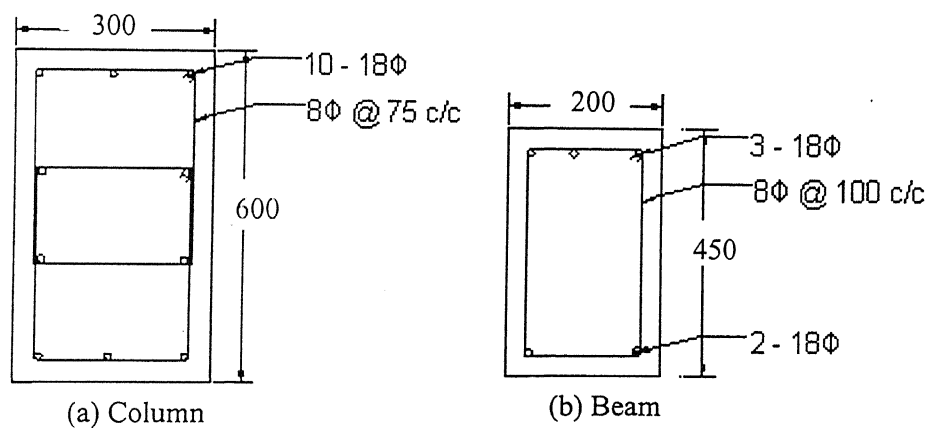


Fig. 2.8: Cross section of frame-A in EQ2 case

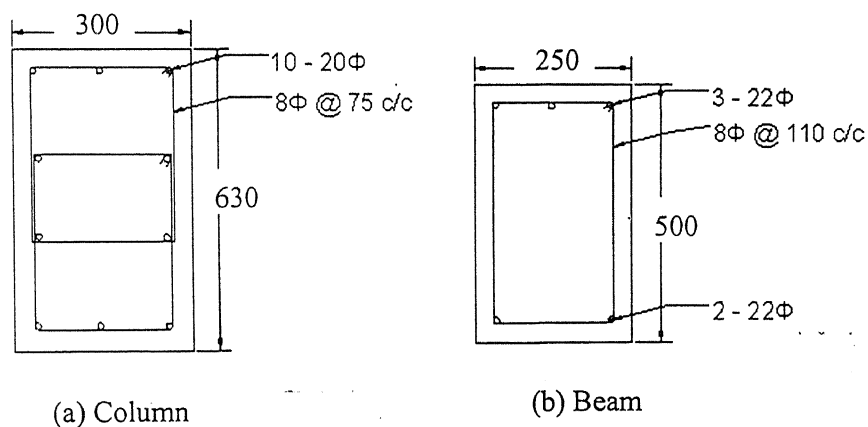


Fig. 2.9: Cross section of frame-A in EQ3 case

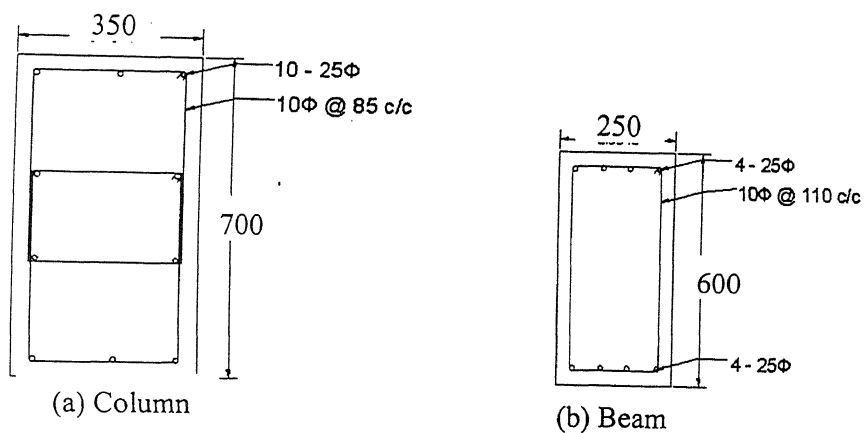


Fig. 2.10: Cross section of frame-A in EQ5 case

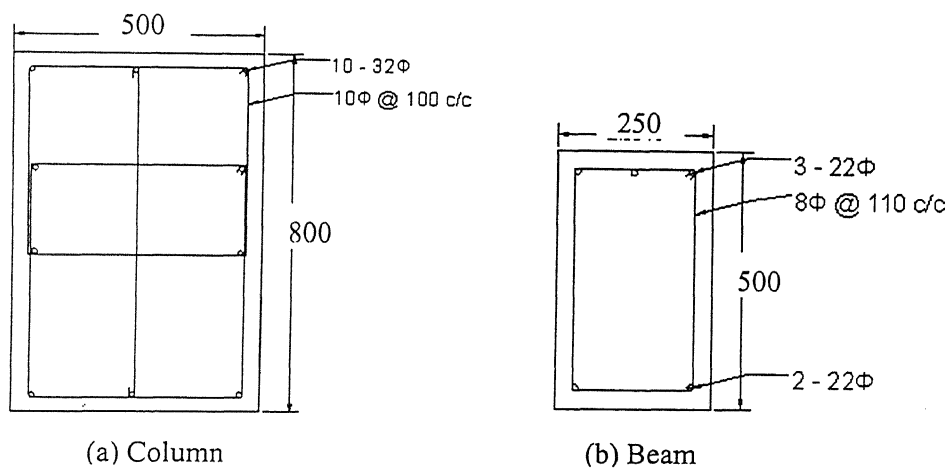


Fig. 2.11: Cross section of frame-A in EQC3 case

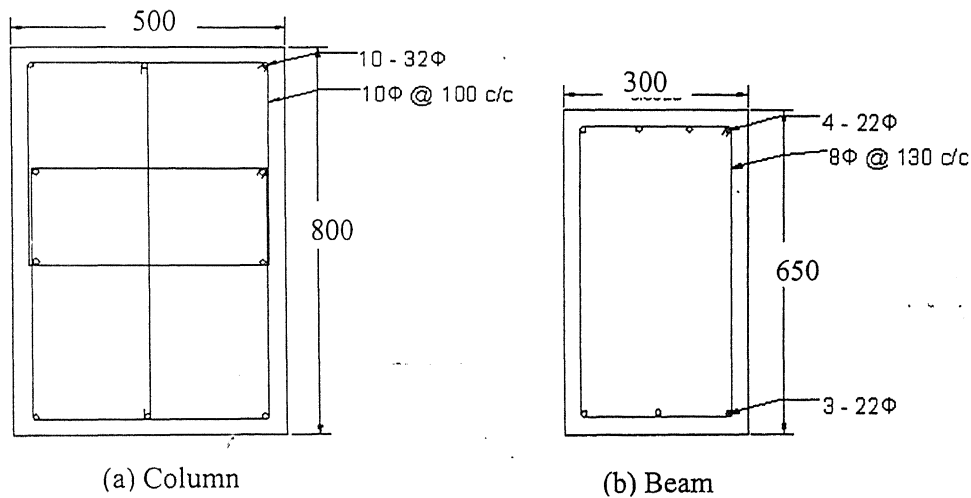


Fig. 2.12: Cross section of frame-A in EQCB3

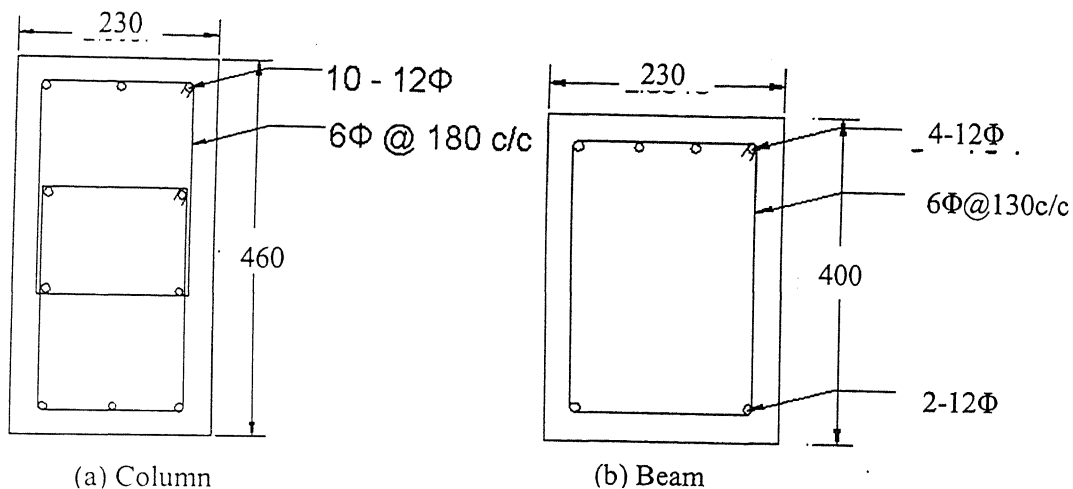


Fig. 2.13: Cross section of frame-B in GRAV case

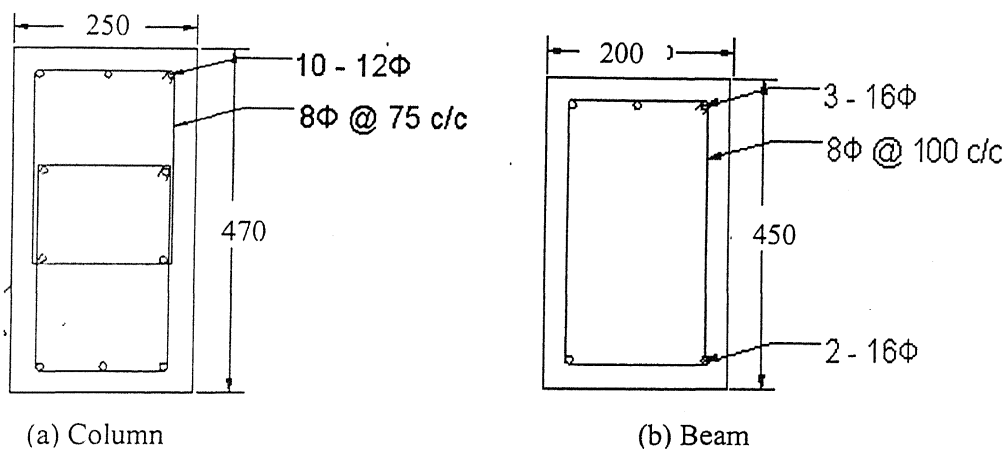


Fig. 2.14: Cross section of frame-B in EQ2 case

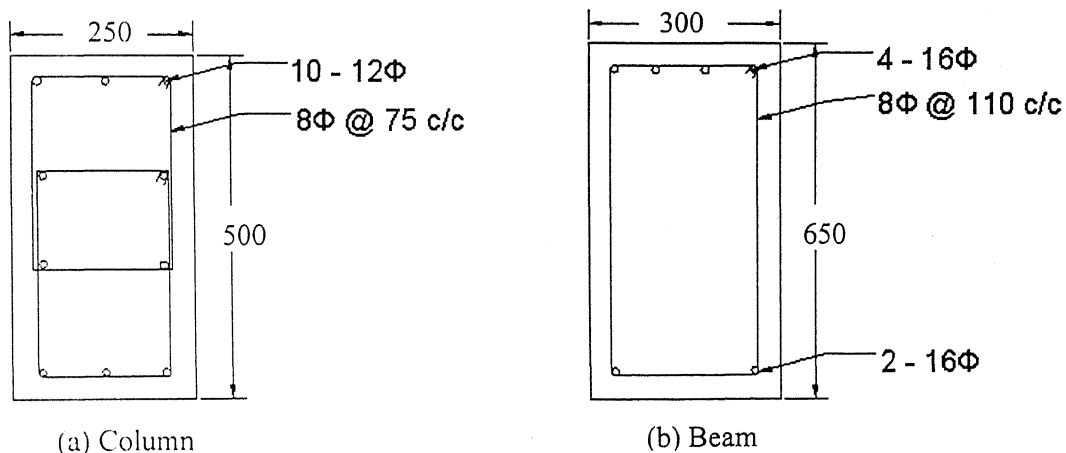


Fig. 2.15: Cross section of frame-B in EQ3 case

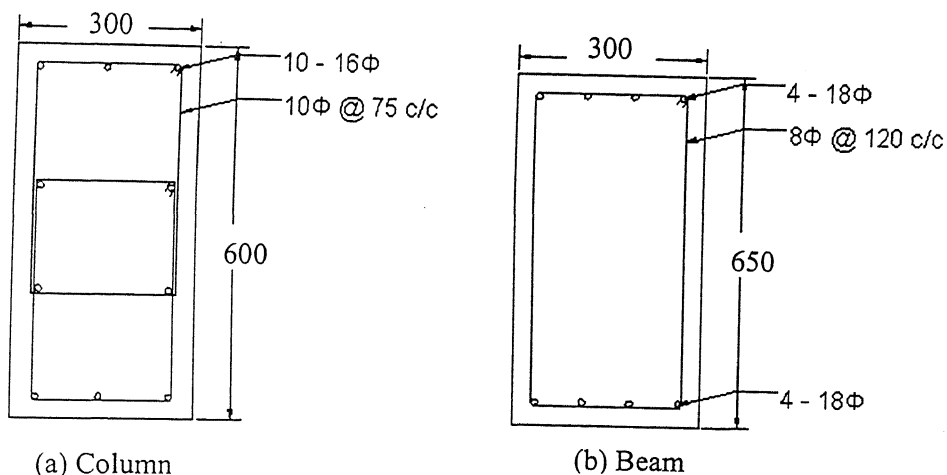


Fig. 2.16: Cross section of frame-B in EQ5 case

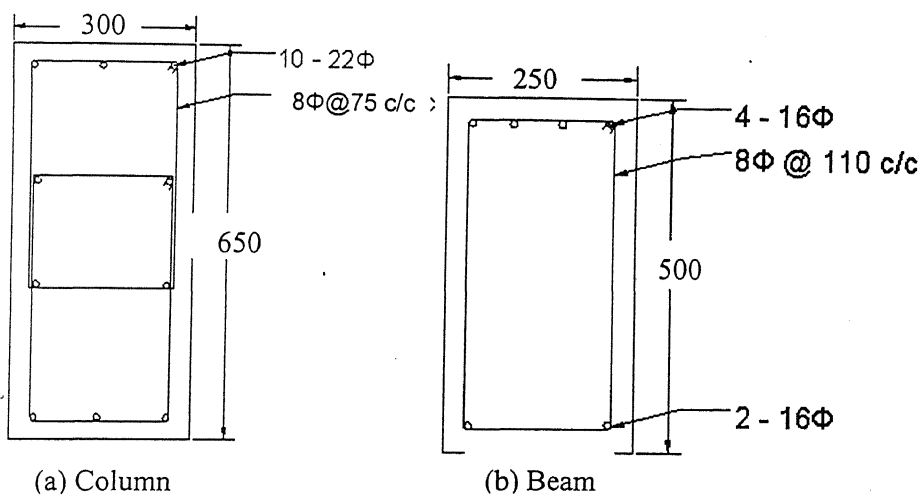


Fig. 2.17: Cross section of frame-B in EQC3 case

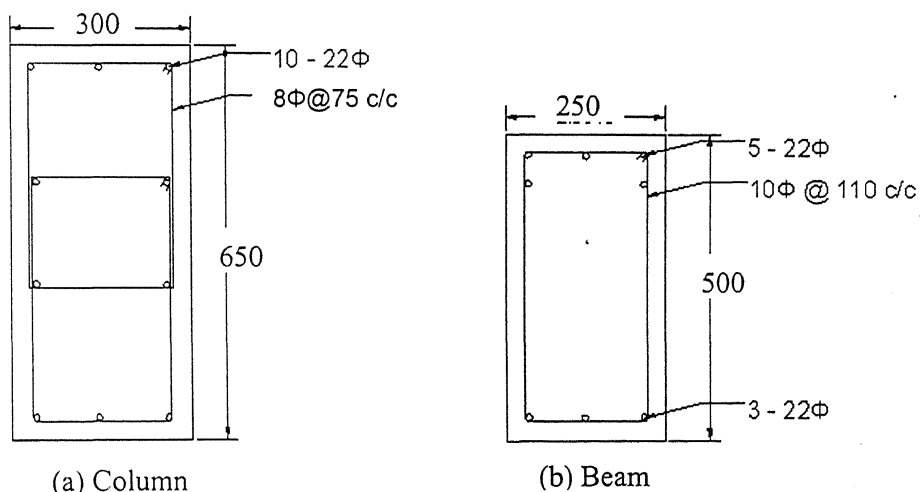


Fig. 2.18: Cross section of frame-B in EQCB3

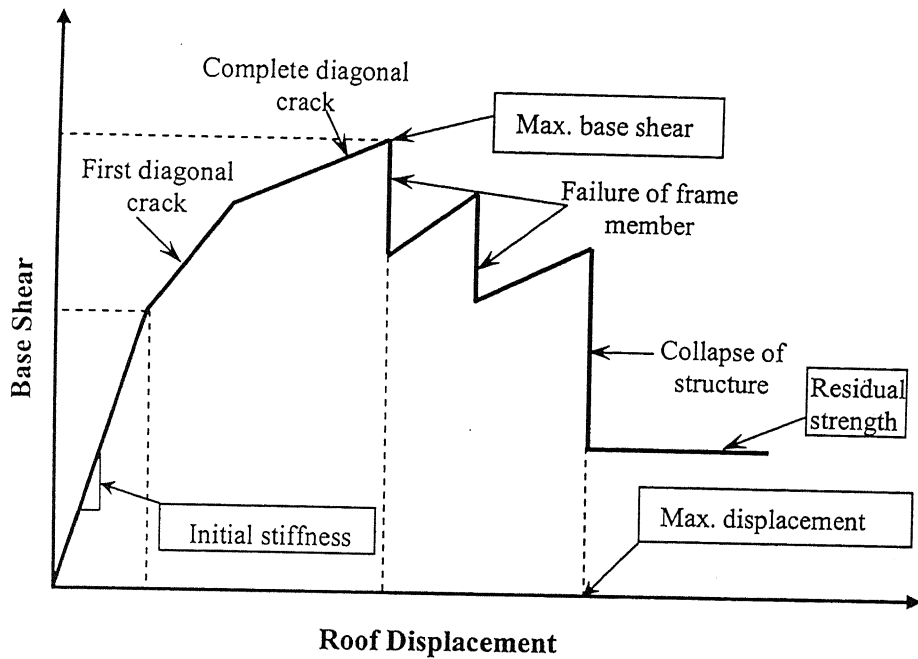


Fig. 3.1: Idealized pushover curve with salient features for infilled frame structure

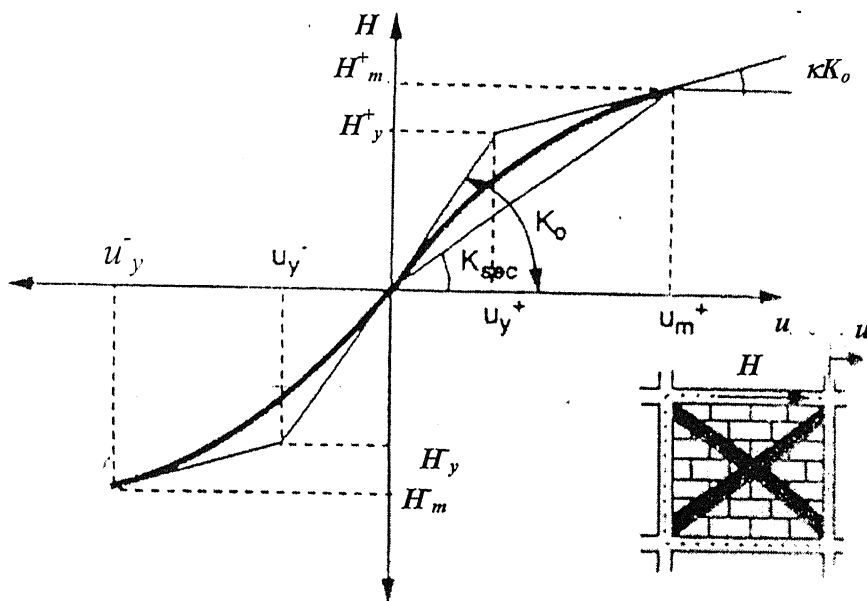


Fig. 3.2: Load-deformation relationship by Reinhorn et al. [Reinhorn et al., 1995]

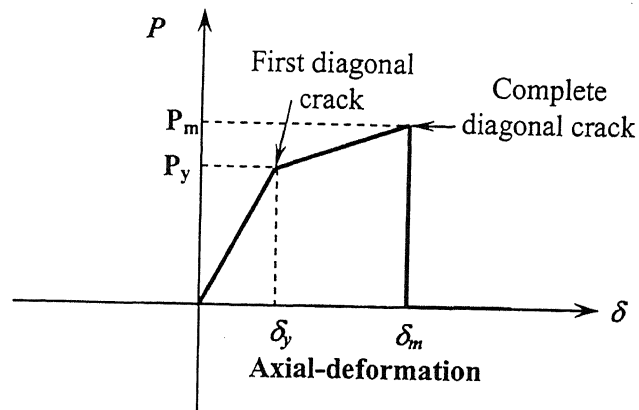


Fig. 3.3: Idealized axial load-axial deformation relationship for equivalent diagonal strut [Das, 2000]

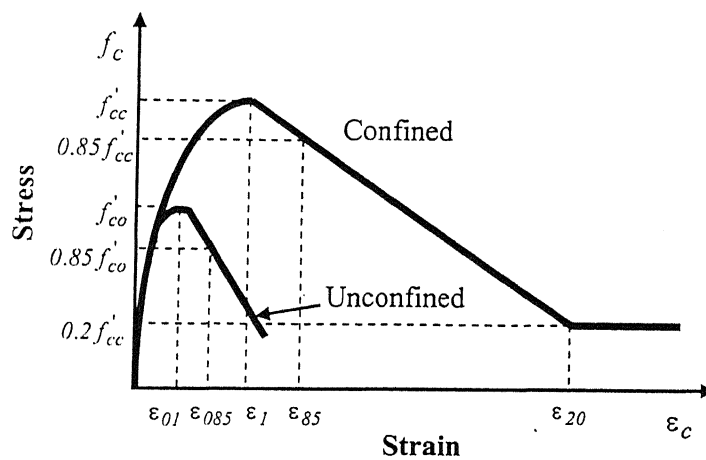


Fig. 3.4: Stress-strain curve for confined concrete [Razvi et al., 1999]

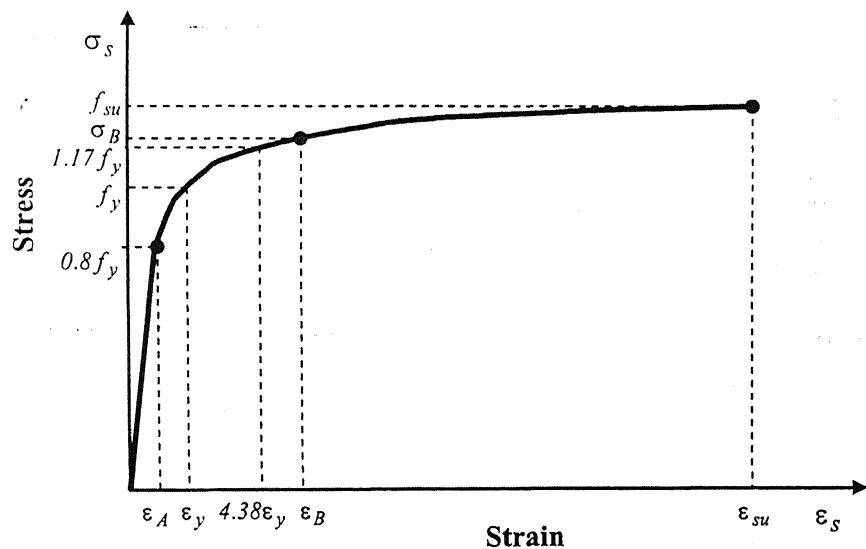


Fig. 3.5: Stress-strain curve of HYSD steel bars [Dasgupta, 2000]

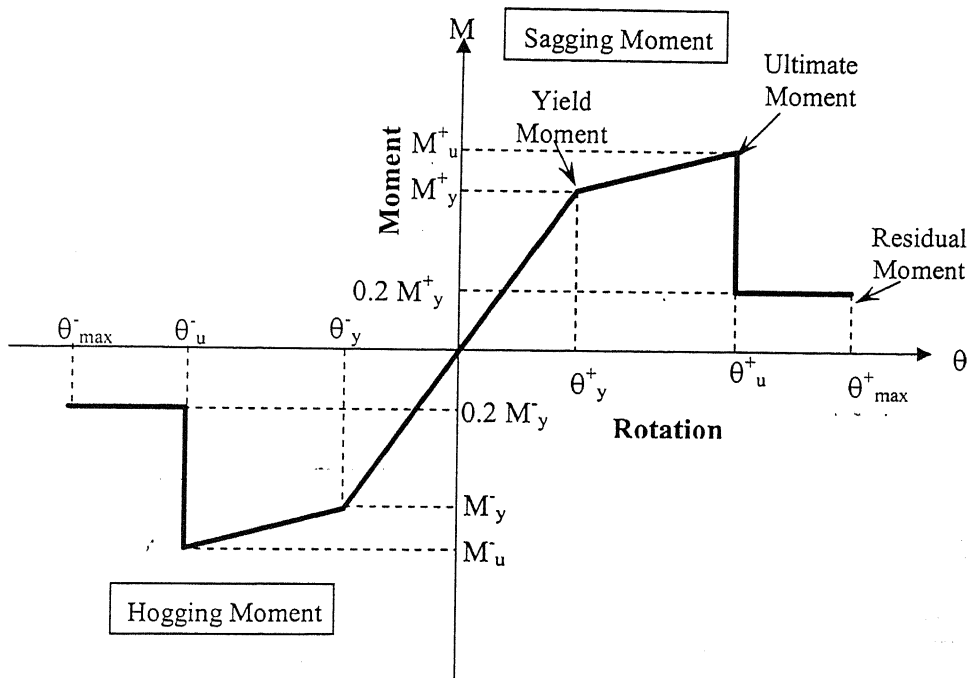


Fig. 3.6: Moment-rotation relationship for frame members [FEMA 273]

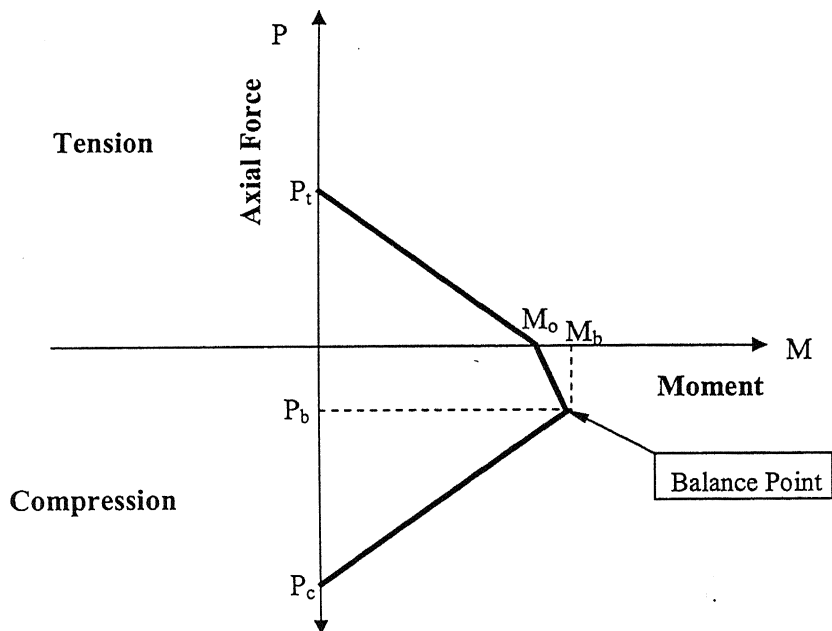


Fig. 3.7: Axial force-moment interaction curve for columns

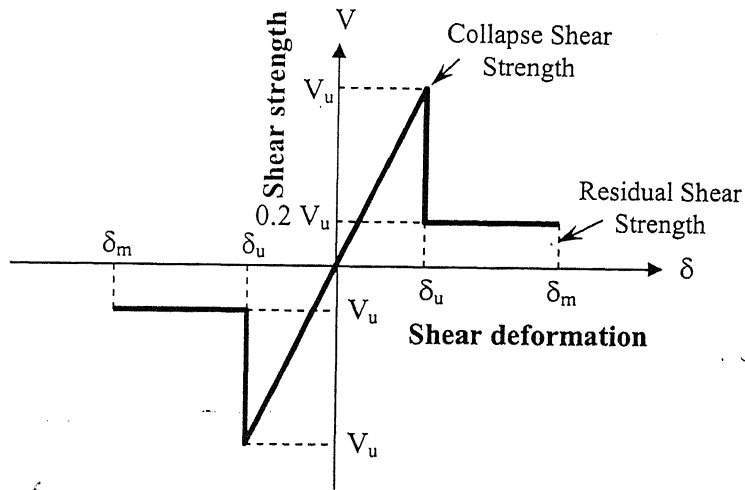


Fig. 3.8: Shear strength - shear deformation relationship for frame members [FEMA 273]

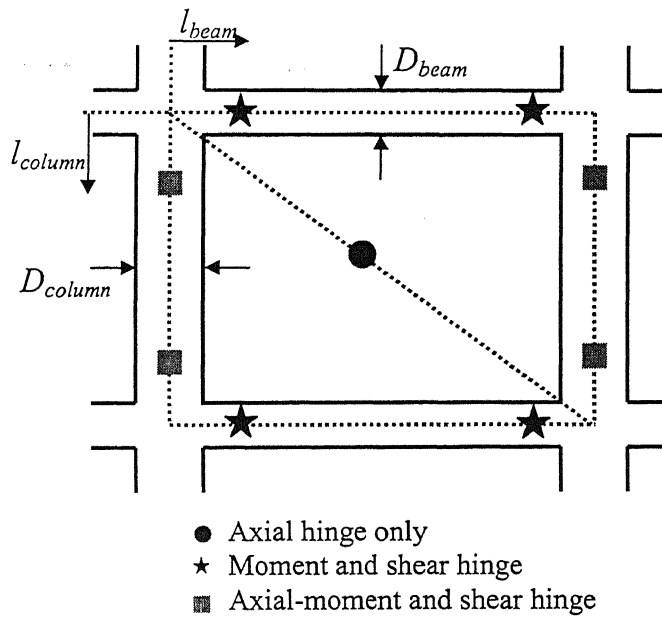


Fig. 3.9: Type and location of hinges in infilled frame

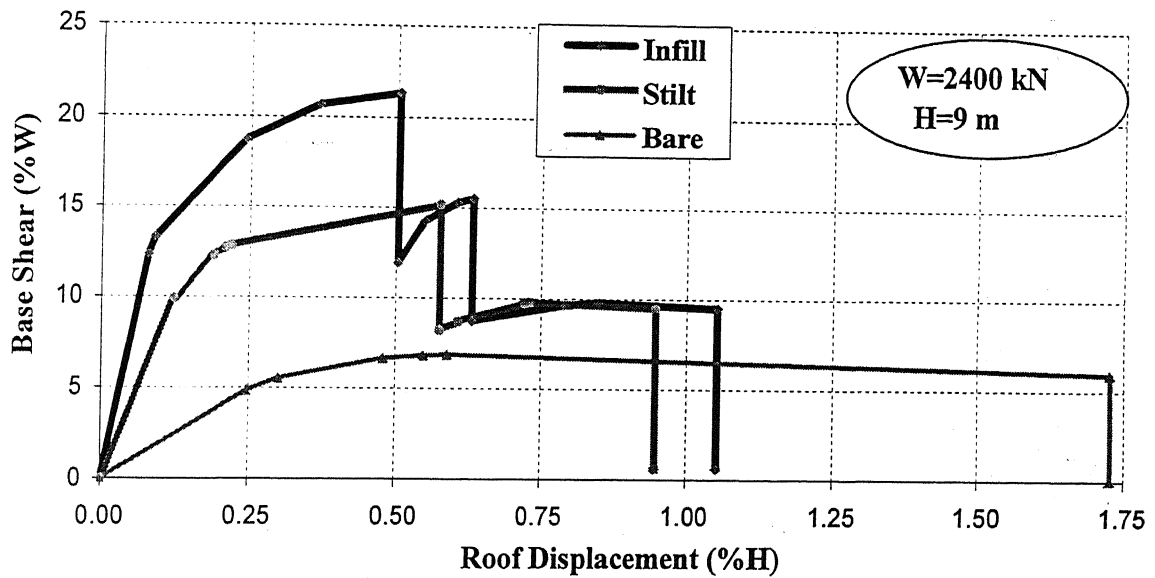


Fig. 4.1: Pushover curve of frame-A design case GRAV

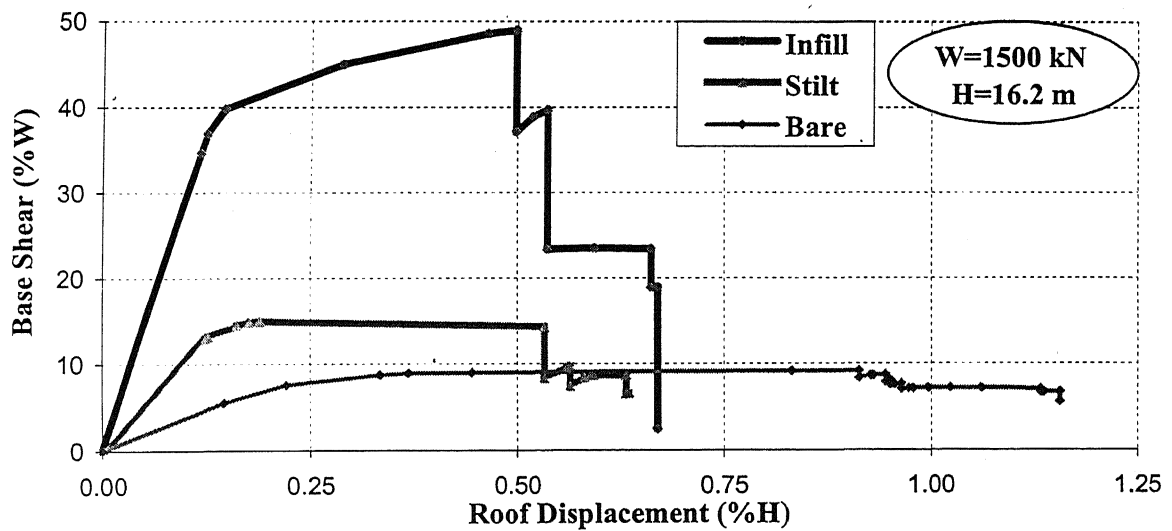


Fig. 4.2: Pushover curve of frame-B design case GRAV

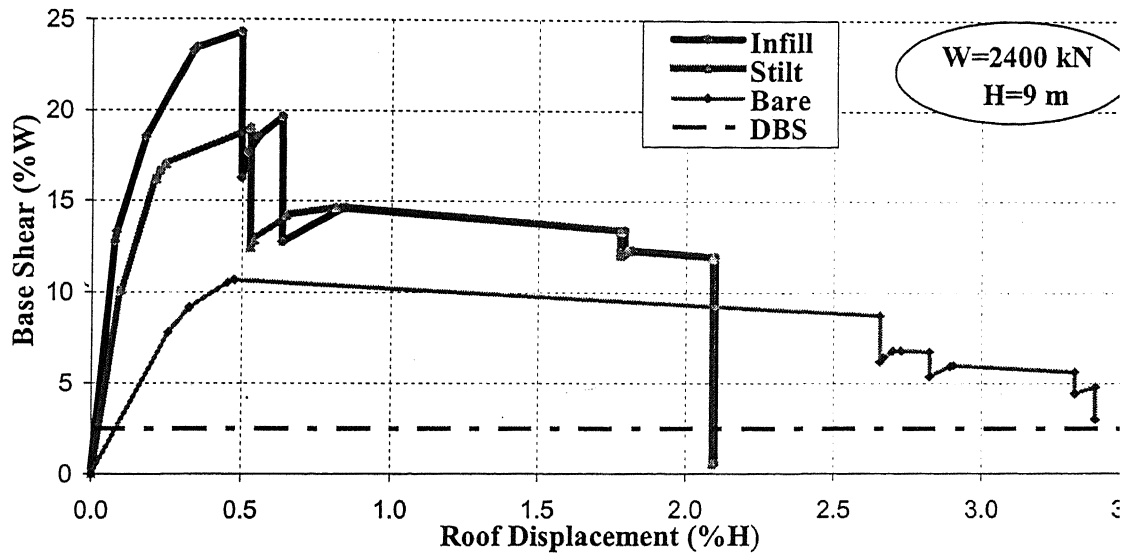


Fig. 4.3: Pushover curve of frame-A design case EQ2

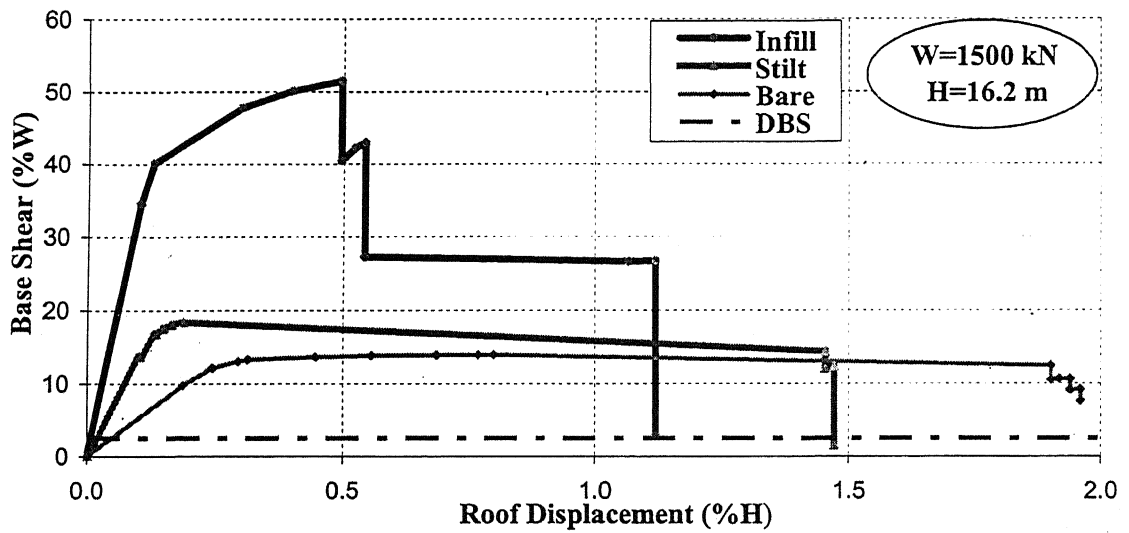


Fig. 4.4: Pushover curve of frame-B design case EQ2

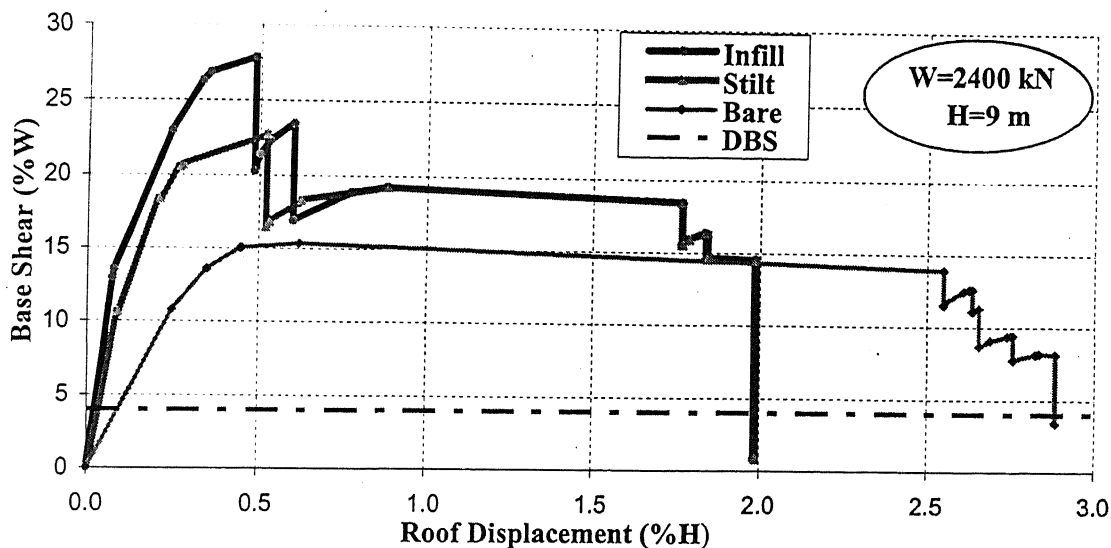


Fig. 4.5: Pushover curve of frame-A design case EQ3

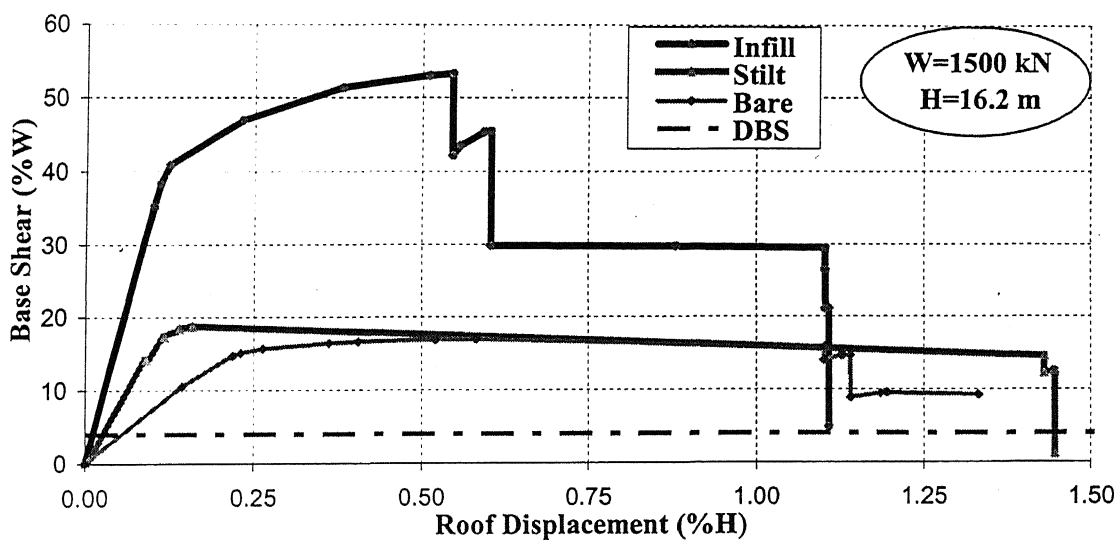


Fig. 4.6: Pushover curve of frame-B design case EQ3

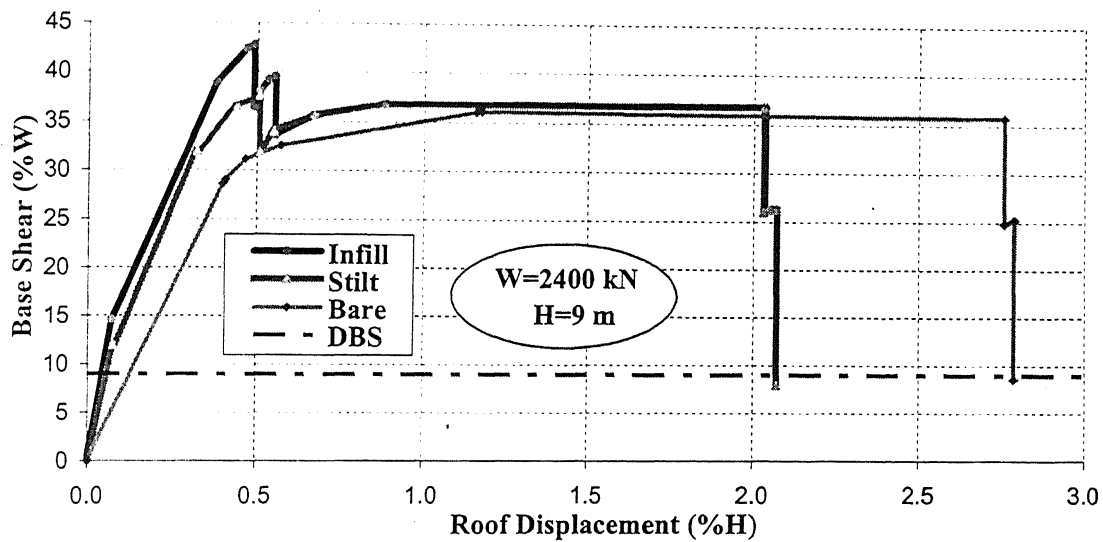


Fig. 4.7: Pushover curve of frame-A design case EQ5

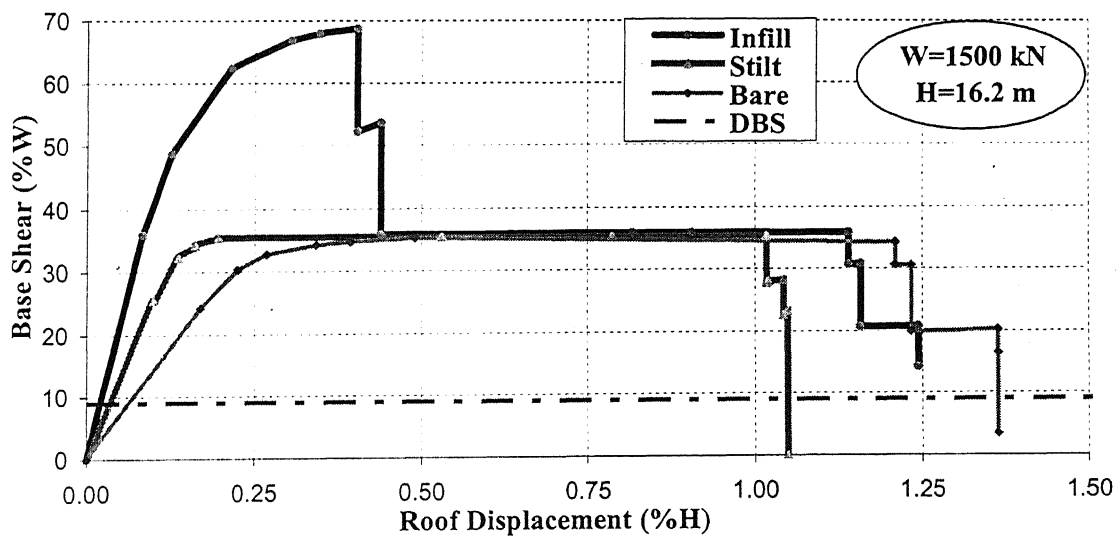


Fig. 4.8: Pushover curve of frame-B design case EQ5

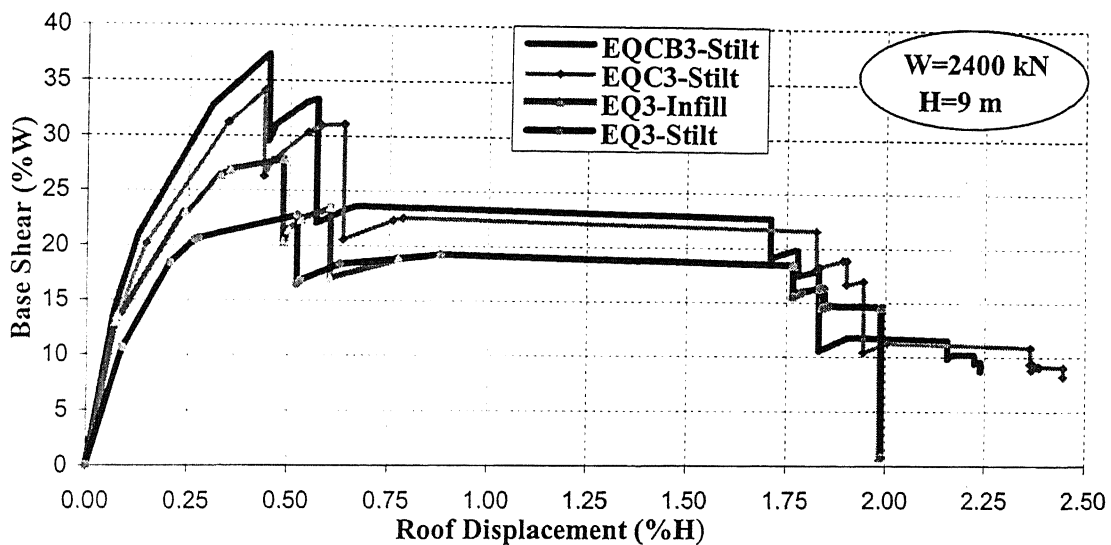


Fig. 4.9: Pushover curve of stilt and infill frames of frame-A

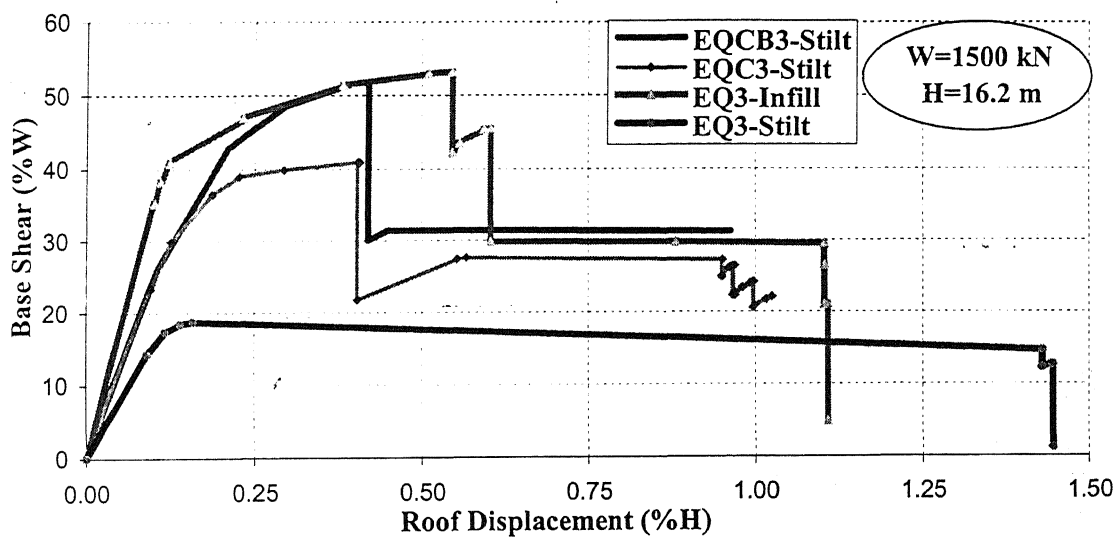


Fig. 4.10: Pushover curve of stilt and infill frames of frame-B

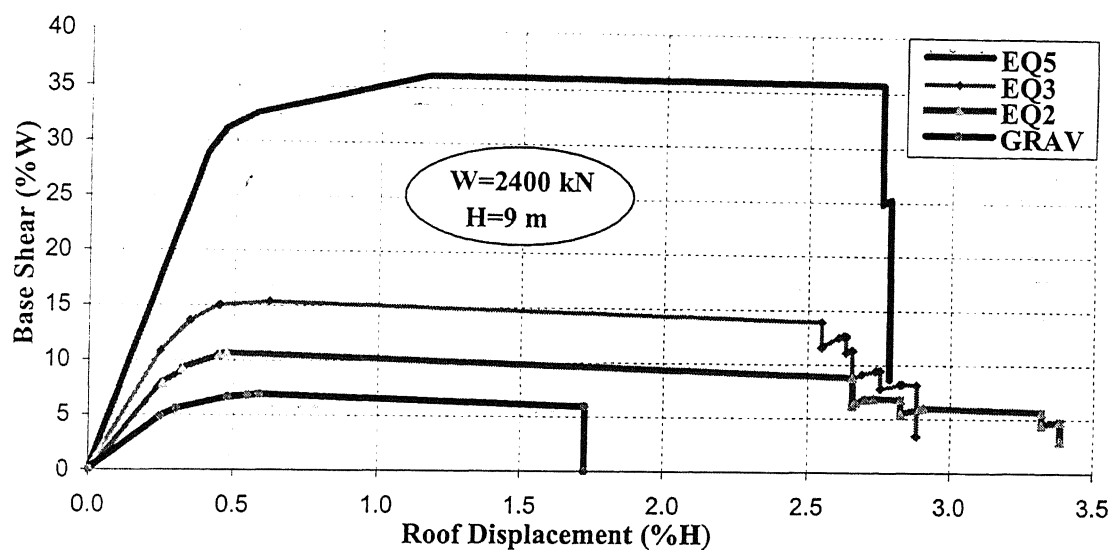


Fig. 4.11: Pushover curve of bare frames of frame-A

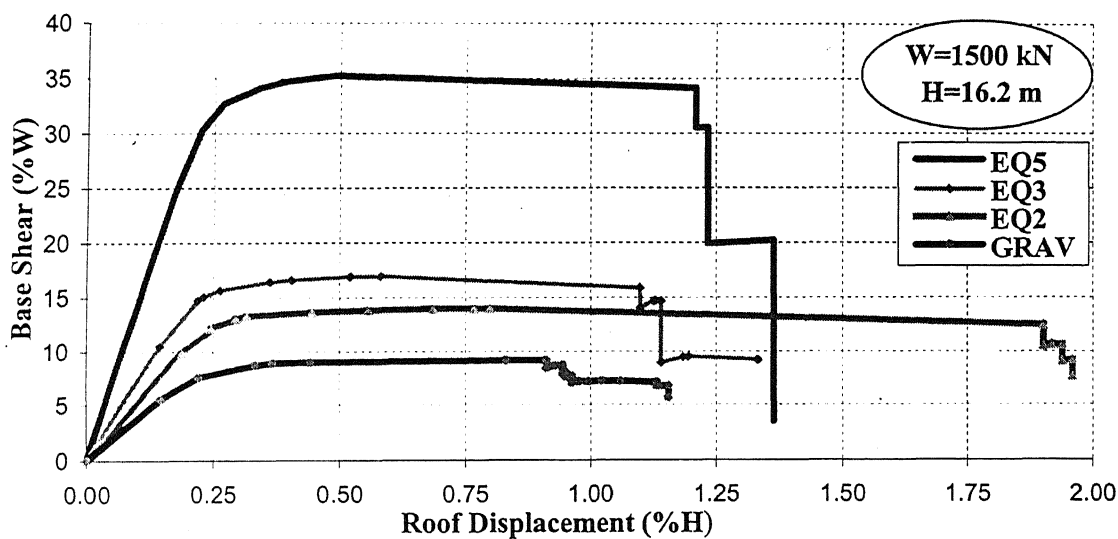


Fig. 4.12: Pushover curve of bare frames of frame-B

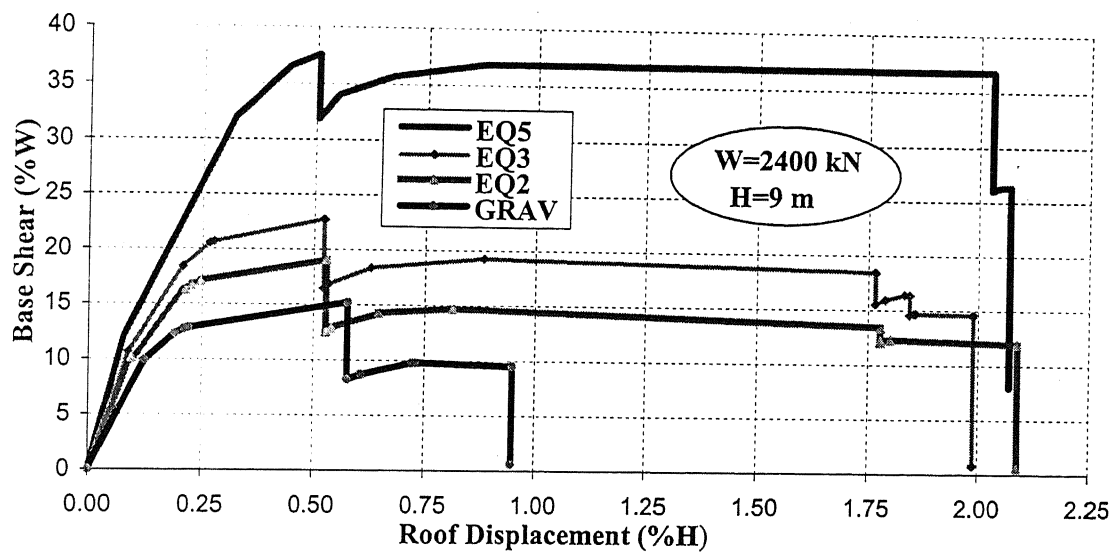


Fig. 4.13: Pushover curve of stilt frames of frame-A

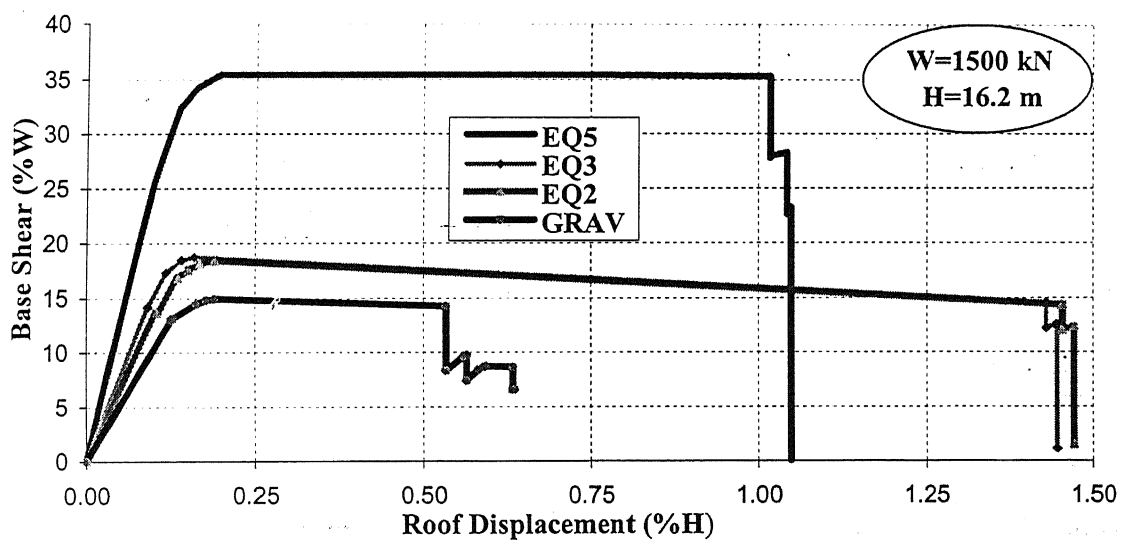


Fig. 4.14: Pushover curve of stilt frames of frame-B

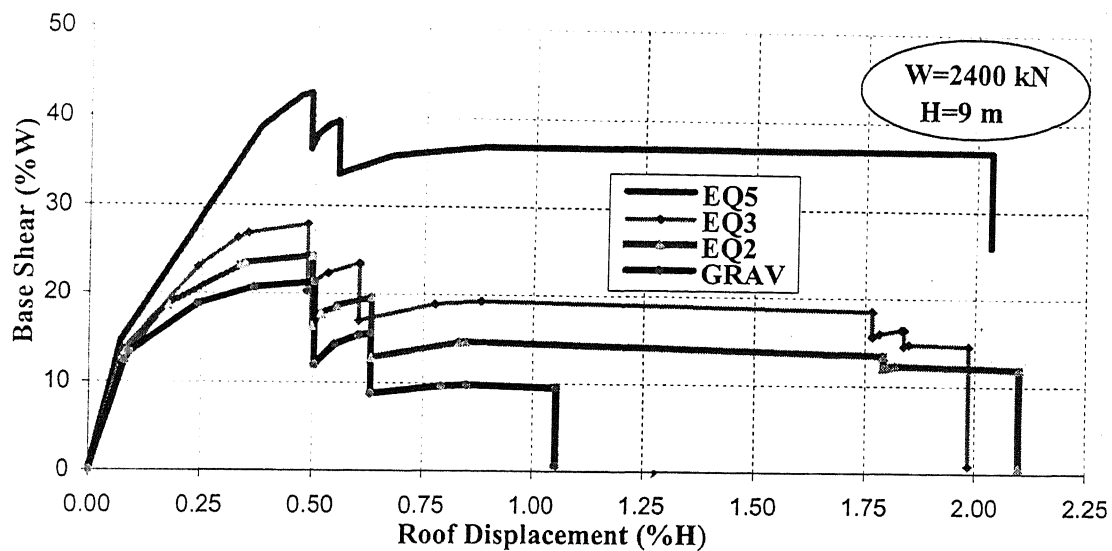


Fig. 4.15: Pushover curve of infill frames of frame-A

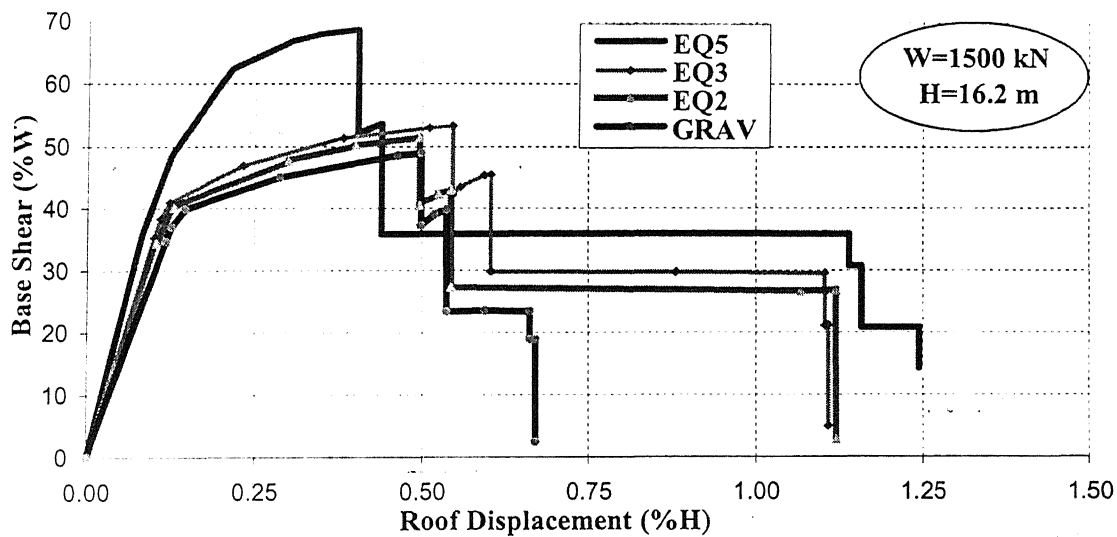


Fig. 4.16: Pushover curve of infill frames of frame-B

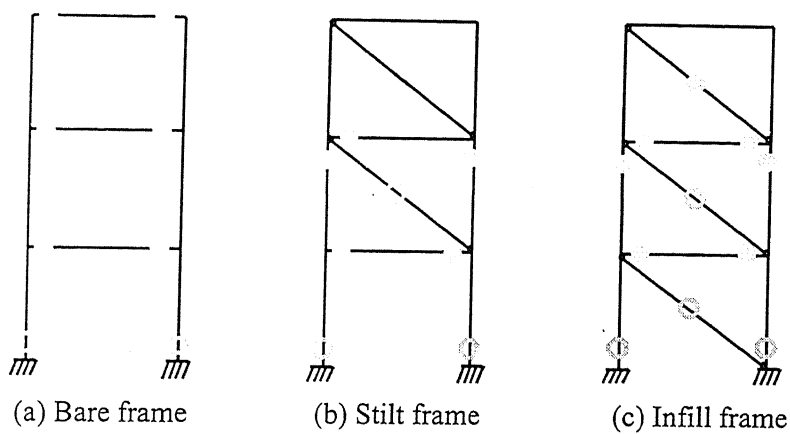


Fig. 4.17: Location of hinges at failure in frame-A of design case GRAV

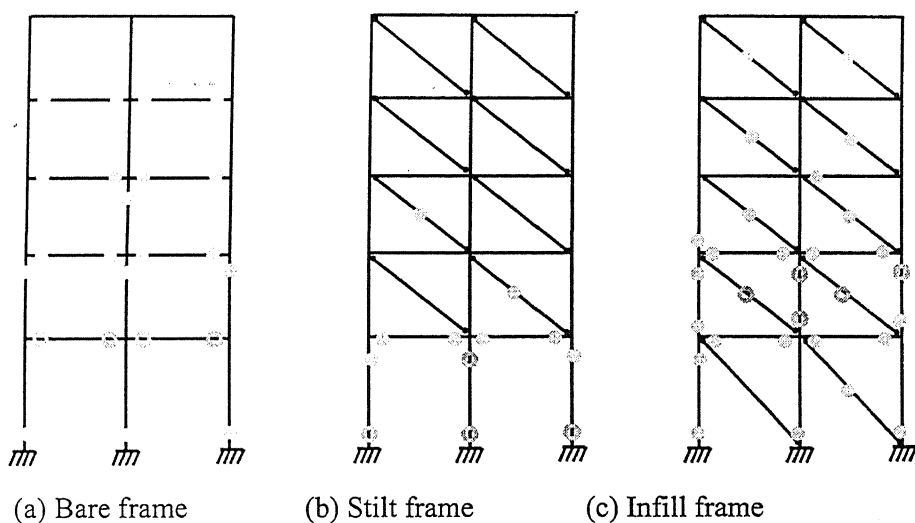


Fig. 4.18: Location of hinges at failure in frame-B of design case GRAV

In strain hardening region
 Failed

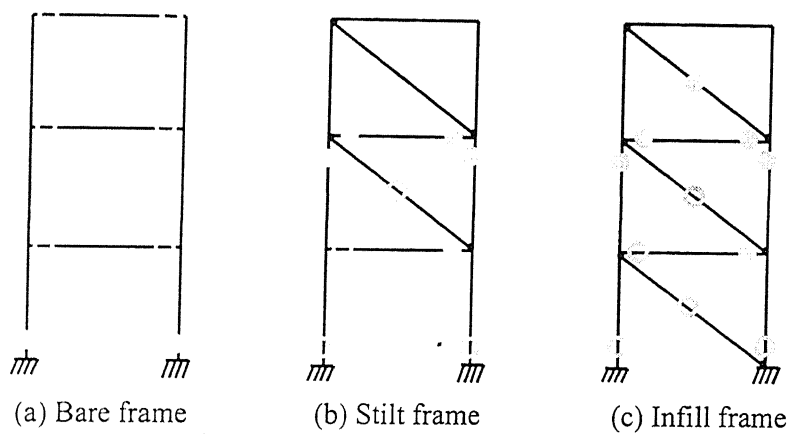


Fig. 4.19: Location of hinges at failure in frame-A of design case EQ2

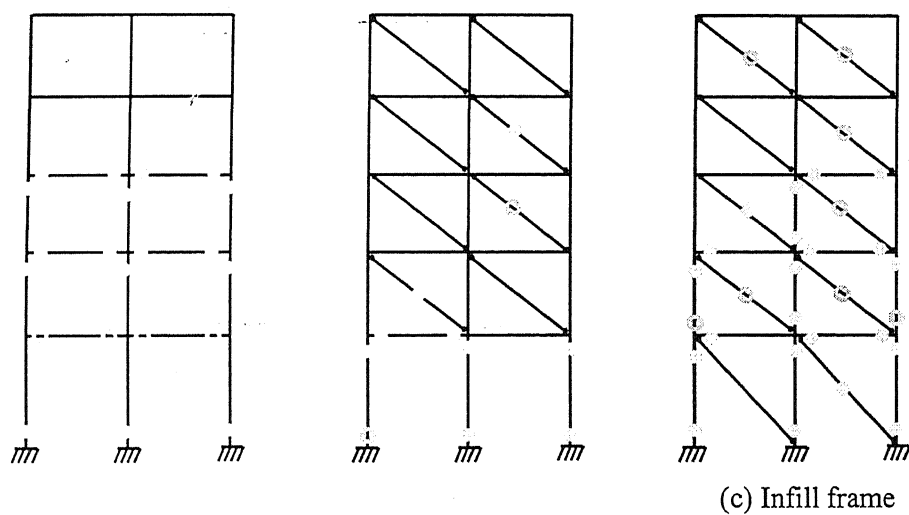


Fig. 4.20: Location of hinges at failure in frame-B of design case EQ2

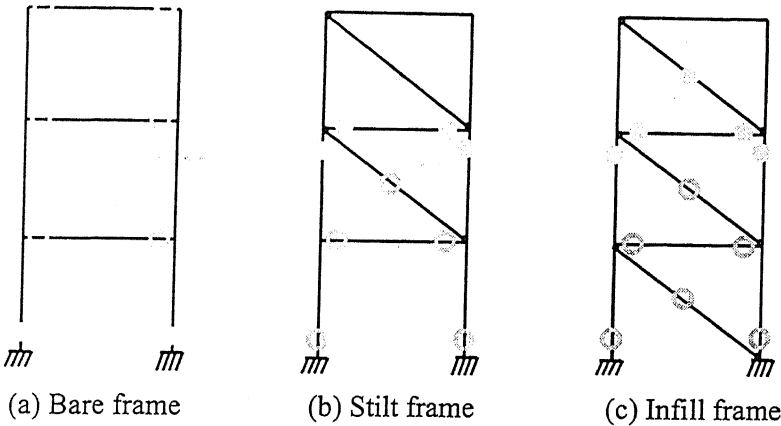


Fig. 4.21: Location of hinges at failure in frame-A of design case EQ3

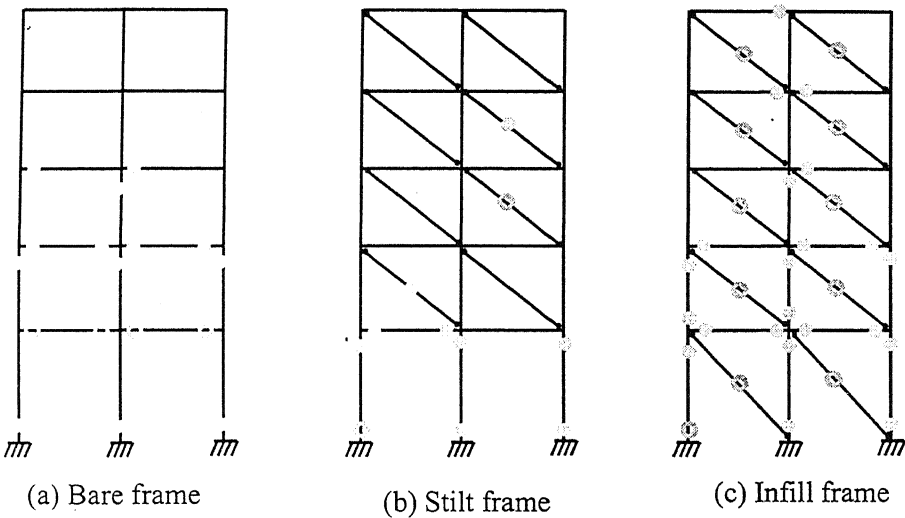


Fig. 4.22: Location of hinges at failure in frame-B of design case EQ3

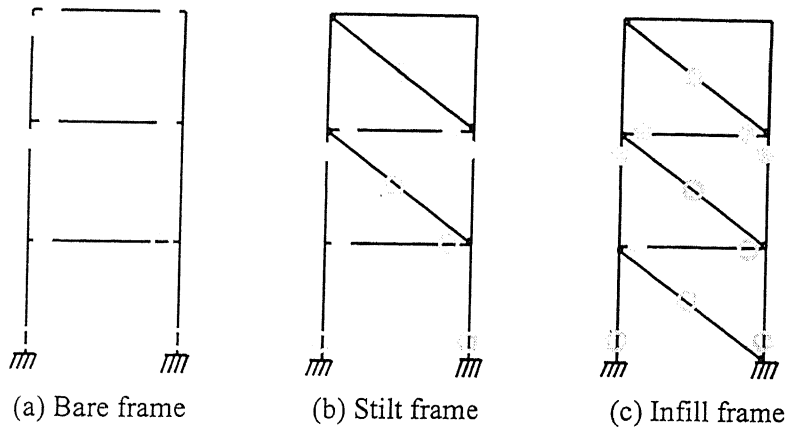


Fig. 4.23: Location of hinges at failure in frame-A of design case EQ5

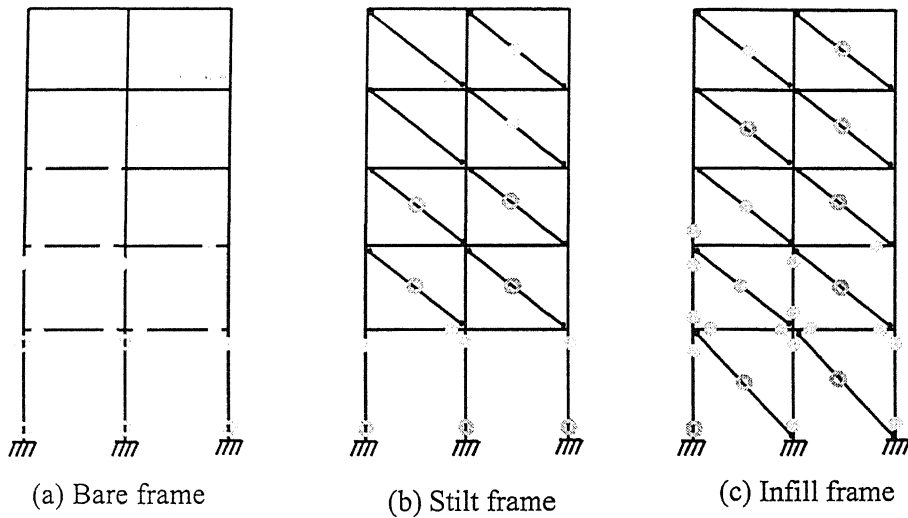


Fig. 4.24: Location of hinges at failure in frame-B of design case EQ5

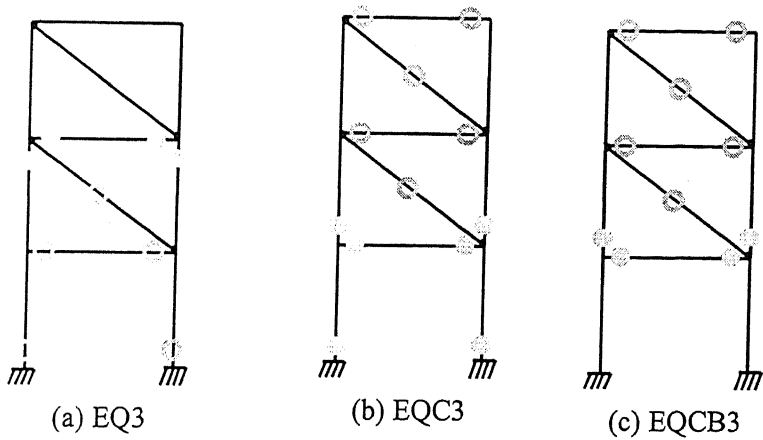


Fig. 4.25: Location of hinges at failure in stilt frame-A

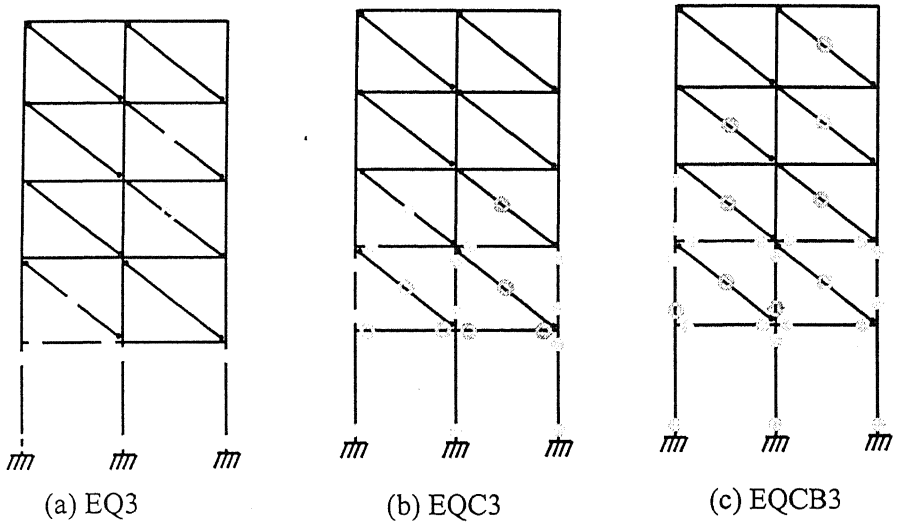


Fig. 4.26: Location of hinges at failure in stilt frame-B

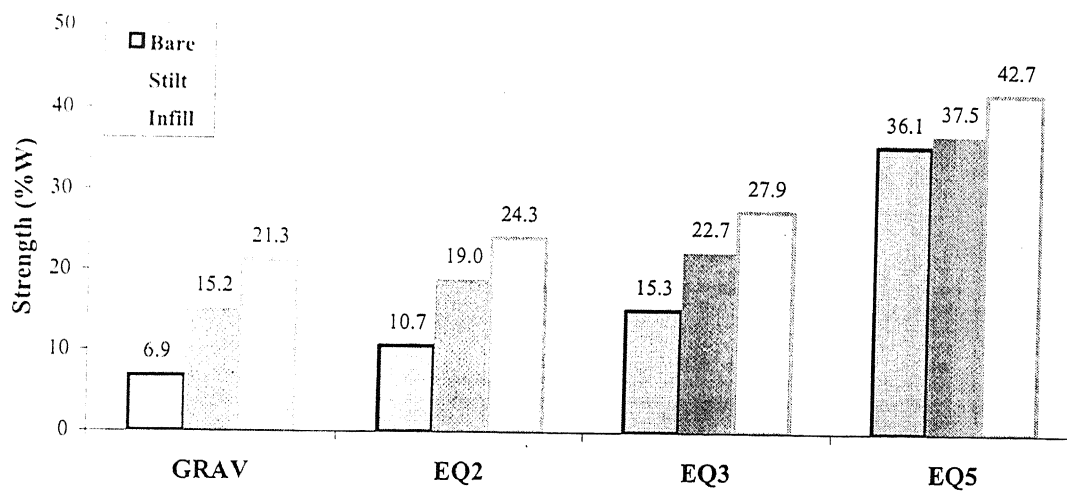


Fig. 4.27: Lateral strength of frame-A

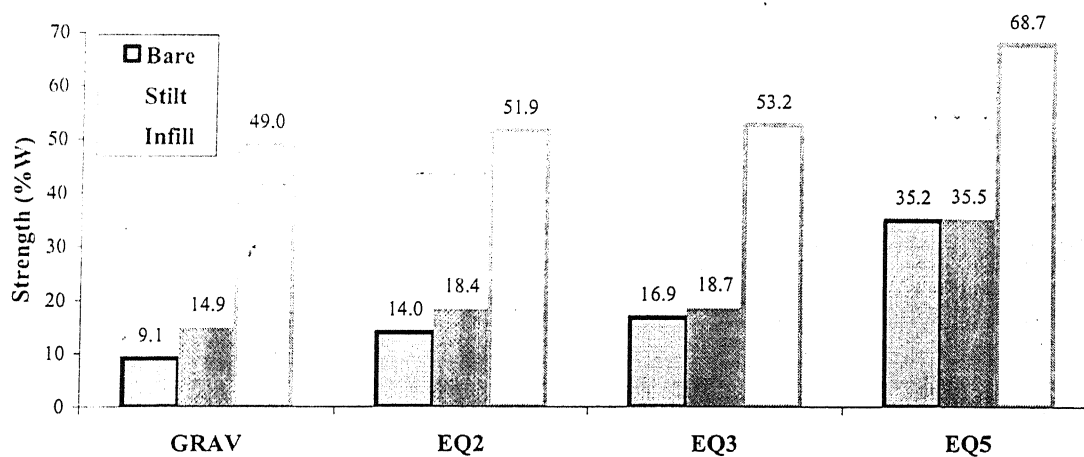


Fig. 4.28: Lateral strength of frame-B

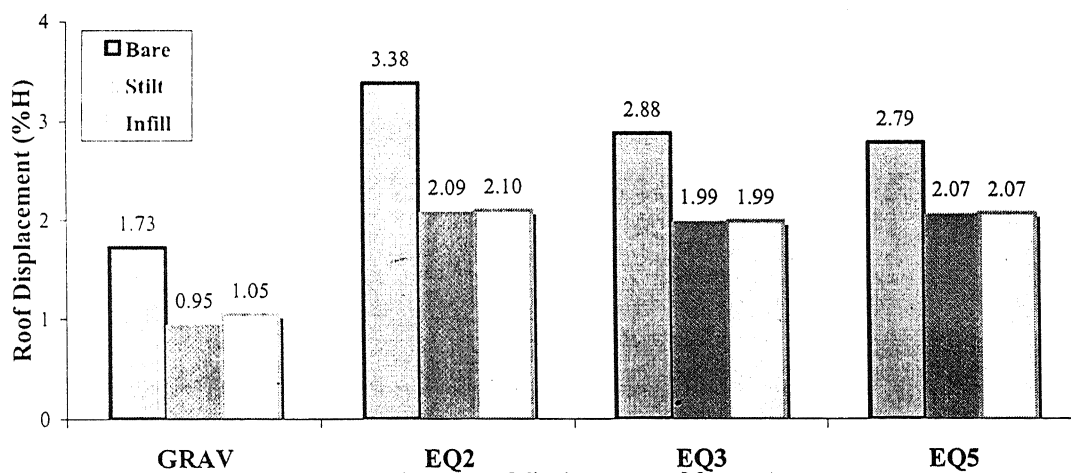
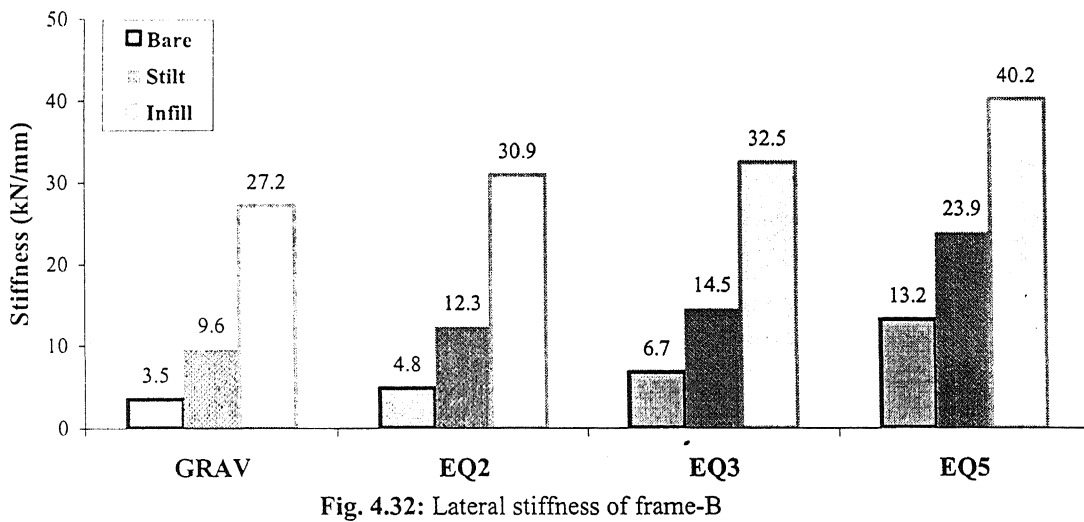
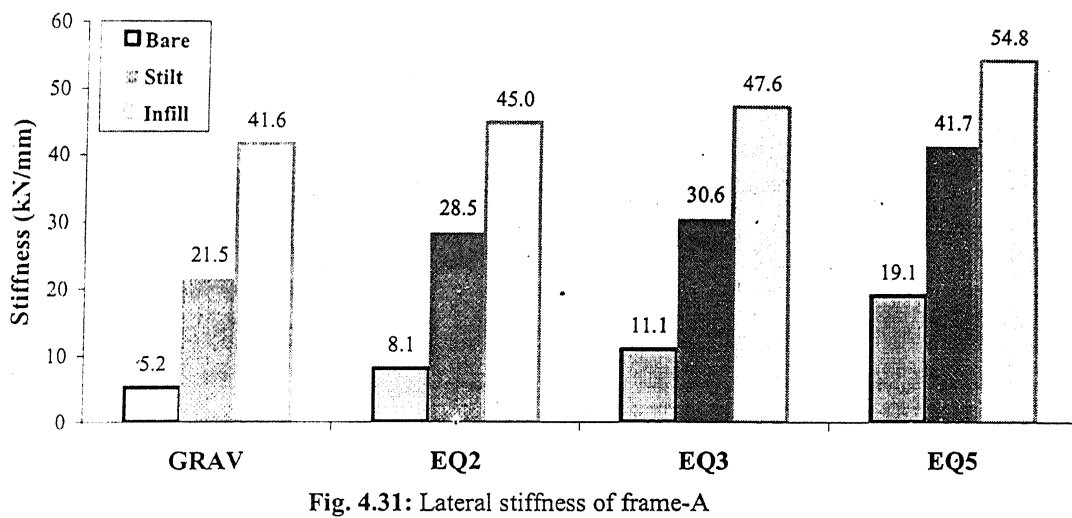
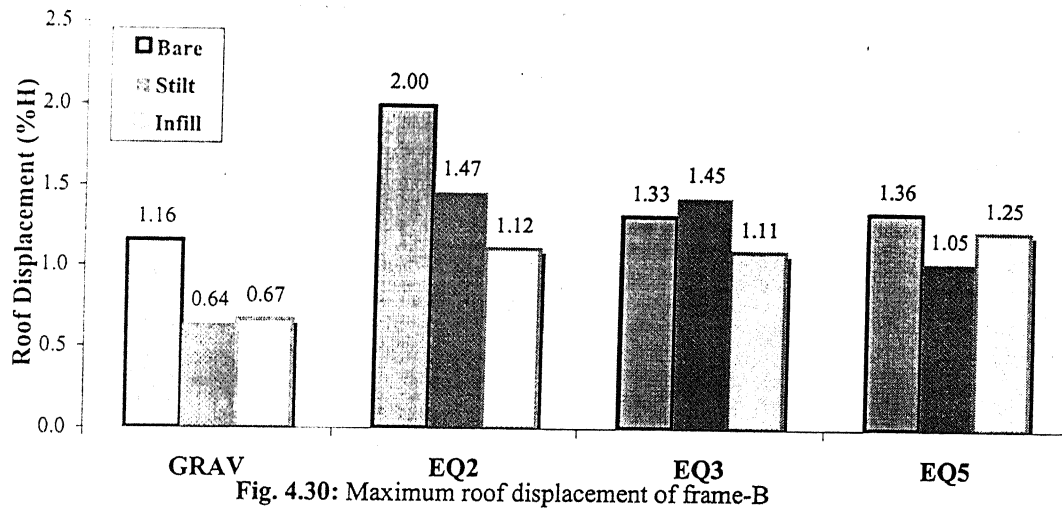


Fig. 4.29: Maximum roof displacement of frame-A



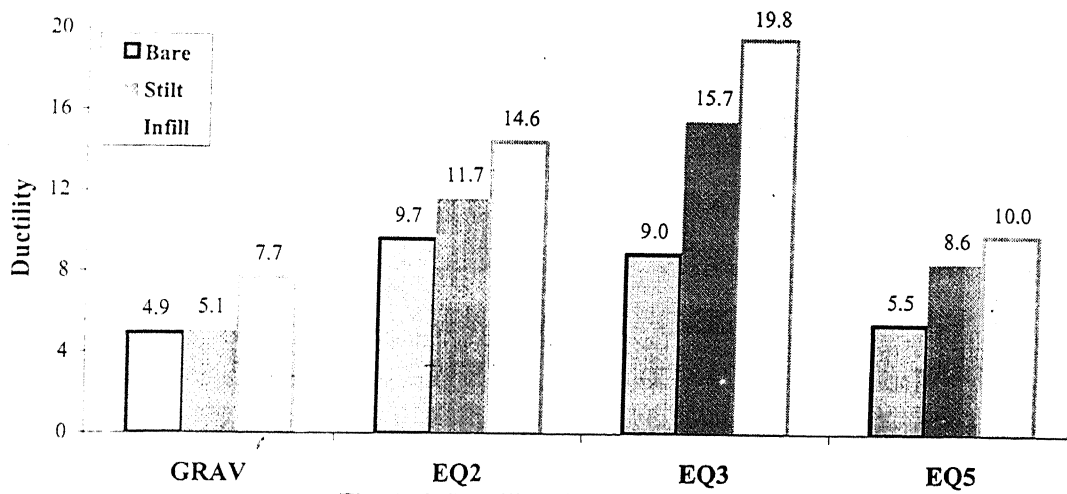


Fig. 4.33: Ductility of frame-A

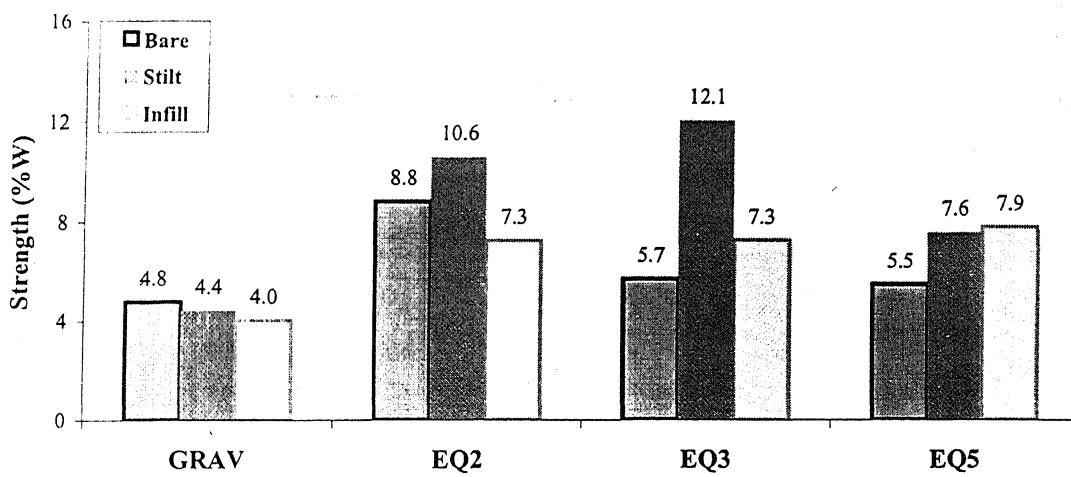


Fig. 4.34: Ductility of frame-B